



CZECH TECHNICAL UNIVERSITY IN PRAGUE

Faculty of Biomedical Engineering
Department of Natural Sciences

***DEVELOPMENT OF ACTIVE PART OF OPTICAL FIBER BIOSENSOR
USING GENETICALLY MODIFIED ORGANISMS***

Doctoral Thesis

Ing. Jakub Zajíc

Ph.D. Program: Biomedicínská a klinická technika
Branch of study: Biomedicínská a klinická technika
Supervisor: doc. Ing. Marie Pospíšilová, CSc.
Supervisor-Specialist: Ing. Gabriela Kuncová, CSc.

Kladno
December 2020

Poděkování

Rád bych poděkoval následujícím lidem, bez nichž bych nemohl dokončit tento výzkum a bez kterých bych se nedostal až do tohoto bodu! Moje vedoucí Dr. Pospíšilová, její podpora a pomoc byly během mého studia zásadní; Dr. Kuncová a Dr. Trögl, jejichž vhlad do problematiky a znalosti mě vedly tímto výzkumem; a Dr. Ripp, který mi pomohli zařídit stáž na University of Tennessee v Knoxville a bez kterého bych tento výzkum nemohl dokončit. Moje největší díky mé rodině za veškerou podporu, kterou mi během těchto studií a výzkumů projevili.

Acknowledgement

I would like to thank the following people, without whom I would not have been able to complete this research, and without whom I would not have made it to this point! My supervisor Dr. Pospíšilová, her support and help were crucial throughout my studies; Dr. Kuncová and Dr. Trögl, whose insight and knowledge into the subject matter steered me through this research; and Dr. Ripp, who have helped me to arrange an internship at the University of Tennessee in Knoxville and without whom I would not have been able to finish this research. And my biggest thanks to my family for all the support they have shown me through these studies and research.

"Biomedical engineering is an interdisciplinary professional and scientific discipline that uses and combines engineering, physical, mathematical and biological experience and skills to solve practical problems of medicine and biology (ecology, genetics, etc.)." (1)

Prohlášení

Prohlašuji, že jsem disertační práci s názvem “DEVELOPMENT OF ACTIVE PART OF OPTICAL FIBER BIOSENSOR USING GENETICALLY MODIFIED ORGANISMS” vypracoval samostatně a použil k tomu úplný výčet citací použitých pramenů, které uvádím v seznamu přiloženém k práci.

Nemám závažný důvod proti užití tohoto školního díla ve smyslu §60 Zákona č.121/2000 Sb., o právu autorském, o právech souvisejících s právem autorským a o změně některých zákonů (autorský zákon).

Declaration

I declare that I have elaborated my dissertation thesis titled “DEVELOPMENT OF ACTIVE PART OF OPTICAL FIBER BIOSENSOR USING GENETICALLY MODIFIED ORGANISMS” independently and have used a complete list of citations of used sources, which I present in the list attached to this work.

I have no compelling reason against the use of this schoolwork within the meaning of Section 60 of Act No. 121/2000 Coll., On Copyright, on Rights Related to Copyright and on Amendments to Certain Acts (the Copyright Act).

Abstrakt

Využití optických vlastností geneticky modifikovaného organismu (GMO) *Pseudomonas putida* TVA8, který je schopen produkovat bioluminiscenci ($\lambda \approx 500\text{nm}$) ve styku s benzenem, toluenem, etylbenzenem a xyleny, je jedním z možných principů optických biosenzorů detekujících tyto nebezpečné látky a další analyty. S využitím fyzikálně-chemických modelů buněčných interakcí s pevnými povrchy je poukázána snadnější adsorpce buněk *P. putida* TVA8 na křemenný povrch po ošetření γ -aminopropyltriethoxysilanem (APTES), bez použití nestabilní chemické matrice. Je demonstrována imobilizace mikroorganismů ve formě biofilmu na optovláknový element (OVE), který byl navržený pro zesílení slabého bioluminiscenčního signálu, čímž byl získán nejméně 135 dní aktivní optický prvek schopný on-line detekce přítomnosti toluenu v médiu ($26,5 \text{ mg L}^{-1}$) a reálného vzorku odpadní vody. Opakovatelnost přípravy sondy OVE a její použití bylo prokázáno s pěti OVE různých geometrií. Byly otestovány také další mikroorganismy, konkrétně *E. coli* 652T7, *S. cerevisiae* BLYR a *P. fluorescens* HK44 citlivé na různé analyty a jejich biologickou toxicitu.

Intenzita měřené bioluminiscence byla ovlivněna OVE s transmitancí mezi 1,4 a 5 %. Je popsán ideální tvar a geometrii OVE včetně porovnání bioluminiscenční odpovědi pěti OVE s různými geometriemi. Intenzita detekované bioluminiscence pomocí OVE byla několikrát větší než u PCS optického vlákna. Intenzity bioluminiscence se postupně snižovaly v důsledku uvolňování adsorbovaných buněk; a byly nižší, když byly indukovány kontaminovanou podzemní vodou, než v minerálním médiu (MSM) se stejným obsahem toluenu. Koncentrace toluenu $26,5 \text{ mgL}^{-1}$ byla detekována do 30 minut po ponoření sondy do vzorku. Imobilizace dalších mikrobiálních kmenů na povrchu křemičitého skla, funkcionalizovaného APTES, byla neúspěšná a je třeba zvážit další imobilizační techniky – i.e. prokázanou imobilizaci *E. coli* 652T7 pomocí polyethyleniminu. Prvek je použitelný jako detekční sonda pro vícenásobné použití v laboratoři a online monitorování biologicky dostupné kontaminace ve vzdálených lokalitách.

Prezentované experimenty byly realizovány v laboratoři Ústavu chemických procesů AV ČR v Praze-Suchdole a v laboratoři partnerského centra pro environmentální biotechnologie na University of Tennessee v americkém Knoxville.

Klíčová slova: Znečištění, Kontaminace, Endokrinní disruptory, Biosensor, Bioreportér, Luminiscence, Optovláknový prvek, Imobilizace, Biofilm, *Pseudomonas putida* TVA8

Abstract

The use of optical properties of the genetically modified organism (GMO) *Pseudomonas putida* TVA8, which is capable of producing bioluminescence ($\lambda \approx 500\text{nm}$) in contact with benzene, toluene, ethylbenzene and xylenes, is one of possible principles of optical biosensors detecting hazardous and other analytes. Facilitation of adsorption of *P. putida* TVA8 cells on quartz surface, after its treatment with γ -aminopropyltriethoxysilane (APTES), without the use of an unstable chemical matrix, is presented with the use of physico-chemical models of interactions of cells with solid surfaces. Immobilization of microorganisms in the form of biofilm on the optical fiber element (OFE), designed to amplify weak bioluminescent signal, was demonstrated and an active optical element capable of on-line detection of the presence of toluene in the medium (26.5 mg L^{-1}) and a real sample of wastewater for at least 135 days was obtained. Repeatability of preparation of OFE probe and its use was demonstrated with five OFEs of different geometries. Other microorganisms, namely *E. coli* 652T7, *S. cerevisiae* BLYR, and *P. fluorescens* HK44 sensitive to different analytes and their biological toxicity were also tested.

The intensity of measured bioluminescence was influenced by shapes of OFEs possessing transmittances between 1.4 and 5 %. The ideal shape and geometry of an OFE was described and compared to the real bioluminescence responses of five OFEs with different geometries. Intensity of detected bioluminescence with OFE was several times greater than with an PCS optical fiber. The intensities of bioluminescence gradually decreased due to release of the adsorbed cells; and were lower when induced with contaminated ground water than in the mineral medium (MSM) with the same content of toluene. Toluene concentration 26.5 mgL^{-1} was detected within 30 minutes of immersion of the probe into a sample. Immobilization of other microbial strains on APTES functionalized silica glass surface was unsuccessful, other immobilization techniques needed to be considered - i.e. demonstrated immobilization of *E. coli* 652T7 using polyethyleneimine. The element is conceivable as a detection probe for multiple use in a laboratory and the online monitoring of bioavailable contamination in remote localities.

Presented experiments were carried on in laboratory of the Institute of Chemical Process Fundamentals of the Czech Academy of Sciences in Praha-Suchdol and at laboratory of the partner Center for Environmental Biotechnology of the University of Tennessee in Knoxville, USA.

Key words: *Pollution, Contamination, Endocrine Disruptors, Biosensor, Bioreporter, Luminescence, Fiber-optic Element, Immobilization, Biofilm, Pseudomonas putida TVA8*

Table of Contents

Abstract	IV
List of used symbols and abbreviations	VII
List of used chemicals and media.....	VIII
List of figures and List of tables.....	IX
1. Introduction.....	11
1.1 Goals.....	14
2. Theoretical part	15
2.1. Sensors and detectors.....	15
2.1.1. Fiber optic sensors.....	18
2.1.2. Fiber optic whole-cell biosensors.....	19
2.1.3. Immobilization of microorganisms.....	22
2.2. Aromatic hydrocarbons - BTEX.....	25
2.3. Endocrine disrupting chemicals	27
2.3.1. Polychlorinated biphenyls (PCB)	27
2.3.2. Dioxins	28
2.3.3. Phytoestrogens.....	28
2.3.4. Pesticides.....	29
2.3.5. Phthalates.....	29
2.4. Bioluminescent bioreporters.....	30
2.4.1. <i>Pseudomonas putida</i> TVA8.....	30
2.4.2. <i>Escherichia coli</i> 652T7	34
2.4.3. <i>Pseudomonas fluorescens</i> HK44.....	35
2.4.4. <i>Saccharomyces cerevisiae</i> BLYR	36
2.4.5. Currently used and applied bioreporters	37
3. Experimental part.....	39
3.1. Used devices and software.....	40
3.2. Used media and solutions	51

3.3.	Sterilization and disinfection	53
3.4.	Growing bioreporter organisms	53
3.5.	Tapered optical fiber element.....	54
3.5.1.	Measurement of surface contact angles and zeta potentials.....	56
3.6.	Surface modification of the OFE.....	57
3.7.	Cell adsorption on the modified OFE	57
3.8.	Measurement of induced bioluminescence.....	58
3.9.	Scanning electron microscope visualization	60
4.	Results and discussion.....	62
4.1.	Tapered optical fiber element.....	62
4.2.	OFE surface characterization - contact angles and zeta potential.....	64
4.3.	Repeated immobilization of bioreporters and their visualization in SEM	66
4.4.	Time records of induced bioluminescence - ICP	67
4.5.	Time records of induced bioluminescence - UTK.....	68
4.6.	ICP experiment	73
4.6.1.	Contaminated water induced bioluminescence	75
4.7.	UTK experiment.....	76
4.7.1.	Immobilization and induction of <i>E. coli</i> 652T7	78
5.	Outcomes and future course of research	81
5.1	Future goals.....	83
6.	Attachments	84
6.1.	List of author's publications	84
6.2.	List of author's conference contributions	84
6.3.	Proof of first and second bioluminescent peak	85
6.4.	SEM images of immobilized <i>P. putida</i> TVA8.....	86
6.5.	Real polluted water sample composition test	88
7.	Bibliography.....	91

List of used symbols and abbreviations

°C – degree of Celsius	MSM – mineral salt medium
cps – counts per second	n – refraction index
AB – acid-base	L, l – liter or length
ADWG - Australian Drinking Water Guidelines	LW – Liftshitz-van der Waals
A.U. – arbitrary units	M – molar (concentration)
b – radius	m – meter
BBIC – biolum. bioreporter integrated circuit	OD – optical density
BOX – BIO-OPT-UVX project	OFE – optical fiber element
BTEX – benzene, toluene, ethylbenzene, xylenes	OVE – optovláknový element (OFE in czech)
CA – contact angle	Pa – pascal
CAS – Czech Academy of Sciences	PAH - polyaromatic hydrocarbon
cfu – colony forming unit	PCB – polychlorinated biphenyls
CTU – Czech Technical University	PCS – polymer-clad silica
CZ – Czech Republic	ppb – particles per bilion
DWG - Drinking Water Guidelines	PVC - polyvinyl chloride
EC – European commission	RCF - rotational centrifugal force
ED – endocrine disruptors	rpm – rotations per minute
EDC – endocrine disrupting chemicals	s - second
e.g. - exempli gratia – for example	SEM – scanning electron microscope
EL - elctrostatic	SPR - surface plasmon resonance
EPA - Environmental Protection Agency	T – time
EPS – extracellular polymeric substance	t – true value
etc. - et cetera, and others	UCHT – University of Chemistry and Technology
et al. - et alii - and others	USA – United States of America
ε - error	US NPDWS - United States National Primary Drinking Water Standards
FBE – Faculty of Biomedical Engineering	UTK – University of Tennessee in Knoxville
FOBS – fiberoptic biosensor	QHPR - Queensland Public Health Regulation
FOE – fiber-optic element	WHO - World Health Organization
FOS – fiber optic sensor	WP – with permission
G – gravitational force	ZP – zeta potential
g - gram	x – sensor response
GC – gas chromatography	Y – measurand value
GDP – gross domestic product	λ – wavelength
GMO – genetically modified organism	
ICP – Institute of Chemical Processes	
mbp – million base pairs	

List of used chemicals and media

Agar		
APTES	-	(3-Aminopropyl)triethoxysilane
C ₇ H ₈	-	toluene
CaCl ₂	-	Calcium chloride
CuSO ₄ · 5H ₂ O	-	Copper sulfate pentahydrate
FeCl ₃ · 6H ₂ O	-	Ferric chloride hexahydrate
H ₂ O	-	Water
H ₂ SO ₄	-	Sulfuric acid
H ₃ BO ₃	-	Boric acid
HCl	-	Potassium chloride
Kan	-	Kanamycin
KH ₂ PO ₄	-	Monopotassium phosphate
LB	-	Lauria-Bertani medium
MgSO ₄ · 7H ₂ O	-	Magnesium sulfate heptahydrate
MSM	-	Mineral salt medium
MnSO ₄ · H ₂ O	-	Manganese sulfate monohydrate
Na ₂ HPO ₄ · 12H ₂ O	-	Di-sodium hydrogen phosphate dodecahydrate
Na ₂ MoO ₄ · 2H ₂ O	-	Sodium Molybdate Dihydrate
NaCl	-	Sodium chloride
NaOH	-	Sodium hydroxide
NH ₄ NO ₃	-	Ammonium nitrate
O ₂ H ₂	-	Hydrogen peroxide
PB	-	Phosphate buffer
piranha solution		
Tet	-	Tetracycline
Y1771	-	Synthetic drop-out supplement (without LEU,URA,TRY)
yeast nitrogen base without amino acids		
ZnSO ₄ · 7H ₂ O	-	Zinc sulfate heptahydrate

List of tables

Table 1: <i>Reported BTEX concentrations in water</i>	26
Table 2: <i>Water BTEX guidelines</i>	26
Table 3: <i>Bioluminescent responses of P. putida TVA8 to 24 different chemicals</i>	34
Table 4: <i>Available OFE approximations by bi-exponential equations</i>	55
Table 5: <i>Calculated transmittance, cell number and OFE efficiency</i>	63
Table 6: <i>Zeta potential of tested samples</i>	64
Table 7: <i>Contact angles of tested samples for 3 different liquids</i>	64
Table 8: <i>Sums of bioluminescence intensities and maxima of bioluminescence for five OFEs</i>	77

List of figures

Fig. 1:	Sensor characteristics.....	17
Fig. 2:	Scheme of FOS in reflection and transmission arrangement.....	18
Fig. 3:	Extrinsic and intrinsic FOS	19
Fig. 4:	General representation of classic and whole-cell biosensor elements	21
Fig. 5:	BTEX, molecules of benzene, toluene, ethylbenzene and xylene.....	25
Fig. 6:	Polychlorinated biphenyls.....	28
Fig. 7:	Polychlorinated dibenzo-p-dioxins and Polychlorinated dibenzofurans	28
Fig. 8:	Chemical structure of orthophthalates.....	29
Fig. 9:	<i>P. putida</i> TVA8, SEM image	31
Fig. 10:	Bacterial luciferase luminescence reaction.....	32
Fig. 11:	Bioluminescence spectrum of <i>P. putida</i> TVA8	33
Fig. 12:	<i>P. fluorescens</i> HK44 biofilm on silica glass, SEM image	36
Fig. 13:	<i>Saccharomyces cerevisiae</i> BLYR cell, SEM image	37
Fig. 14:	Alginate-immobilized bioreporter onto exposed optical fiber core	38
Fig. 15:	AB15 pH meter with probe and RL150 pH meter	40
Fig. 16:	700LS-E Steam sterilizer	41
Fig. 17:	TR-104 balances and APX-602 balances.....	41
Fig. 18:	Lab-Line 3597 shaker and PsycroTherm shaker.....	42
Fig. 19:	Shaker - Unimax 1010DT, Heidolph	42
Fig. 20:	Laminar flow box HH1.2 Basis, Helta-Holten AIS	43
Fig. 21:	Thelco 17 oven and Memmert UM300 oven	43
Fig. 22:	Ultrasonic cleaner PS04000A	44
Fig. 23:	Oriel 7070 detection system with photomultiplier tube Oriel 70680.....	44
Fig. 24:	MP-984-RS Perkin Elmer photon counting module	45
Fig. 25:	Variomag Multipoint 6/15 magnetic stirrer	45
Fig. 26:	CAM 200 goniometer setup	46
Fig. 27:	Luminometer Berthold FB12	46
Fig. 28:	Centrifuge Universal 32R and Sorvall Legend XTR	47
Fig. 29:	Velp ZX3 advanced vortex mixer and Baxter SP vortex mixer	47
Fig. 30:	Zeiss Auriga scanning electron microscope and Tescan VEGA3 SEM	48
Fig. 31:	SPI module sputter coater.....	49
Fig. 32:	IVIS Lumina K series III, Perkin Elmer, In-vivo imaging System	49
Fig. 33:	SurPASS analyzer	50

Fig. 34:	Scheme of OFEs preparation	54
Fig. 35:	Tapered optical fiber element with marks for measurement of diameters	55
Fig. 36:	Tapered OFEs available for experiments at UTK.....	56
Fig. 37:	Experimental set-ups for monitoring bioluminescence.....	59
Fig. 38:	OFE immersed in the induction solution.....	60
Fig. 39:	Quartz cones.....	61
Fig. 40:	Transmittance calculated for five theoretical OFEs with different bends	63
Fig. 41:	Likelihood of adhesion of the <i>P. putida</i> TVA8 to APTES quartz	65
Fig. 42:	<i>P. Putida</i> TVA8 biofilm-like layer, 2 and 130 days after initial immobilization	66
Fig. 43:	OFE-0 - Time-records of daily inductions of bioluminescence.....	67
Fig. 44:	OFE-0 - Time-records of daily inductions of bioluminescence.....	67
Fig. 45:	OFE-0 - Time-records of daily inductions of bioluminescence.....	68
Fig. 46:	OFE-0 - Time-records of daily inductions of bioluminescence.....	68
Fig. 47:	OFE-A - Time-records of daily inductions of bioluminescence.....	69
Fig. 48:	OFE-B1 - Time-records of daily inductions of bioluminescence.....	69
Fig. 49:	OFE-B2 - Time-records of daily inductions of bioluminescence.....	69
Fig. 50:	OFE-C - Time-records of daily inductions of bioluminescence.....	70
Fig. 51:	OFE-D - Time-records of daily inductions of bioluminescence	70
Fig. 52:	Typical time-record of daily induction of <i>P. putida</i> TVA8 adsorbed on OFE.....	71
Fig. 53:	Daily bioluminescence maxima, aggregated data from six OFEs.....	72
Fig. 54:	Time of the first bioluminescence maxima, aggregated data of six OFEs.....	72
Fig. 55:	OFE with adsorbed <i>P. putida</i> TVA8 induced daily for 135 days	74
Fig. 56:	Main peak bioluminescence integrals and max bioluminescence of each OFE.....	76
Fig. 57:	<i>E. coli</i> 652T7 immobilized on an APTES modified quartz cone	78
Fig. 58:	Time records of bioluminescence of <i>E. coli</i> 652T7 immobilized on OFE in PEI.....	79

1. Introduction

Economical and industrial growth require natural, human, and capital resources. Resources that are either qualitative such as particular material and work force, or quantitative such as increasing qualification of workers and increasing process efficiency. Most discussed environmental topics that relate to the increase of global gross domestic product (GDP) are Sustainable Development and Global Problems, such as depletion of natural resources, overpopulation, migration of population and environmental pollution. These problems deserve attention because they affect humanity and human health in short but also in long term periods. It is not only an environmental issue, but the problem also reaches to the political, economic and medical spheres. (2) (3)

The various industries from which the modern society benefits and produces large number of chemicals. Such chemicals are released into the environment either on purpose (fertilizers, drinking water treatment), or by leakage. It is important to distinguish between the term contamination that is used for chemicals that cause no harm to the environment and humans, and the term pollutant that is *“any substance introduced into the environment that adversely affects the usefulness of a resource.”* Any substance can pollute in concentration high enough, but it is mostly the industrial chemicals that are emphasized in environmental monitoring. Primarily controlled chemicals identified in regulations (i.g. World Health Organization or United Nations Environment Programme) are selected due to their toxicity in low concentrations, bioaccumulativity, persistency, carcinogenicity and repeated assessment in monitoring programs. (2) (3)

Both usage and production of the petroleum-based products were caused by Industrial revolution and expansion. Nowadays there are many places potentially contaminated by petroleum chemicals due to this phenomenon. Increasing population require steady supply of drinking water. Chemical and biological composition of such a source must meet local regulations. Regular analyses are required to control tap water as well as ground and surface waters and effluents from industrial areas. Benzene, toluene, ethylbenzenes, and xylenes (BTEX) are the main partially water-soluble contaminants. Monitoring of so-called endocrine disrupting chemicals, derived from petroleum and other industrial products, also became one of the main research interests in recent years. (4) (5)

BTEX compounds are normally degraded when exposed to atmospheric oxygen. The problem occurs when they pollute soil and ground waters, where the oxygen is depleted. Moreover, the BTEX is highly mobile in ground waters. Besides these properties of BTEX compounds, attention is also paid to the accumulation of these pollutants, negative effects on human nervous system and carcinogenicity. (6)

Past decades also experienced exponential growth of number of pharmaceutical and agricultural chemicals. A wide variety of those chemicals were found to have the potential to disrupt the endocrine system of animals, including humans. The term endocrine disrupting chemicals (EDC) was first used in 1991 (7), and later the Endocrine society implicated EDCs as a significant concern to public health. Many studies found significant amounts of EDCs in our environment and supplies of drinking water. EDCs were reported to cause adverse developmental, reproductive, neurological, and immune effects in humans. Together with BTEX related health problems those chemicals put research and financial pressure on our health care system. (7) (5) (8) (9) (10) (11) (12)

Numerous analyses are required to check tap water as well as ground and surface waters and the effluents from industrial areas. The gas chromatography (GC) is among the most used analytical methods for separation of gasses, liquids and solids (including BTEX and EDCs). This method has very low limits of detection of volatile compounds, nevertheless this method is time consuming, expensive and dependent on the sample quality and its storage. (13) The author therefore proposes a new way of detecting the discussed pollutants. It is based on a novel optical fiber element (OFE) with immobilized genetically modified organism, which produces bioluminescence in the presence of a compound of interest – author demonstrates the use of developed sensor for toluene detection. Highlights of such a detector would be low price in comparison with standard methods, ability to perform a long-term online detection of BTEX in remote sites without the need of sample preparation. Besides analytical information, the biosensor can also provide functional information such as the effect of a substance on a living organism, specific aspect of cellular metabolism or the information about cellular toxicity. Nevertheless, bioreporter cells have also several drawbacks such as the need of optimal living conditions (temperature, pH, nutrients) or lower sensitivity.

This work discusses the principle of detection in biomedical applications using genetically modified organisms (GMO) and fiber-optic elements. This general principle of biosensor arrangement could be applied in many applications (in-vivo toxicity and carcinoma screenings, pollution, industrial processes control). The detection principle is shown specifically on the chemical pollution of aquatic environment where the author deals with the development of pollution detectors, namely a detector of toluene in contaminated water employing the *Pseudomonas putida* TVA8 bacteria. Author also discusses possible use of other modified microorganisms in pollution detection, including contamination by endocrine disrupting chemicals.

First part of this work was conducted at the **Faculty of Biomedical Engineering of the Czech Technical University in Prague** (FBE, CTU), Sítňá 3105, 272 01, Kladno 2, and at the **Institute of Chemical Processes of the Czech Academy of Sciences** (ICP, CAS), Rozvojeová 135, 165 02 Praha 6. It was elaborated as a part of the project named: BIO-OPT-UVX (BOX) Research Team Advancement at the Faculty of Biomedical Engineering, Czech Technical University in Prague (Registration number: MEYS ESF CZ.1.07/2.3.00/20.0092; duration: July 1, 2011 – May 30, 2014; Project sustainability ended in June 30, 2019; Project administrator: prof. Ing. Miroslava Vrbová, CSc). Results of the experiment, which were carried out at the IPE, were published in Chemical Papers journal in 2016 (4).

Second part of this work was elaborated at the **University of Tennessee in Knoxville, USA, Center for Environmental Biotechnology** (UTK), 76 Dabney Hall, 1416 Circle Drive, Knoxville, TN, 37996-1605. This institution provided all the necessary equipment and instrumentation. Students supervisor at the foreign institution was Steven A. Ripp, PhD. The internship was partially financed from the grant of the Dean of FBE, CTU and internal CTU grants with the following identification numbers: SGS17/110/OHK4/1T/17 and SGS18/097/OHK4/1T/17. Results of this internship were presented at IEEE Sensors and Nano 2019 conference in Penang, Malaysia, financed from the internal CTU grant: SGS19/085/OHK4/1T/17 and were published in Sensors journal in 2020 (14).

The thesis was prepared under supervision of **doc. Marie Pospíšilová, CSc.** from the Department of Natural Sciences at the FBE, CTU. The experimental work was carried out under the supervision of **Ing. Gabriela Kuncová, CSc.** from the ICP, CAS; and **Steven A. Ripp, PhD.** from the UTK.

1.1 Goals

1. To suggest an approach for development of active part of optical fiber biosensor based on literature research.
2. To construct new active layer of the biosensor in form of biofilm and test different available bioreporter cells in the setup.
3. To characterize the designed active part of optical fiber biosensor using laboratory and microbiological procedures and test it on a real polluted water sample.
4. To discuss results for the six available optical fiber elements and suggest future research goals.

2. Theoretical part

Beginning of the theoretical part discuss sensors in general, further focusing on fiber optic sensors and biosensors. Subsequently two environmental threats that are in the focus of this thesis are described - namely BTEX group of aromatic hydrocarbons and endocrine disrupting chemicals. Author also provides information about bioluminescent microorganisms that were used in experiments for development of the active part of biosensor.

2.1. Sensors and detectors

Broadest definition of a sensor is that it is “anything that responds to an input of interest.” We think of it as of a device that can detect a physical or chemical quantity and converts it into a signal which can be read by an observer or by an electronic device. A **sensor** provides us with continuous information about a measurand, on the contrary a device registering solely the presence or absence of a quantity is called **detector**. Another term related to sensors is a transducer. It is a material or a device that converts energy from one form into another. Sensors can be thus considered as forms of transducers. (15)

Sensors development is driven by various needs, such as to increase production, to decrease cost, to detect a pollutant or a disease etc. The need for sensors drives their development in agriculture, food industry, healthcare and many other areas. When there is a need, a measurand of interest needs to be defined prior to the sensor development. When the measurand is identified it needs to be converted through the chemical, physical or biological interaction into an entity suitable for creating a sensor output. Detection means (biological, chemical, electromagnetic, temperature, displacement, radiation ...) are than identified by the nature of this interaction. (16)

Signals can be divided based on the generated or received energies into the following categories – mechanical, thermal, electrical, magnetic, radiant, and chemical. (15)

Sensors need to be appropriately characterized in terms of certain parameters and characteristics. Basic classification divides sensors into passive ones, that do not need any power supply and generate signal by itself (photovoltaic or piezoelectric sensors),

and active ones, that need an external energy source (temperature resistive sensor). Based on the sensor output, they can be divided into analog or digital. (17)

Accuracy of a sensor is the difference between measured and true value. It tells us how good the measured value is compared to a recognized standard and could be specified by an error ε (A). Errors of a systems can sum up; the resulting error is than given by (B).

$$\varepsilon (\%) = \frac{x_m - x_t}{x_t} \times 100 \quad (A)$$

$$\varepsilon_0 = \left[\sum_i \varepsilon_i^2 \right]^{1/2} \quad (B)$$

Where x is the measurand and indexes t, m are the true value and the measured value, respectively. (17)

Basic sensor parameters are:

1. **Range** of a sensor is defined by the minimum and maximum value between which the sensor works well, under defined parameters.
2. **Resolution** of a sensor tells us, what is the smallest possible physical change of a measured variable, which can be measured by the sensor.
3. **Repeatability** of a sensor describes how consistent is repeated measurement. A sensor with high repeatability gives us a narrow range of measured values that are repeated under the same conditions.
4. **Stability** of a sensor describes how much the sensor characteristics remain constant over time. The stability (drift) is a result of a sensor or its components aging, or it could be a function of another variable such as signal frequency.
5. **Linearity** can be defined by a deviation from the best fit straight line obtained by regression analysis or a straight line that connects the end points of the measured curve. (17)
6. **Sensitivity** of sensor is determined by the slope of the calibration curve. It is defined as a change of output variable related to the change of an input variable (dY/dX).

All the above characteristics are known as static characteristics. Dynamic characteristics involve the response time of a sensor that is defined as a time needed for the output to change from its previous state to a final value within some tolerance. They also involve the determination of transfer function, frequency, or impulse response. Some of the characteristics are depicted in Fig. 1. Besides all the mentioned characteristics, the sensor itself is also influenced by the external variables such as temperature, humidity, or vibrations. These needs to be considered and/or eliminated to a maximum extent. (17)

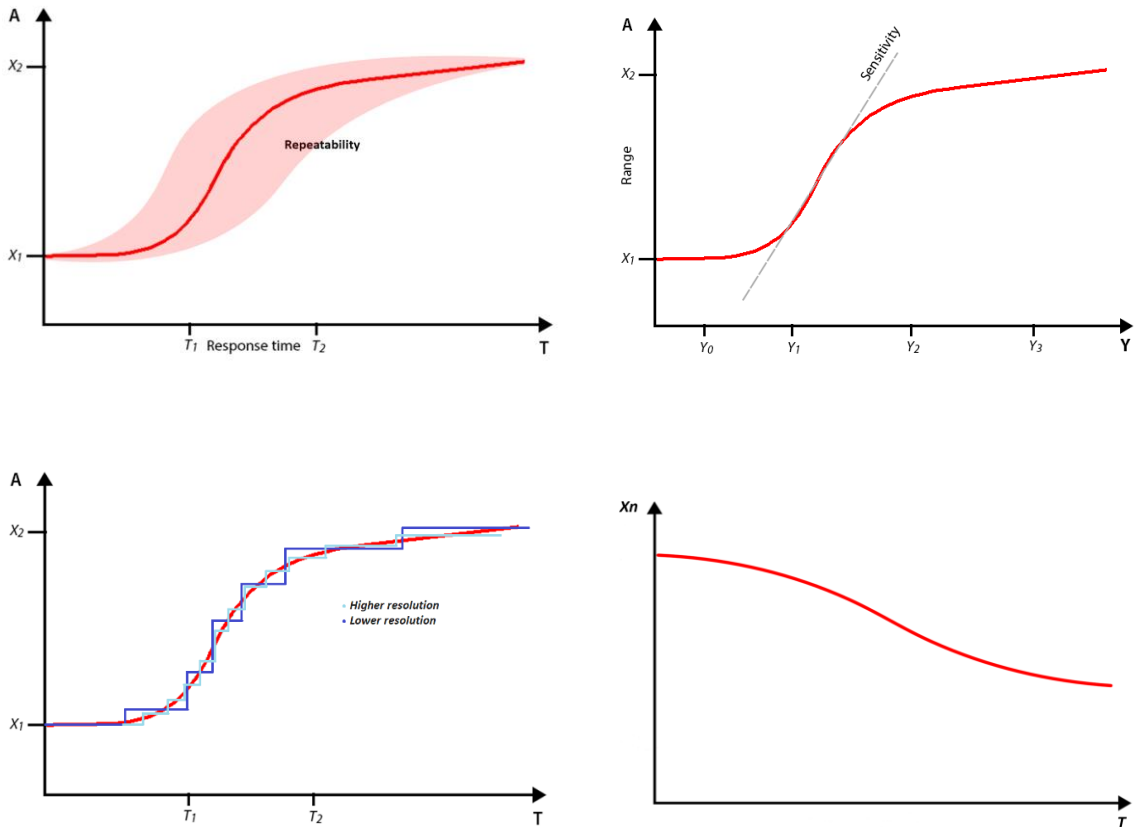


Fig. 1: Sensor characteristics - response time and repeatability (response X within time T , top left); calibration curve and sensitivity (response X to measurand value Y , top right); resolution (response X within time T , bottom left); stability (point X_n within time T , bottom right)

2.1.1. Fiber optic sensors

Optical sensor uses the principle of interaction of light with mass for sensing physical and chemical parameters. Fiber optic sensors (FOS) are thus a subset of optical sensors, which use optical fiber in their design. Optical fibers fundamentals and light propagation in optical fibers are described in (18) (19).

Fiber optic sensors (FOS) use various types of optical fibers (ex. PCS, PVC; single/multi-mode; step/gradient refraction index) to guide light of the spectral range from 180 nm up to 10 μm . The advantages of the use of optical fibers in FOS are small dimensions, low attenuation on long distances, resistance to electromagnetic noise, possibility of measuring small volume samples and possibility of performing online measurements in flammable or in normally inaccessible sites. (18)

FOS consists of a light source, optical fiber, light detector, and a processing unit. It is based on registering changes of light characteristics such as intensity, phase, polarization or spectrum. FOS can be divided based on their arrangements to intrinsic and extrinsic. Extrinsic sensor uses optical fiber only as a passive element to transmit light from a source to a detection site and/or further to a detector. Intrinsic sensor uses the fiber as an active element, where the detection site is located within the fibers core or cladding. Another division is according to transmission and reflection arrangement of a FOS (Figs. 2-3).

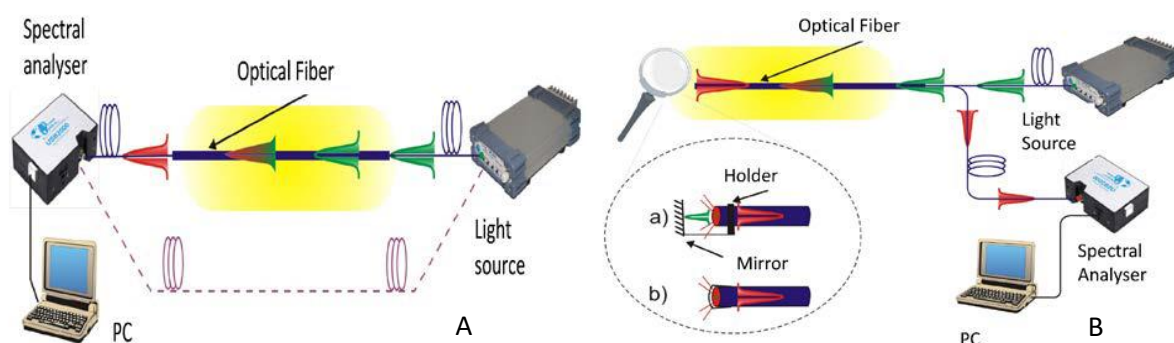


Fig. 2: (A) Scheme of FOS in reflection arrangement;
(B) Scheme of FOS in transmission arrangement. (WP) (18)

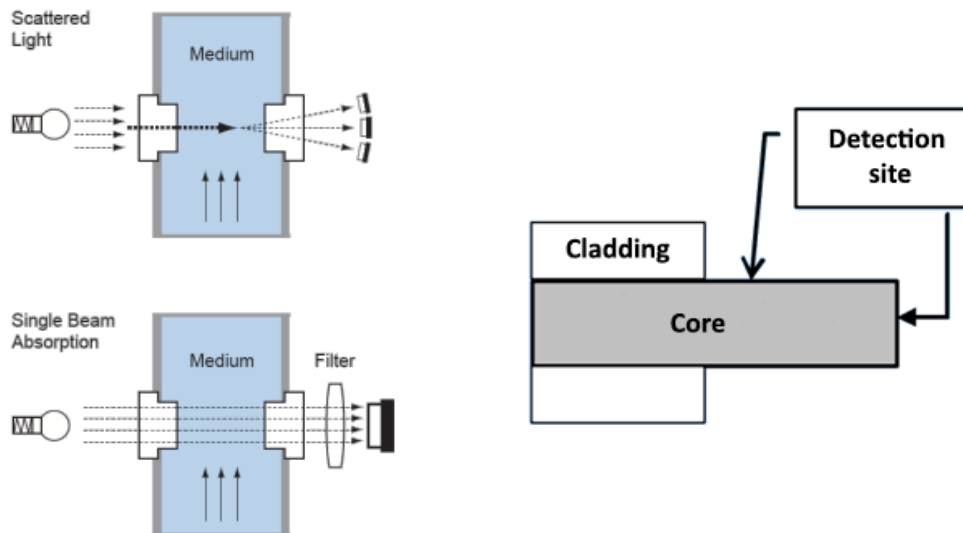


Fig. 3: Extrinsic FOS (left) and intrinsic FOS (right) (WP) (19)

2.1.2. Fiber optic whole-cell biosensors

Biosensors are devices that incorporate a biological sensing element in their design. The aim of this is to increase the sensitivity and sometimes also selectivity by the use of a biological element. Biological elements are of more or less complex nature. Namely: organisms, tissues, cells, organelles, membranes, enzymes, receptors, antibodies, nucleic acids, and organic molecules could be used as a sensing element. Advantage of biological elements is their biocompatibility compared to an inorganic fluorophore.

Pospíšilová et al. (2015) describe four fiber optic biosensors (FOBS) classifications. **Enzyme** FOBS employ various catalytic enzymes, which are the most widespread type of biosensor. In general, they have great specificity and sensitivity, but the preparation and enzymes purification are time consuming and costly. The glucose sensor by Pasic et al. (2007); hydrogen peroxide, xanthine, and hypoxanthine sensor by Spohn et al. (1995); or dopamine sensor by Yuanting et al. (2012) could be mentioned as an example. **Whole cells** FOBS use microbial cells that react to an analyte. An indicator (pH, oxygen) or optical properties of cells are than the subject of detection (fluorescence, luminescence). Microbial cells are easy to manipulate, more viable and stable in-vitro. The toluene biosensor by Kalabova et al. (2013) could be mentioned as an example. **Immunoassay** FOBS exploit the binding between an antibody and antigen, which is detected through a fluorescent label or by evaluation

of reflectivity or refractive index. The fiber optic SPR probe by Mai et al. (2019) could be mentioned as an example. **Nucleic acid** FOBS use the single-stranded DNA that forms double strands with a complementary strain, usually labeled with an optical indicator. The adenosine sensor by Xiyu et al. (2019) could be mentioned as an example. (18) (20) (21) (22) (23) (24) (25)

“According to their mode of action, optical biosensors have been subdivided into five subgroups: (a) plain fluorometric sensors; (b) direct and indirect indicator-mediated chemical sensors; (c) direct enzymatic biosensors; (d) indicator-mediated enzymatic biosensors; and (e) affinity biosensors.” Typical optical measurement methods include absorbance or reflectance, fluorescence, bioluminescence or chemiluminescence. (18)

Wang and Wolfbeis (2020) published an extensive updated review of Fiber-Optic Chemical Sensors and Biosensors. (26)

This work aims to design an active part of whole cell fiber optic biosensor of BTEX contaminants. As it was described above, this biosensor uses whole cells as recognition elements. Whole cell biosensors allow us to obtain functional information (effect of stimulus on a living system, effect of a substance on other aspect of cellular metabolism, cell toxicity, etc) and qualitative or quantitative analytical information (what substance is present and in what concentration). Sensitivity of a cell to a substance is determined by its receptor/ligand binding constant. A relatively new approach is to genetically modify a cell strain to increase its specificity and sensitivity to a specific substance. Monitoring the state of cells to obtain desired information is carried out either on its energy metabolism - measurement of pH, O₂ consumption, CO₂ production, lactate production or it uses specific features of some cells such as potential on nerve cells or bioluminescence. Whole-cell biosensors employing GMO is reviewed by Wei et al. (2015). (27)

The design of whole cell biosensor was chosen for its low cost in comparison to lengthy chemical analysis, simplicity, and relatively fast analysis. It allows us to perform continuous monitoring in remote sites, it is possible to make the biosensor small, compact and it could detect several measurands at the same time (28). Furthermore, it could measure the total bioavailability of a pollutant rather than its free form. Nevertheless, the chosen approach also has potential drawbacks, such as worse handling, limited lifetime of living components, lower

sensitivity in comparison to chemical analysis, response time to an analyte from tens of minutes up to hours, and legal obstacles to employ GMO in the environment or living organism, but there already have been several exceptions (29) (30). General representation of a whole-cell biosensor is shown in Fig. 4.

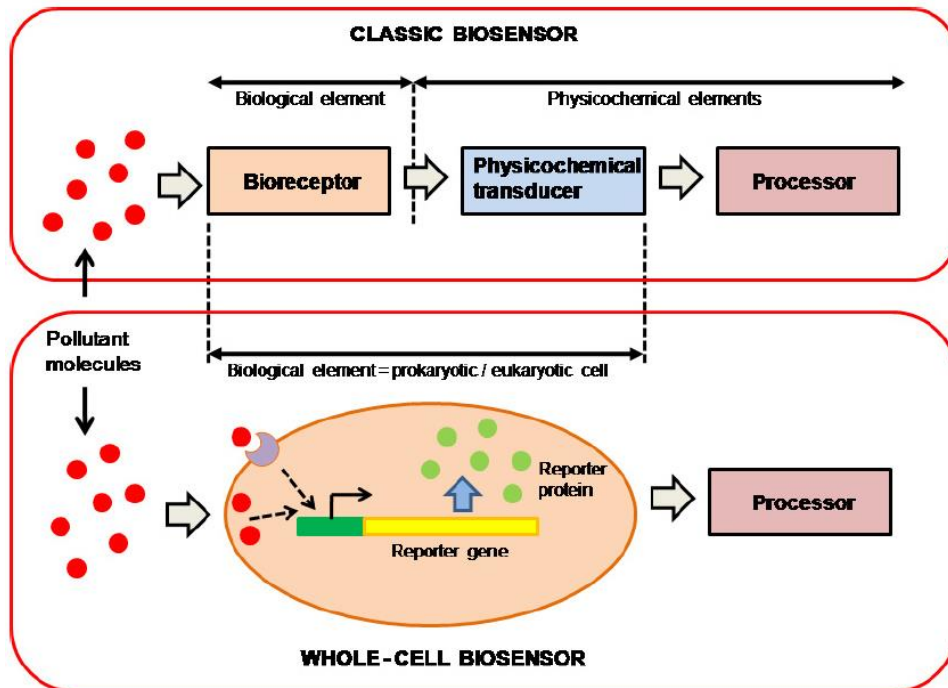


Fig. 4: General representation of classic and whole-cell biosensor elements (31)

This work focuses on the development of BTEX detector in an environmental sample with the use of a specific bioreporter organism, but the same principle of sensing and detection could be used in general, using different microorganisms in different fields and applications. This also opens endless possibilities for fast and inexpensive determination of numerous analytes in medicine.

2.1.3. Immobilization of microorganisms

A whole-cell biosensor, as an analytical instrument, requires the integration of living cells into a device, e.g. by immobilization, in close contact with the transducer, which is a light detector in the case of an optical sensor. Many immobilization strategies, recently reviewed by Xu et al., have been employed. (32) Their list comprises cell adsorption, entrapment or encapsulation into polymers or a combination of hydrogel entrapment and cryopreservation, plasma-deposited films, the application of photolithography or electrospinning and electrodeposition (33) (34). In portable sensors, as the bioluminescent bioreporter integrated circuit (BBIC) (35) or field deployable sensors (36) (37), the immobilized reporter organisms were used as a disposable material. The reproducibility of fabrication of the component with immobilized living cells and their storage stability were checked in (38) (39), but there is a lack of data on their repeated use.

Sustained analytical responses of immobilized cells are required for a sensor used repeatedly in the laboratory as well as for the on-line monitoring of pollution in remote localities. Longevity is needed in the case of the integration of bioluminescent bioreporters into the optical structures of intrinsic optical fiber sensors (e.g. evanescent field sensor). In combination with quartz optical fibers, living bioluminescent bioreporters might serve for on-line and in-situ monitoring in remote hazardous localities and, unlike electrical sensors or portable sensors with electrical components, might be applied in places with an explosive atmosphere.

Among immobilization techniques, cell adsorption and **entrapment** into silica gel by sol-gel method possess the properties of transparency, chemical inertness and biocompatibility which are of primary importance for optical sensors. The porous gel also permits nutrients to reach microorganisms immobilized within a certain depth. Sol-gel method involves transformation from a liquid colloidal suspension into a gelatinous gel, subsequently transiting into a solid material. The method has been used to immobilize various biological sensing elements, including whole cells. For this matter, one needs to overcome extreme pH values and high alcohol concentrations during the process e.g. by adding the living cells into the sol after partial hydrolysis of the precursor. (40) Microbial cells do not react with the matrix but are rather captured in the aging gel. This method was used to entrap *P. putida* TVA8

in a drop of silica gel on tapered element to form a biorecognition layer of a biosensor that detected toluene in water repeatedly for over two weeks. (41)

The **adsorption** of cells onto solid surfaces is one of the initial steps of microbial biofilm formation, which can be regarded as a natural method of whole cell immobilization (42). Adhesion of living cells to a wide variety of suitable solid-liquid interfaces is a prerequisite to biofilm formation. Rough, hydrophobic, and nonpolar surfaces increase the likelihood and rate of the cell attachment and biofilm development. Conditioning films composed of attached polymers form a growth medium or targeted chemical modification, also play a positive role in microbial attachment. Another variable affecting microbial attachment is the hydrodynamics of the medium, in which the cells behave as particles. Higher linear velocities of a medium result in thinner hydrodynamic boundary layer on the solid-liquid interface and faster association of cells with the surface, until velocities become high enough to overcome shear forces on the attaching cells. Microbial attachment is also affected by aqueous medium characteristics such as pH, nutrient levels, ionic strength, and temperature. For last but not least, properties of microbial cells also influence the attachment of cells to a surface. These include surface hydrophobicity, size, motility, presence of fimbriae and flagella, and production of various extracellular polymeric substances (EPS). Targeted selection or modification of the surface properties of solid materials can significantly enhance the adsorption of cells. In order to predict and understand the process of microbial adsorption onto solid surfaces, different physicochemical models (e.g. the thermodynamic model and the extended Derjaguin–Landau–Verwey–Overbeek (DLVO) theory) can be applied. (43) (44) (45) (46)

In a biofilm, cells are enclosed in a matrix, mainly consisting of polysaccharides and possibly other non-cellular material and particles. The behavior of a biofilm microorganisms could be diametrically different from their planktonic state. In biofilm cells are organized in heterogenic structures, distributed over a surface in homogenous or heterogenous microcolonies, rather than in continuous monolayer, surrounded by interstitial voids. External and internal influences and processes affect biofilm architecture by making it more compact, loose it, or dissolve it. External particles trapped in EPS can function as a cell protection, support growth or enhance environmental conditions of the biofilm (e.g. erythrocytes and fibrin in pathological heart valve biofilm; precipitation of minerals in

biofilm and encrustation of a medical catheter). Structure of a biofilm provides an ideal environment for creation of nutrient gradients, exchange of genes (conjugation occurs more frequently than in planktonic state), and quorum sensing. The key biofilm characteristics were described by Donlan (2002) or Kokare et al. (2009). The challenge is to completely understand what makes the biofilm so different from the planktonic phenotype. (43) (47) (48) (49)

Continuous monitoring with whole cell biosensors requires repeated inoculation (50) or immobilization (51) of cells on the sensing element. In comparison with other immobilization techniques, the immobilization of bioluminescent bioreporters by attachment on a surface of the sensing element has two advantages: the formation of a layer of cells attached to a surface does not involve any dropping or printing machines, and the cells adhere tightly to the sensing element to minimize loss of the detected bioluminescence signal. (14)

Reporter cells immobilized on the tip of an optical fiber can enable continuous measurements in small volume samples and remote localities. The tiny dimensions of an optical fiber (diameter <600 μm) make it possible to immobilize only a few cells on the fiber tip. However, such a small number of cells provides a low light intensity, resulting in low biosensor sensitivity. To increase the signal intensity, the light coupling efficiency can be increased by etching the fiber tip and increasing the number of adhered reporter cells by encapsulation into alginate beads (52).

Present work sought to demonstrate the repetitive use of a whole-cell sensor with the biorecognition layer prepared by the adsorption of living cells on the wider end of a tapered optical fiber in the form of biofilm, which also resulted in an increase in the detected bioluminescence signal intensity.

2.2. Aromatic hydrocarbons - BTEX

One of the most stressed chemicals in environmental monitoring are aromatic hydrocarbons. Also known as arenes, they are molecular compounds with sigma bonds and delocalized pi electrons between carbon atoms forming mono- or polycyclic rings.

Benzene, toluene, ethylbenzene and xylenes are organic, aromatic, hydrocarbon chemicals (Fig. 5). They belong to volatile organic compounds that have high vapor pressure at room temperature. BTEX are associated with petroleum and its products. They can be present in gasoline, rubbers, plastics, paints or even in car exhausts or in cigarette smoke. Besides these human made products, these compounds can also be found in petroleum production and usage sites as environmental contaminants. Natural sources of BTEX are gas and petroleum deposits, emissions from volcanos or forest fires. (53)

BTEX are partially water-soluble, thus it is obligatory to monitor BTEX concentrations in the drinking water, industrial areas, and other risk localities (benzene – 1.84 g/L at 30°; toluene - 0.52 g/L at 20 °C; ethylbenzene - 0.15 g/L at 20 °C; xylenes – 0.12 g/L at 20°).

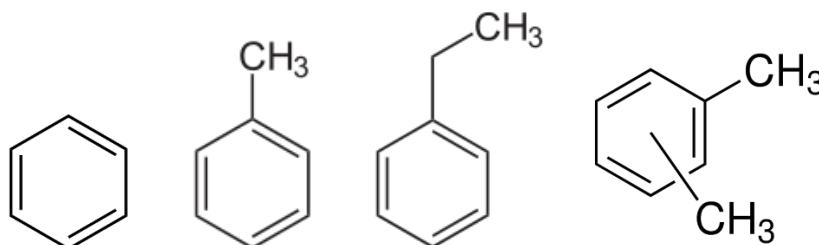


Fig. 5: BTEX, molecules of benzene, toluene, ethylbenzene and xylene respectively from the left

The following effects of BTEX on human health can be distinguished: Short term effects include skin and sensory irritation, central nervous system problems (tiredness, dizziness, headache, loss of coordination) and effects on the respiratory system (eye and nose irritation). Long term effects include kidney, liver, and blood system problems. Chronic exposure to benzene compound can lead to leukemia and cancers of the blood-forming organs. (54)

Concentrations of BTEX compounds in the environment range from 0.1 to over 100 ppb in air. Concentration in ground water is generally below 3 ppb, but in polluted sites it can reach values over 3500 ppb. Higher concentrations are generally detected in urban

areas, high traffic density areas, gas stations, and daily consumer products (especially cigarette smoke). Table 1 shows typical reported concentrations of BTEX in water. (53)

Table 1: Reported BTEX concentrations in water (53)

[ppb or µg/L]	Benzene	Toluene	Ethylbenzene	Xylenes
Surface water	<0.1 – 2.1	<1 - 15	<0.1 - 1.8	<0.1 - 1.2
Contaminated surface water	Up to 100	NA	Up to 15	Up to 32
Groundwater	<0.1 - 1.8	<1 - 100	<0.1 - 1.1	<0.1 - 0.5
Contaminated groundwater	Up to 330	Up to 3500	Up to 2000	Up to 1340
Drinking water	<0.1 - 5	<1 - 27	<1 - 10	<1.0 - 12

Public health guidelines, based on an acceptable daily intake, were published by numerous agencies operating worldwide – i.g. World Health Organization Drinking Water Guidelines (WHO DWG); Queensland Public Health Regulation (QHPR); Australian Drinking Water Guidelines (ADWG); United States National Primary Drinking Water Standards (US NPDWS). Some of the guidelines values are listed in the Table 2. (53)

Table 2: Water BTEX guidelines (53)

[ppb or µg/L]	WHO DWG	QHPR	ADWG	US NPDWS
Benzene	10	1	1	5
Toluene	700	800	800	1000
Ethylbenzene	300	300	300	700
Xylene	500	600	600	10000 (total xylenes)

Regulation (EC) No 1907/2006 of the European Parliament and of the Council sets toluene concentration limits for work environments at 680 µg/L in freshwater environment. The regulation also defines the acute toxicity to algae and daphnia (6-245 mg/L within 1-2 days) and fish (7.63 mg/L within 4 days); and chronic toxicity to fish (5.44 mg/L within 7 days). Taiwanese agencies have set acceptable limits for toluene in drinking water and groundwater at 7.6–10.9 µM (900 µg/L). (55)

2.3. Endocrine disrupting chemicals

Endocrine disruptors (ED, EDC) are a wide range of chemicals with effects on humans and wildlife. There is an evidence that these chemicals have adverse effects upon the exposure to relatively high concentrations. There is also an evidence of worsened fertility and increased number of certain types of cancers in humans in past decades, which is considered as the result of human exposure to EDC, but scientific uncertainty still exists. The main idea of long or short-term effects of EDC is based on the fact that all organ systems of a human body are regulated by endocrine factors. Changes in normal levels of these factors are thus logically connected with adverse effects of these chemicals, especially during periods of human development, pregnancy, or lactation. The current research focuses on whether the amounts of EDC present in our environment can possibly influence humans, what concentrations and exposure times are harmful and to what extent, and also what is the effect of a mix of two or more EDC. (9)

2.3.1. Polychlorinated biphenyls (PCB)

PCBs are biphenyl compounds with 1-10 hydrogen atoms replaced by chlorine (Fig. 6). They were widely used in the mid-20 century and were prohibited in most of western countries in late 1970s and 1980s due to extremely low rate of biodegradation and carcinogenicity. PCBs were used in transformers, capacitors, inks, adhesives, paper, paints, insulators, and pesticide extenders. PCBs are no longer produced, nevertheless they are still present and cycle in global environment, including living organisms, in significant quantities. PCBs tend to concentrate in sea ecosystems, where they sorb to sediments and organic matter. Upon ingestion PCBs are concentrating in fatty tissues and liver, increasing the risk of cancer. (56) (12)

At 25 °C they range from light to dark-yellow oily liquids to white crystalline solids and hard noncrystalline resins. There are 209 possible PCB congeners. They have low water solubility at about 0.7 mg/L, molecular weight of 326 ± 24 , and melting point at 357 ± 17 °C. Maximum contaminant level in drinking water, set by the United States Environmental Protection Agency (EPA), is set to 0.5 ng/L. (56)

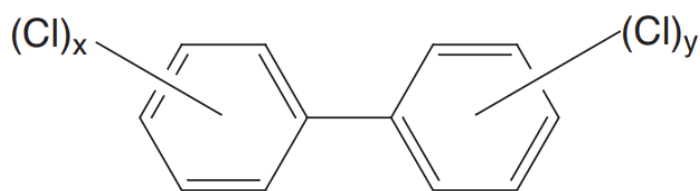


Fig. 6: Polychlorinated biphenyls (number of chlorine atoms $[x + y] = 1-10$)

2.3.2. Dioxins

Dioxins are highly toxic and environmentally persistent compounds, accumulating in the food chain, mainly in the fatty tissue of animals. Term dioxins is often used for the family of structurally and chemically related polychlorinated dibenzo-para-dioxins and polychlorinated dibenzofurans (Fig. 7). They are a byproduct of manufacturing processes including chlorine bleaching of paper pulp and the manufacturing of some herbicides and pesticides. Human exposure is mainly through food - meat and dairy products, fish and shellfish. List of effects on human health include reproductive and developmental problems, immune system damage, interference with hormones and cancer. (8) (12)

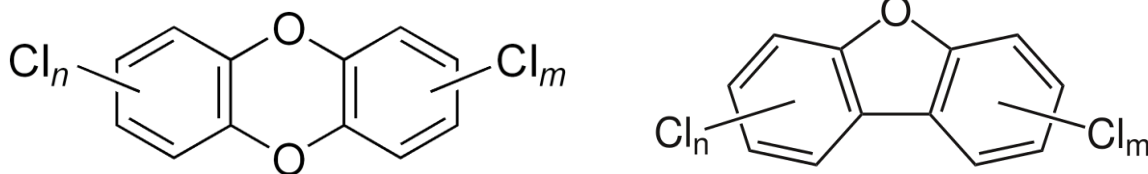


Fig. 7: Polychlorinated dibenzo-p-dioxins and Polychlorinated dibenzofurans respectively

2.3.3. Phytoestrogens

Family of plant hormones, similar to natural human estrogens. They are suspected to act as endocrine disruptors. Exposure occurs mainly through food - mainly tofu, soymilk, and other soy products. Intake has the potential to cause adverse health effects, particularly when exposure occurs during development. Consumption by infants is of increased concern because their brain and reproductive system are undergoing sexual differentiation and maturation. Structural and functional alterations in the developing reproductive tract were reported. (11)

2.3.4. Pesticides

Pesticides are group of substances or mixtures of substances that are used to kill pests, including insects, rodents, fungi and unwanted plants. They protect plants from pests, weeds or diseases, and humans from vector-borne diseases, such as malaria or dengue fever. Pesticides can be found in a variety of everyday foods and beverages. Safe limits were set by EPA and other organizations, but the limits underestimate the real health risk of simultaneous synergic exposure to two or more chemicals in real-life conditions. Countless negative health effects that have been associated with pesticides include dermatological, gastrointestinal, neurological, carcinogenic, respiratory, reproductive, and endocrine effects, mentioned by Nicolopoulou-Stamati et al. (10)

2.3.5. Phthalates

Another group of man-made chemicals primarily used as plasticizers in the manufacture of flexible plastics which are used in everyday consumer products (flooring, food covers, parenteral medical devices etc.), including cosmetics and pharmaceuticals (perfumes, lotions etc.) (Fig. 8). Human exposure is widespread and occurs through ingestion, inhalation, and dermal contact. Phthalates were reported to alter sexual differentiation and cause worsening of semen quality. (5)

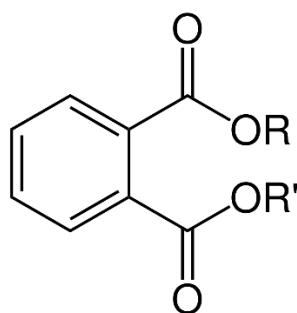


Fig. 8: Chemical structure of orthophthalates. (*R* and *R'* are general placeholders)

2.4. Bioluminescent bioreporters

This part briefly describes used bioreporter organisms. *Pseudomonas putida* TVA8 is in the main focus of this thesis. Other tested and potential microorganisms, suitable for the detection of pollutants, are also mentioned.

2.4.1. *Pseudomonas putida* TVA8

Pseudomonas putida is characterized as a gram negative, aerobic, non-sporeforming, oxidase positive bacteria with one or more flagella. It has the shape of rod and size of about 2 μm (Fig. 9). It is ubiquitous bacteria that can be found in soil and water. Ideal growth temperature of the bacteria is about 25 °C. *P. putida* species are regarded as non-pathogenic bacteria, however few cases of *P. putida* infections were found in immunocompromised patients who came in contact with contaminated commercial anti-fog solution. (57)

Strains as for example *P. putida* F1 are capable of metabolizing aromatic hydrocarbons such as toluene, benzene, and ethylbenzene, utilizing them as a sole source of carbon. This ability makes the bacteria suitable as a remedy for contaminated soil (where it is usually found) or as a transducer in sensors and detectors of contamination of human environment. Genetically engineered strain *P. putida* TVA8, derived from the F1 strain, produces bioluminescence when metabolizing toluene and similar compounds. Taking all these facts in consideration *P. putida* TVA8 was chosen as the bioreporter organism for the researched biosensor. The strain was also used in other studies at our institution, thus it was one of the main goals of this study to immobilize the TVA8 strain on bare OFE in the form of biofilm. (58) (59)

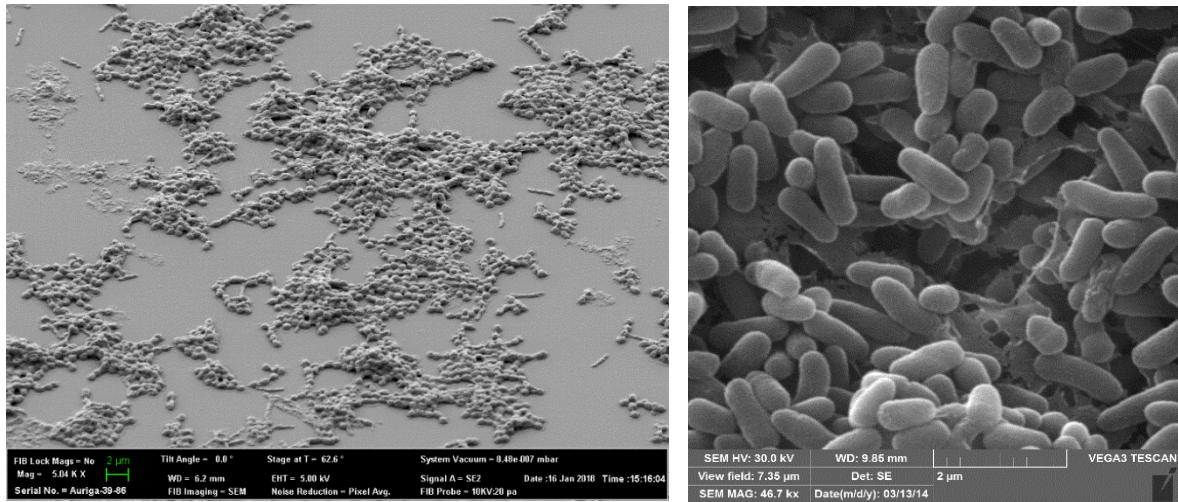


Fig. 9: *P. putida* TVA8, SEM image

“In *P. putida* F1 the toluene is degraded by enzyme system composed of four protein components encoded by the genes identified as *todA*, *todB*, *todC1*, and *todC2*. These proteins create the enzyme called toluene dioxygenase. This enzyme acts by incorporating two atoms of molecular oxygen into the aromatic toluene ring to give cis-toluene dihydrodiol. This compound is further broken down by sequential action of the protein products of *todD*, *todE* and *todF*. The *tod* genes, arranged in *tod* operon, are induced coordinately by toluene.” (60) (61)

For the use in biosensors it is necessary to quantify the analyte concentration by the gene expression. From about 30 chemically independent bioluminescence genes of different organisms, emitting light of different wavelengths from one to the other end of visible spectrum, bioluminescence *lux* genes from bacterium *Vibrio fischeri* were chosen and inserted into the *tod* operon of *P. putida* F1. “The *lux* cassette of genes contains *lux CDABE* genes. *LuxAB* encodes the luciferase enzyme responsible for bioluminescence. Luciferase converts an aldehyde group to a carboxyl group with the use of molecular oxygen (substrate oxygenation). This process regenerates a fatty acid, and it is the aldehyde that provides the substrate for light production (Fig. 10). The *luxC* encodes for the reductase, *luxD* for the transferase and *luxE* for the synthetase enzymes. Together these genes *luxCDE* encode the fatty acid reductase enzyme complex. This *lux* gene cassette is then fused to the promoter for the degradation genes so that the *lux* genes are transcribed simultaneously with the degradation genes upon induction. The result is the production of light when the operon

of choice is induced. If the whole *lux* cassette of *CDABE* is used, no substrate needs to be added because the substrate, aldehyde, is produced by the enzymes encoded by the *lux CDE* genes. These constructs can be made with any inducible catabolic gene system. “ (60) (61)

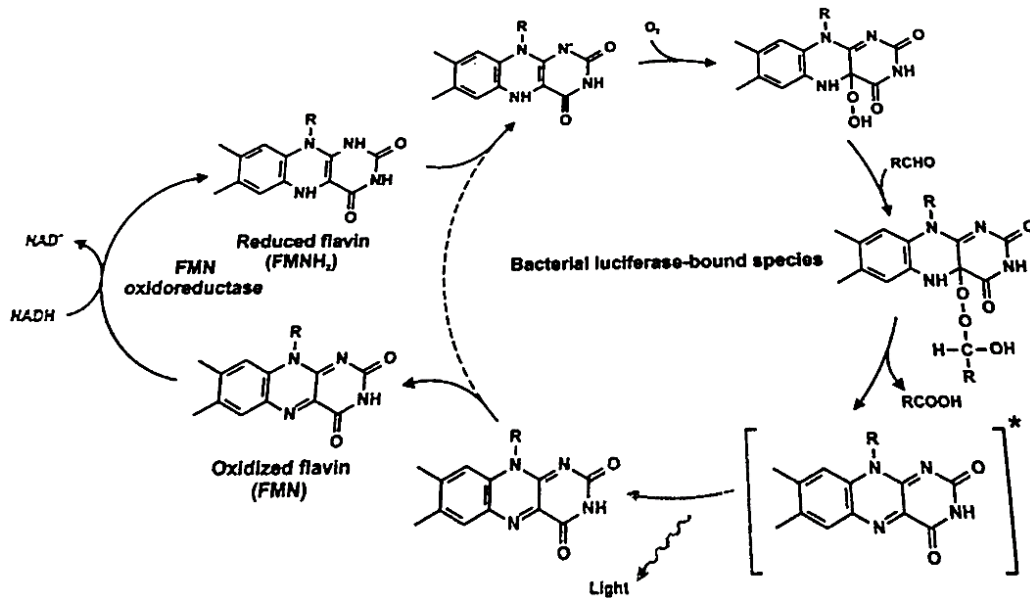


Fig. 10: Bacterial luciferase luminescence reaction (60)

P. Putida TVA8 is a genetically modified strain, tailored to produce bioluminescence in the presence of aromatic hydrocarbons (e.g. BTEX contaminants). It was constructed by introducing the *tod-luxCDABE* fusion directly into the chromosome of *P. putida* F1 strain by a constructed transposon. According to the research of Applegate et al. (1998) the insertion of the genes is stable and has no negative effect on cell growth. Cell growth in Minimal Salt Medium (MSM) with added toluene showed the ability of TVA8 strain to utilize toluene as a sole carbon source. Fig. 11 shows bioluminescence spectrum of *P. putida* TVA8 (luciferase) with maximum at about 500 nm (Fig. 11). (60)

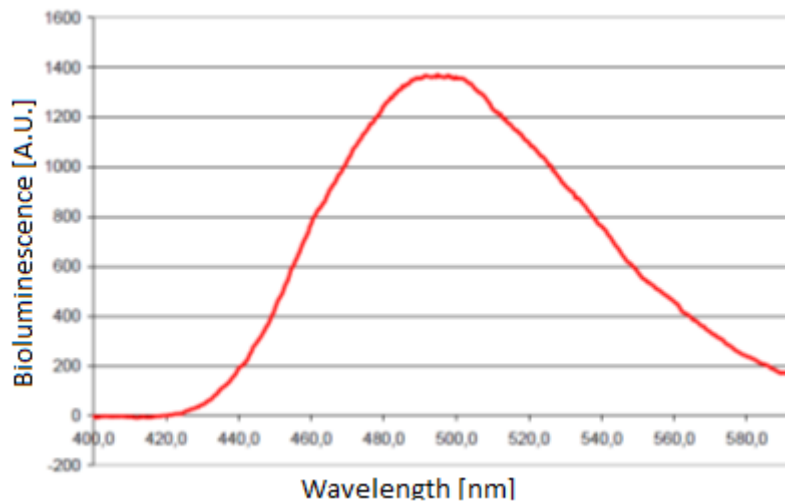


Fig. 11: *Bioluminescence spectrum of P. putida* TVA8 (*luciferase*)

Applegate et al. (1998) determined the toluene detection limit of free cells in MSM to 30 $\mu\text{g/l}$ and measured light responses to other chemicals such as benzene, xylenes, phenol, JP-4. Kuncová et al. (2011) tested the response of TVA8 strain to other chemicals listed in the Table 3. The responses show the advantage of sensing various environmental pollutants, nevertheless the authors also don't suggest the TVA8 for selective detection of BTEX. Quorum sensing could play a role in production of bioluminescence. Kuncová et al. (2011) determined the optimal temperature of 25 °C, and the cell concentration of 10^8 cfu/mL for high and fast toluene induced bioluminescence. (60) (62)

Table 3: Bioluminescence maxima produced with free *Pseudomonas putida* TVA8 induced with the thousand times diluted saturated solution (10 μ L of the saturated solution in 10 mL of MSM) containing 10^8 cell/mL at 25 °C. The compounds are lined up from the highest to the lowest bioluminescence maximum. (WP) (62)

Compound	Solubility* (g/L)	Bioluminescence	
		AU of 10^{-3} satur. sol.	AU/mol
Ethylbenzene	0.161	18,706,000	12,327,370
Toluene	0.53	5,630,000	978,345
Phenol	83.0	5,300,000	6009
Benzene	1.78	2,590,000	113,640
4-Ethyltoluene	0.095	2,380,000	3,011,326
4-Fluortoluene	1.24*	1,390,000	124,540
Cumene	0.05	998,000	2,399,192
Isobutylbenzene	0.01	954,000	12,675,921
Styrene	0.25	487,000	202,787
Trichlorethylene (TCE)	1.28	315,000	32,337
o-Xylene	0.175	247,000	149,753
p-Xylene	0.198	198,000	106,100
o-Cresol	31.0	196,000	683
m-Xylene	0.135	175,000	137,537
2-Methylnaphthalene	0.03	39,400	186,756
Benzylchloride	0.49	33,200	8578
Naphthalene	0.03	18,600	79,484
Salicylic acid	2.0	6660	460
Hexachlorobenzene	0.005	6220	354,291
2-Chloronaphthalene	0.1	5300	8618
Biphenyl	0.004	3060	117,963
2-Bromnaphthalene	0.005*	2800	124,540
1,3,5-Triethylbenzene	0.004	1690	50,785
Negative control	-	1200	-

The bioluminescent reporter *P. putida* TVA8 was first constructed at the University of Tennessee in Knoxville. For the purpose of this study the TVA8 strain was kindly donated by the center of Environmental Biotechnology, UTK. First part of this study was conducted at the Institute of Chemical Processes, CAS. The TVA8 strain was also available for experiments at UTK.

2.4.2. *Escherichia coli* 652T7

E. coli is characterized as a gram negative, facultatively anaerobic, coliform bacteria with a shape of rod and size of about 2 μ m. It is considered as one of the most diverse bacterial species, about 190 serogroups are described to the present day. Ideal grow temperature of the bacteria is about 37 °C. It has circular chromosome with the size of about 4.5-5.5 Mbp, often carrying plasmids encoding a pathogen. *E. coli* is a normal part of human bacterial flora in guts, but some pathogenic strains could cause mild or severe diseases such as gastroenteritis or urinary tract infections. (63)

E. coli's 652T7 genome contains a plasmid-based phage lambda T7 promoter fusion to the *P. luminescens luxCDABE* gene cassette. Genes encode luciferase enzyme together with

necessary aldehyde substrate for its function. This bioreporter bacterium produces bioluminescence constitutively at 500 nm. (64)

The strain was used in the studies of Wen-Juan Shi et al. (2014) and Liyu Du et al. (2015) as a control of toxicity of mercury, C60 and cellulose nanocrystals. The toxicity was expressed as inhibition of bioluminescence relative to control samples. The 652T7 strain was picked as one of suitable candidates for immobilization on bare OFE in this study. (64) (65)

2.4.3. *Pseudomonas fluorescens* HK44

P. fluorescens is characterized as a gram negative, rod-shaped bacterium, obligatory aerobic, oxidase positive bacteria with multiple flagella. It has size of about 2 μm (Fig. 12). It is ubiquitous bacteria that can be found in soil and water. Ideal grow temperature of the bacteria is about 27 °C but its permissive growth range is from 4 - 35 °C. *P. fluorescens* species are regarded as non-pathogenic bacteria, however cases of *P. putida* infections were reported in immunocompromised patients who received contaminated heparinized saline flushes. (66) (67)

P. fluorescens HK44 is derived from *P. fluorescens* 18H. Strain HK44 was engineered to contain a naphthalene catabolic plasmid, pUTK21, mutagenized by transposon insertion of the *luxCDABE* (bioluminescent) gene cassette. Genes encode luciferase enzyme together with necessary aldehyde substrate for its function (bioluminescence at 500 nm). Due to the naphthalene catabolic pathway carried on pUTK21, strain HK44 degrades a number of two- and three-ring polyaromatic hydrocarbons (PAHs) and produces bioluminescent light in response to naphthalene, salicylate, or 4-methyl salicylate. (68)

The *P. fluorescens* HK44 was released in the field as the first genetically engineered microorganism to monitor bioremediation potential by Ripp et al. (2000). It was also used as active part of whole-cell biosensor by Kalabova et al. (2018). It was picked as one of suitable candidates for immobilization on bare OFE in this study. (29) (69)

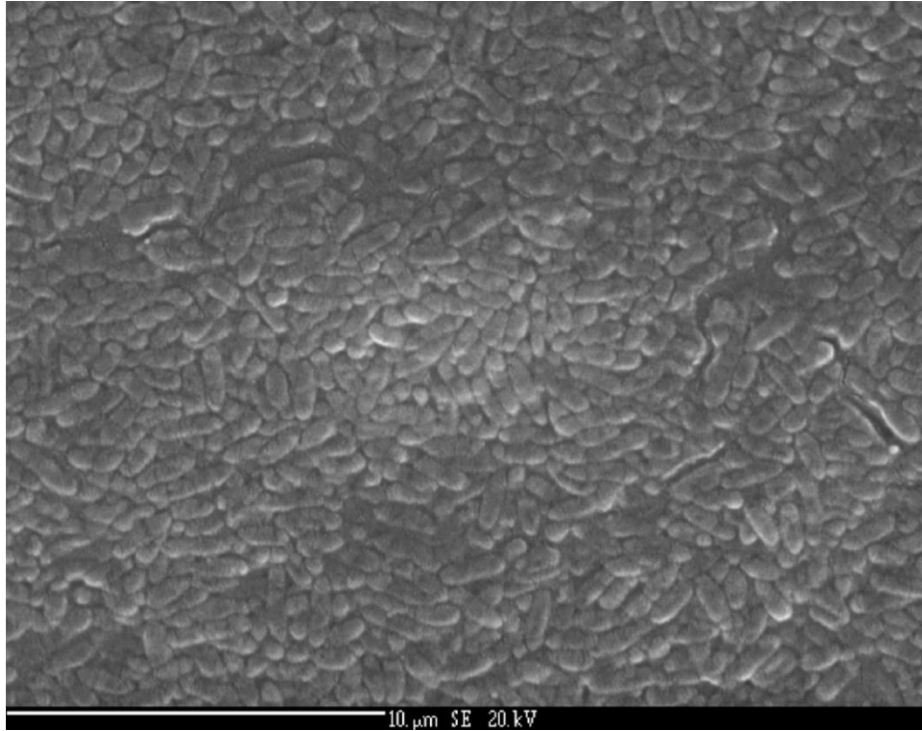


Fig. 12: *P. fluorescens* HK44 biofilm on silica glass, SEM image (WP) (69)

2.4.4. *Saccharomyces cerevisiae* BLYR

Saccharomyces are unicellular and saprotrophic fungi, unable to use nitrate and able to ferment carbohydrates. They divide asymmetrically by process known as budding. Their colonies grow rapidly and mature within 3 days. Genus *Saccharomyces* includes several species which are commonly isolated from mammals, birds, trees, plants, and soil. Pneumonia, endocarditis, liver abscess, and sepsis have been reported in immunocompromised patients. *Saccharomyces cerevisiae* is a round yeast with size of about 5-10 μm (Fig. 13). It is widely used in food industry and also the most studied eukaryotic model organism. (70)

Saccharomyces cerevisiae BLYR strain, used in this study, was created by inserting pUTK401 and pUTK404 plasmids into *S. cerevisiae*, which already contained human AR (hAR) gene in its chromosome. Plasmids encode luciferase enzyme together with necessary aldehyde substrate for its function. Constitutive bioluminescent reporter for monitoring of toxicity of chemicals was then created (bioluminescence at 540 nm). The full procedure is described by Eldridge et al. (2007), who also used the strain for the detection of androgens and estrogens associated toxicity. (71)

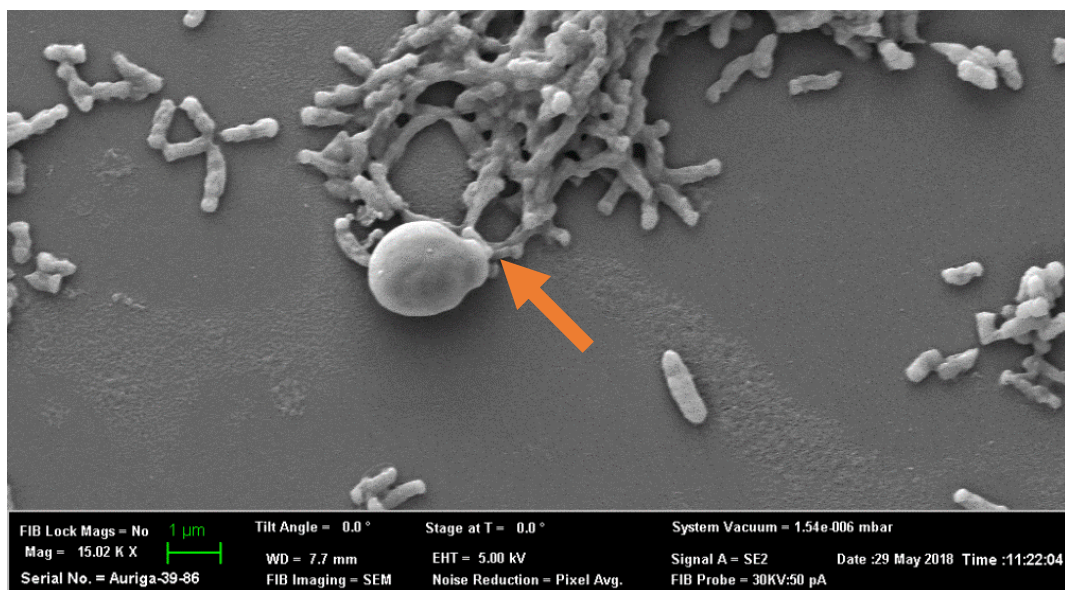


Fig. 13: *Saccharomyces cerevisiae* BLYR cell, SEM image

2.4.5. Currently used and applied bioreporters

Zhaohui Xu et al. (2003) developed a whole-cell bioassay for the detection of bioavailable BTEX. This bioassay is an example of a biosensing that employ free microbial cells with an indicator. Authors used “genetically engineered *E. coli* strain expressing toluene dioxygenase (TDO) and toluene dihydrodiol dehydrogenase (TodD), enabling the conversion of BTEX into their respective catechols, which were quickly converted into colored products by a horseradish peroxidase (HRP). The intensity of the color formation was correlated to concentrations of the BTEX compounds. The bioassay was selective toward BTEX-related compounds with no interference observed with commonly used pesticides, herbicides, and organic solvent. The bioassay was stable for over 10 weeks.” (72)

Free cells are not suitable for all applications. In many studies authors try to immobilize cells in an organic or inorganic matrix. As an example could be mentioned the work of Polyak et al. (2001) who used genetically modified strain *Escherichia coli* which produce bioluminescence in the presence of genotoxic agents. Modified strain was alginate-immobilized onto an exposed core of an optical fiber (Fig. 14). The performance of this whole-cell FOS system was examined as a function of parameters such as gel probe matrix volume, bacterial cell density, and numerical aperture of the fiber core or working temperature. Authors used a model genotoxicant mitomycin C. (52)

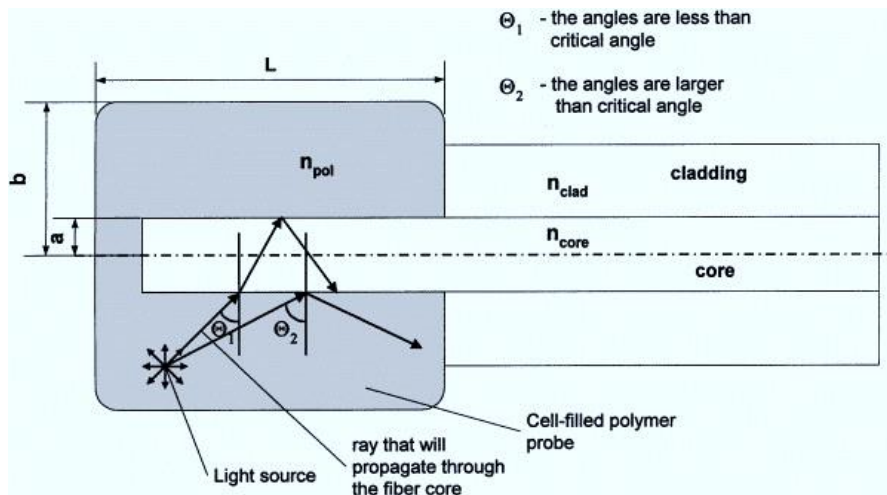


Fig. 14: Optical ray paths of a single bacterial cell enclosed in a calcium alginate matrix, taken as a single radiating light source. L =length of optical fiber tip, a =radius of the fiber core, b =radius of the polymer probe, n_{pol} =refractive index of the polymer probe, n_{clad} =refractive index of the cladding, n_{core} =refractive index of the fiber core. (52)

Optimal response was achieved with six alginate/bacterial layers on 1 cm exposed fiber-optic core (volume 100 μl , containing suspension of $1.5\text{--}3.0 \times 10^7$ cells). When the core diameter was etched down from 400 μm to 270 μm , photon detection efficiency significantly increased due to compensation of normalized frequency V of active part of fiber and used optical fiber. Optrode response was dose-dependent for at least 6 h, with a lower detection limit of 25 $\mu\text{g/l}$. (52)

The works of Ishizaki T. (73) or Kalábová H. (23) (74) could be mentioned as another example. The authors used an inorganic matrix (Tetramethyl orthosilicate (TMOS), waterglass-ludox mixture as precursors) to immobilize cells onto the OFE. In the demonstration experiments authors used bacteria *Pseudomonas fluorescens* HK44 selective to presence of salicylic acid and naphthalene. Microorganisms were immobilized in the active layers. The measured intensity of bioluminescence using the OFE was six times higher as compared to PCS fiber (600 μm), which was in agreement with the result of mathematical modeling. The applicability of biosensing was demonstrated by detection of BTEX with *Pseudomonas putida* TVA8 in twelve samples of the wastewater in laboratory conditions." Nevertheless, the viability of cells within such a layer was low and the layer itself created another dispersion environment between the immobilized cells and FOE. In addition, the TMOS layer had the maximal lifespan of about 6 weeks. (23)

3. Experimental part

The main task was to construct an active part of fiber optic sensor using tapered optical fiber element connected to a photcounter and genetically modified organism *P. putida* TVA8. First the surface properties of silica glass and available microorganisms were characterized. Fiber element was then chemically treated to ameliorate microorganism adhesion. The bioluminescent microorganism was then immobilized onto the face of the fiber element in form of biofilm-like layer. The sensor was tested for about 135 days using a solution containing toluene. The sensor was also tested using a real polluted water sample from a water purification plant. In the second set of experiments, repeatability of sensor was assessed and best OFE shape was described.

Devices and workplace from the two following institutions were used for all the experiments: Institute of Chemical Process Fundamentals of the Czech Academy of Sciences in Prague (ICP); and the Center for Environmental Biotechnology at the University of Tennessee in Knoxville (UTK).

All chemicals used in this study were commercial products of high quality, purchased from www.sigmaaldrich.com (Merck) and www.fishersci.com.

All used devices and work procedures are described in this chapter.

3.1. Used devices and software

a. pH meters - Fisherbrand accumet AB15; and Thermo Russel RL150

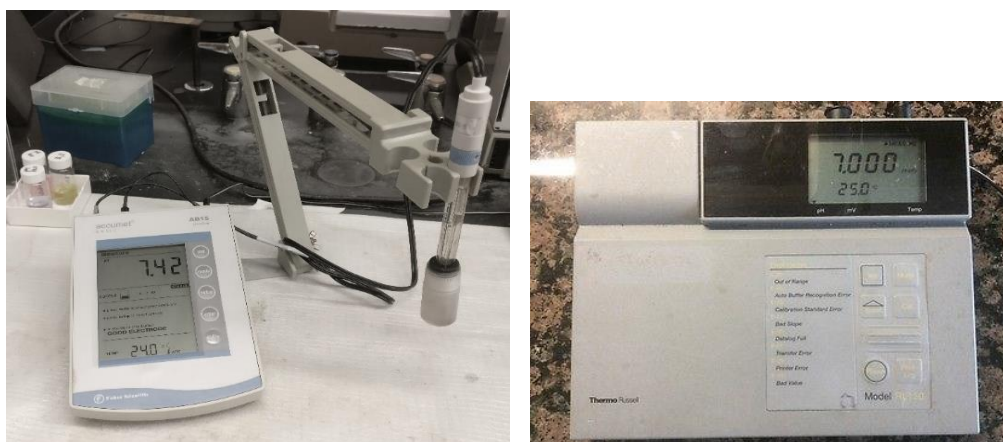


Fig. 15: AB15 pH meter with probe (left, UTK); and RL150 pH meter (right, ICP)

AB15 pH meter includes main unit, pH glass probe, and power source. The device is characterized by pH range of -1.99 to 19.99, resolution of 0.01 pH unit, and accuracy of ± 0.01 pH unit. It has two-point manual calibration. The glass pH probe involves both indication and reference electrodes. The indication electrode is a glass pH electrode. The reference electrode is a saturated silver chloride electrode.

RL150 pH meter includes a main unit, pH glass probe, and power source. The device is characterized by a range of pH from -2 to 20, resolution of 0.001 pH unit, and accuracy of ± 0.002 pH unit. It has two-point manual calibration. The glass pH probe involves both indication and reference electrodes. The indication electrode is a glass pH electrode. The reference electrode is a saturated silver chloride electrode.

b. Fridges - Liebherr GRT21G1HC (ICP); and TSG Glass Door TSG12RPGA (UTK)

Refrigerating systems allowed to set temperatures from -2 to 16 °C and 2 to 10 °C respectively. Systems were suitable for keeping microbial cultures, sterile media, and other chemicals. (Images not available)

c. Sterilizers - Getinge 700LS-E Steam Series; and Autoclave Chirana PS121 V/I



Fig. 16: 700LS-E Steam sterilizer (UTK)

The 700LS-E (UTK) and Chirana PS121 (ICP, image not available) feature programs for gravity and pre-vacuum cycles from 110 °C to 135 °C for hard goods and from 104 °C to 135 °C for liquids.

d. Laboratory Balances - TR-104; and APX-602, Denver Instrument Company, USA

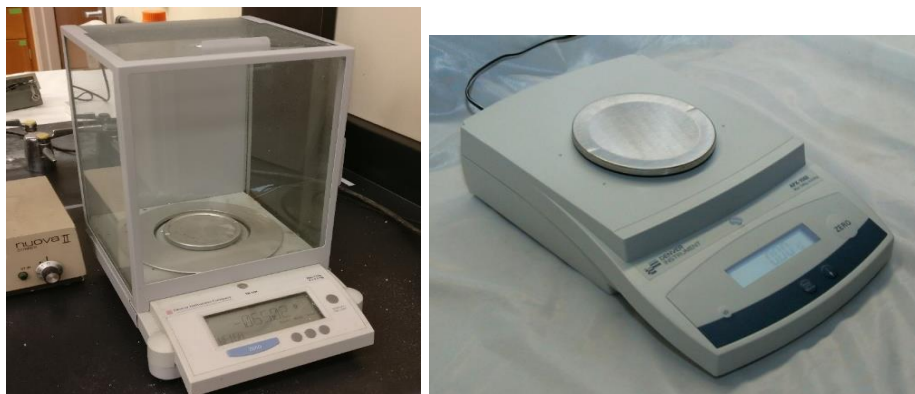


Fig. 17: TR-104 balances (left, UTK); APX-602 balances (right, ICP)

The TR-104 balances have a readability of 0.0001 g, repeatability of 0.1 mg, linearity of 0.2 mg, weighing Range of 110 g, and stabilization time of 10 s. The APX-602 balances have a readability of 0.01 g, repeatability of 0.01 mg, linearity of 0.2 g, weighing Range of 600 g, and stabilization time of 5 s.

e. Environmental Shakers - LabLine 3597 Orbital; PsycroTherm Controlable Shaker



Fig. 18: Lab-Line 3597 shaker (left, UTK); PsycroTherm shaker (right, UTK)

Both shakers allow the temperature to be set between 0 °C - 60 °C with ± 0.3 °C control at 37 °C. Shaking speed is adjustable between 0 and 400 rpm. Both devices have uniformly moving platform in 1-inch orbit, and a stable rack.

f. Horizontal shaker - Unimax 1010DT, Heidolph (ICP)



Fig. 19: Shaker - Unimax 1010DT, Heidolph (ICP)

Shaker has maximum load capacity of 5 kg; shaking orbit of 10 mm; variable speed from 30 to 500 rpm; digital process timer up to 999 min with acoustic alarm.

g. Laminar flow box HH1.2 Basis, Helta-Holten AIS, Denmark



Fig. 20: Laminar flow box HH1.2 Basis, Helta-Holten AIS (ICP)

HH1.2 flow box allows to adjust air flow velocity and has filter replacement indicator.
(UTK flow box info unavailable)

h. Ovens - Thelco Precision Scientific Co Model 17; and Memmert UM300



Fig. 21: Thelco 17 oven (left, UTK); Memmert UM300 oven (right, ICP)

Temperature in both ovens could be set up to 200 °C, temperature was controlled either on the device display (ICP) or by inserting a glass thermometer (UTK).

i. Ultrasonic cleaner PS04000A



Fig. 22: Ultrasonic cleaner PS04000A (ICP; UTK)

The cleaner has ultrasonic power of 100 W at operating frequency of 35 kHz. Its heating power is 180 W. The thermostat could be set up to 77 °C.

j. Detection System Oriel 7070 with photomultiplier tube Oriel 70680



Fig. 23: Oriel 7070 detection system with photomultiplier tube Oriel 70680 (UTK)

Photomultiplier device allows measurements to be made over the range of 200 nm to 1.1 μm . It has adjustable power supply from 0 to 900 V, suitable for exciting photodiode sensors and photomultiplier tubes. Operating temperature is 14 - 40°C. Accuracy at 27 °C is $\pm 0.1\%$ (± 0.001 digital). Linearity of response is 0.05 %. Gain drift is 0.07 %/°C.

k. Photon counting module - MP-984-RS Perkin Elmer



Fig. 24: MP-984-RS Perkin Elmer photon counting module (ICP)

The module is designed for applications in all fields of single photon detection. It excels with high dynamic range of the installed CPM and exceptional low noise in comparison to similar devices. Measurements could be made over the range of 200 to 670 nm.

l. Magnetic stirrer - Variomag Multipoint 6/15 stirrer



Fig. 25: Variomag Multipoint 6/15 magnetic stirrer (ICP, UTK)

The stirring speed is adjustable from 80 to 2000 rpm for volumes up to 3 L. It has 15 stirring points for multiple containers.

m. CAM 200 goniometer - KSV Instruments, Finland

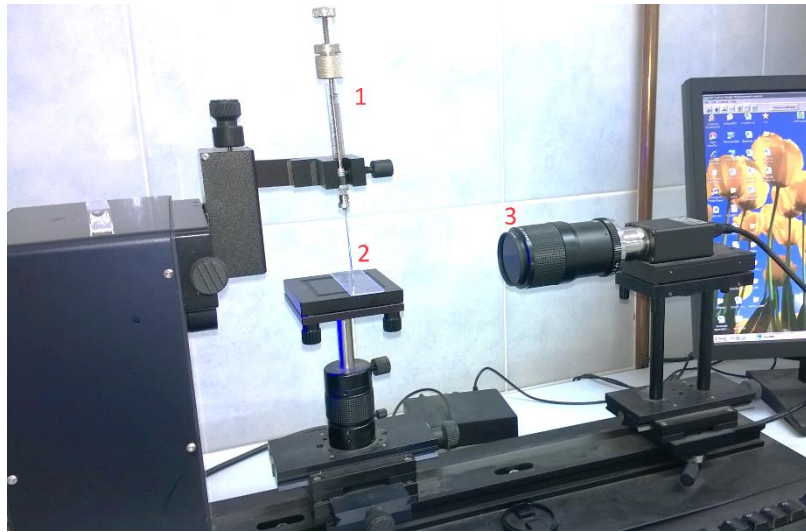


Fig. 26: CAM 200 goniometer (UCHT); 1 – test liquid dispenser; 2 – tested sample; 3 - camera

Three test liquids (water, formamide, 1-bromnaphthalene) are used for hydrophobicity measurements.

n. luminometer Berthold FB12 - Berthold Detection System GmbH



Fig. 27: Luminometer Berthold FB12

The device can fit 35mm culture dishes or 20 ml vials. It has photon counting detector PMT with the spectral range of 300 – 600 nm. Sensitivity is described as better than 1000 molecules of firefly luciferase.

o. Centrifuge - Hettich Universal 32R; and ThermoScientific Sorvall Legend XTR



Fig. 28: Centrifuge Universal 32R (left, ICP, WP); Sorvall Legend XTR (right, UTK)

Universal 32R accommodates standard tubes up to a volume of 100 ml, microtiter plates, Falcon tubes, blood collection systems and cyto accessories. Microlitre/microcentrifuge tubes can be accelerated to a max RCF of 23907.

Legend XTR Centrifuge accommodates up to 40 x 50mL conical tubes, 196 blood tubes or 24 microplates. It controls temperature in the range from -10 to 40 °C. Maximal acceleration reaches RCF of 25314 x G; and maximal speed of 15200 rpm.

p. Vortex Mixers - Velp ZX3 Advanced and Baxter SP



Fig. 29: Velp ZX3 advanced vortex mixer (left, ICP, WP), and Baxter SP vortex mixer (right, UTK)

Mixers has adjustable stirring speed up to 3000 rpm, with touch or continuous mode.

q. SEM - Zeiss Auriga; and Tescan VEGA3



Fig. 30: Zeiss Auriga scanning electron microscope (left, UTK); Tescan VEGA3 scanning electron microscope (right, ICP)

Focused ion beam-scanning electron microscope Auriga is a multi-approach instrument to investigate sample at nanoscale resolution. Specifications of Cobra Zeiss column: resolution of less than 2.5 nm at 30 kV. Magnification range: 300 x - 500 kx. Probe current 1 pA - 50 nA. Acceleration voltage: 1 - 30 kV. Emitter: Ga liquid metal ion source.

The VEGA3 is a high-performance analytical SEM capable of operating in both high-vacuum and low-vacuum modes. It has a LaB6 filament with best resolution of 2 nm at 30 kV in high-vacuum mode; 185-850 nm panchromatic CL detector; and high-count rate silicon drift EDS system.

r. SPI Module Sputter Coater - SPI



Fig. 31: SPI module sputter coater (UTK)

“Etch” and “Sputter” modes deposit conductive coatings onto SEM samples, with a common power/vacuum control base unit. It features fast coating (up to 200Å gold in 20 seconds), with water cooling for sensitive samples. Chamber size - 12.7 x 10.2 cm.

s. In-Vivo imaging system - IVIS Lumina K series III - Perkin Elmer

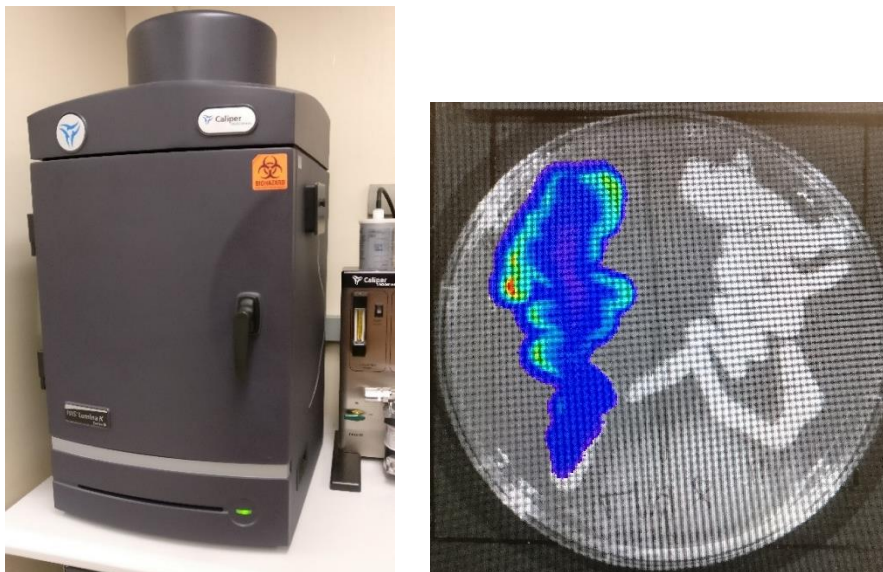


Fig. 32: IVIS Lumina K series III, Perkin Elmer, In-vivo imaging System

The device is capable of imaging both fluorescent and bioluminescent reporters. The system is equipped with up to 26 filter sets that can be used to image reporters that emit from green to near infrared (415-875 nm). Its chamber could be heated from 20 to 40 °C. It has grade 1 CCD camera with 1024 x 1024 imaging pixels; size of 1.3x1.3 cm; and the resolution of 50 microns; cooled to -90 °C.

t. Electrokinetic Analyzer - SurPASS - Anton Paar, Austria



Fig. 33: SurPASS analyzer

SurPASS instrument is capable of routine surface analysis featuring fully automated zeta potential measurements of macroscopic solids at real-life conditions.

The device has streaming potential of $\pm 2000 \text{ mV} \pm (0.2 \% + 4 \mu\text{V})$; Streaming current of $\pm 2 \text{ mA} \pm (0.2 \% + 1 \text{ pA})$; Cell resistance $5 - 20 \text{ M}\Omega \pm (2 \% + 0.5 \Omega)$; Pressure measurement of $1200 \text{ mbar} \pm (0.2 \% + 0.5 \text{ mbar})$; Conductivity of $0.1 - 1000 \text{ mS/m}$; at pH range between 2 – 12; at temperatures between 20 - 40 °C.

3.2. Used media and solutions

a. Luria-Bertani (LB)

Liquid LB medium consisted of NaCl 10 gL⁻¹; Tryptone 10 gL⁻¹; Yeast extract 5 gL⁻¹ in distilled water. For solid medium 17 gL⁻¹ of Agar was added.

Declared amount of chemicals was measured on balances and dissolved in 1 L of distilled water. The medium was divided by 50 ml into 250 ml-Erlenmeyer flasks and sterilized. Solid LB medium was divided by about 20 ml into Petri dishes.

For selective growth **LB_{kan}** medium, kanamycin (filtered using 0.2 µm nitrocellulose filter) was supplemented to the sterilized medium, chilled to about 50 °C, to the final concentration of 50 mgL⁻¹.

For selective growth **LB_{tet}** medium, tetracycline (filtered using 0.2 µm nitrocellulose filter) was supplemented to the sterilized medium, chilled to about 50 °C, to the final concentration of 40 mgL⁻¹.

b. Yeast minimal medium (YMM)

Liquid medium contained yeast synthetic drop-out supplement Y1771 1.46 gL⁻¹; yeast nitrogen base without amino acids 6,7 gL⁻¹ in distilled water. For solid medium 20 gL⁻¹ of agar was added. After sterilization of the medium, chilled to about 50 °C, sterile glucose solution (20%, filtered using 0.2 µm nitrocellulose filter) was added to the final concentration of 2 %.

c. Phosphate buffer (PB)

Buffer contained Na₂HPO₄ · 12H₂O 23.637 gL⁻¹ and KH₂PO₄ 8.98 gL⁻¹ in distilled water. Buffer was then adjusted to pH 7.2 ± 0.2 using 1M NaOH or 1M HCl.

d. Trace element solution

Solution was prepared by the dissolution of H_3BO_3 0.062 g in 1L of 1M HCl and the addition of CaCl_2 2.94 gL^{-1} ; $\text{ZnSO}_4 \cdot 7\text{H}_2\text{O}$ 1.44 gL^{-1} ; $\text{CuSO}_4 \cdot 5\text{H}_2\text{O}$ 0.39 gL^{-1} ; $\text{Na}_2\text{MoO}_4 \cdot 2\text{H}_2\text{O}$ 0.53 gL^{-1} ; $\text{MnSO}_4 \cdot \text{H}_2\text{O}$ 3.5 gL^{-1} ; $\text{FeCl}_3 \cdot 6\text{H}_2\text{O}$ 5.4 gL^{-1} previously dissolved in 1 L of distilled water.

e. Mineral salt medium (MSM)

Medium consisted of $\text{MgSO}_4 \cdot 7\text{H}_2\text{O}$ 0.2 gL^{-1} , NH_4NO_3 0.2 gL^{-1} , trace element solution 0.1 mL, ferric chloride solution 0.1 mL, PB 100 mL and distilled water 900 mL. Ferric chloride solution was filtered using 0.2 μm nitrocellulose filter and added to the final sterile MSM.

f. Piranha solution

Solution contained concentrated H_2SO_4 and 30% H_2O_2 in volume ratio 7:3. Solutions were slowly mixed in a beaker which was cooled with ice.

g. Induction solutions

Toluene induction solution was prepared by mixing 19 ml of MSM and 1 ml of toluene-saturated water (toluene dissolvability - 530 mg/l at 25 °C). The final concentration of toluene was 26.5 mgL^{-1} ; pH 7.2.

LB induction solution contained 75 % of MSM and 25 % of LB medium.

YMM induction solution contained 90 % of MSM and 10 % of YMM.

h. Contaminated ground water sample Aqua43

The Aqua43 sample of ground water contaminated with BTEX was taken from a location in the Czech Republic. The chemical composition of Aqua43 (sample RW6A-43) was analyzed in the certificated laboratory AQUATEST a.s. Liberec, Czech Republic (see analysis in the supplement 5.4.). Contents of the individual BTEX: benzene 0.26 mgL^{-1} , toluene 172 mgL^{-1} , ethylbenzene 7.82 mgL^{-1} and xylene 20 mgL^{-1} .

3.3. Sterilization and disinfection

Every workplace surface was wiped with 98% ethanol. Inoculation wires, tubes and flasks with media were treated with flame during laboratory works.

OFE was cleaned and sterilized in piranha solution and washed in 98% ethanol.

Laboratory glass (tubes, flasks, beakers, pipette tips, cuvettes) were sterilized for 20 min at 120 °C and 0.1 – 1.15 MPa.

All chemicals and media were sterilized for 20 min at 120 °C and 0.1 – 0.15 MPa. Sterilization-sensitive media and chemicals were filter-sterilized using nitrocellulose 0.2µm or polyvinylidene fluoride 0.2µm filter.

Used GMO cultures were sterilized for 50 min at 120 °C and 0.1 - 0.15 MPa and disposed in drain.

3.4. Growing bioreporter organisms

***P. putida* TVA8** culture (initial culture with sterile glycerol 1:1) inoculated from frozen -80°C stock into 100 mL of LB medium supplemented with kanamycin. It was cultivated to stationary phase for about 16 h at 80 rpm and 28 °C to an optical density, measured at $\lambda = 600$ nm, OD₆₀₀ = 0.3 – 0.15.

***S. cerevisiae* BLYR** was inoculated from frozen -80°C stock into 20 ml of YMM medium, cultivated in shaker overnight at 28°C and 30 rpm.

***E. coli* 652T7** culture was inoculated from frozen -80°C stock into 100 mL of LB medium supplemented with kanamycin. It was cultivated for 12 h while shaking (80 rpm) at 35 °C to an optical density, measured at $\lambda = 600$ nm, OD₆₀₀ \approx 0.5.

***P. fluorescens* HK44** culture (initial culture with sterile glycerol 1:1) was inoculated from several different frozen -80°C stocks onto solid LB medium supplemented with tetracycline. The culture did not respond to naphthalene or methyl salicylate induction, bioluminescence was only induced by a temperature change. This pointed out a problem with the stock cultures (loss of plasmid or a mutation). No further stock cultures were available, *P. fluorescens* HK44 was excluded from further experiments.

3.5. Tapered optical fiber element

The tapered optical fiber element (OFE) is a residue of melted quartz preform of optical quality (pure SiO₂) from the production of polymer-cladded silica fibers (PCS). The narrowing part between the dripped part and the fiber was used as an OFE (Fig. 34). The OFE shape is determined by the drawing weight and temperature. (75)

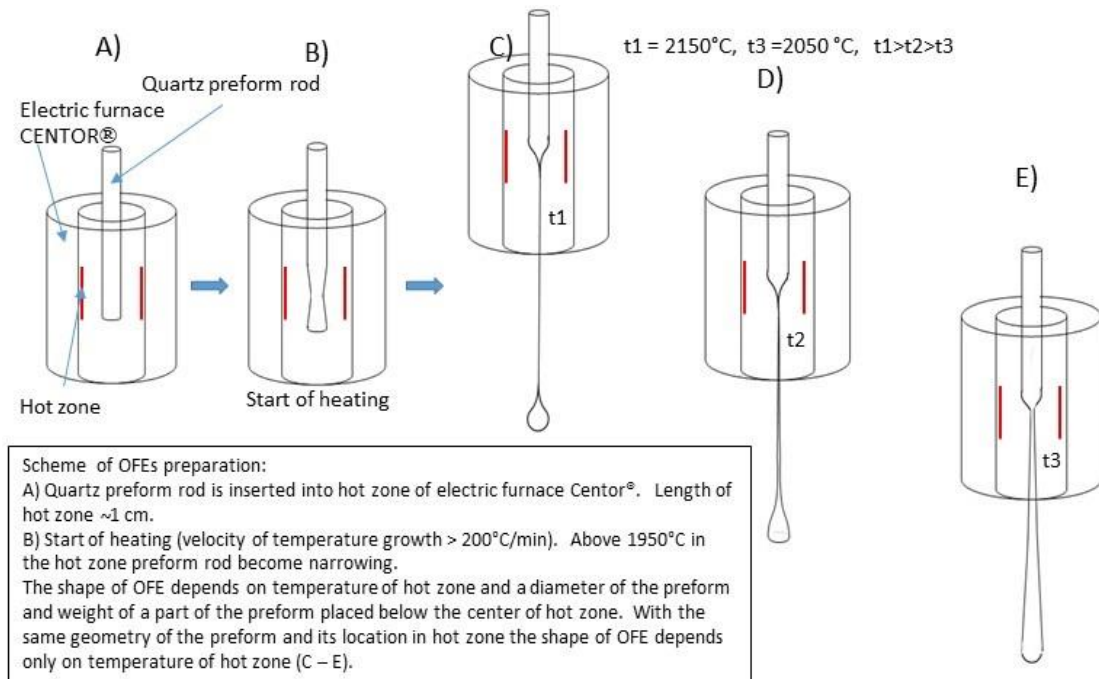


Fig. 34: Scheme of OFEs preparation with description

It was designed to amplify a week bioluminescent signal by increasing the number of light sources (cells) on its face. The ends of OFE were polished to optical quality of $\lambda/2$. The element is characterized by diameters (Dx; from Dmin to Dmax) measured in 10 mm distances along its length (L=Zmax) (Fig. 35). For the purpose of software calculations (transmittance) the available OFE shapes were approximated by a polynomic bi-exponential equation (“Exp2”) in Matlab software (Table 4; in agreement with Kalabova et al. (2018)). (75)

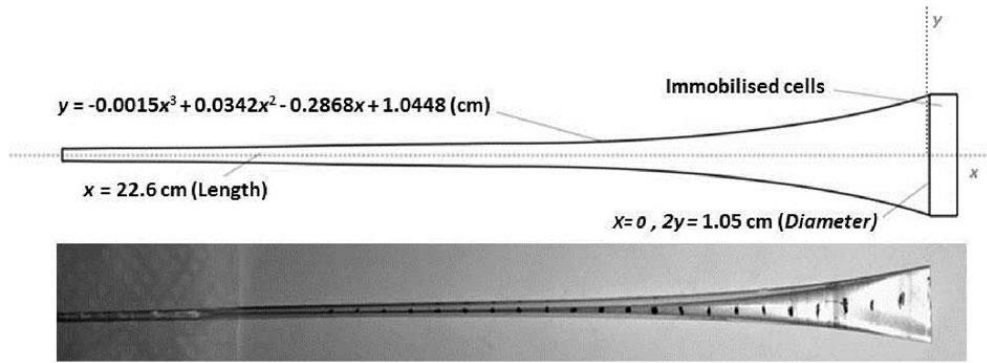


Fig. 35: Tapered optical fiber element "0" with marks for measurement of diameters.

Kalabova et al (2018) successfully compared the model simulations to the real bioluminescence measurements and highlighted one available OFE with best transmittance. One of the aims of this study is to determine the most suitable OFE available for this study and further determine the best geometrical OFE parameters in general. (75)

Elements listed in the Table 4 were used during the experiments at ICP (0) and UTK (A; B1; B2; C; D) - Figs. 35-36.

Table 4: OFEs approximation by bi-exponential equation $y = y_0 + A1 \cdot \exp(-x/t1) + A2 \cdot \exp(-x/t2)$. Equation parameters (A1, t1, A2, t2, $y_0 = 0$), and OFE diameters (Length, Dmax, Dmin).

OFE	Dmax (mm)	Dmin (mm)	Length (mm)	A1	t1	A2	t2
0	10.5	1.6	226	0.906	2.769	0.153	79.177
A	4.97	0.84	328.5	3.093	52.826	1.730	429.369
B1	4.1	0.73	424	3.117	69.541	0.984	1501.727
B2	4.1	0.89	268	3.259	73.314	0.832	12963.443
C	3.04	0.5	532.5	1.789	55.036	1.289	554.939
D	4.85	1.13	208.8	1.606	29.886	3.197	186.254

Elements were kindly donated from the Institute of Photonics and Electronics, Academy of Sciences of the Czech Republic, v.v.i.

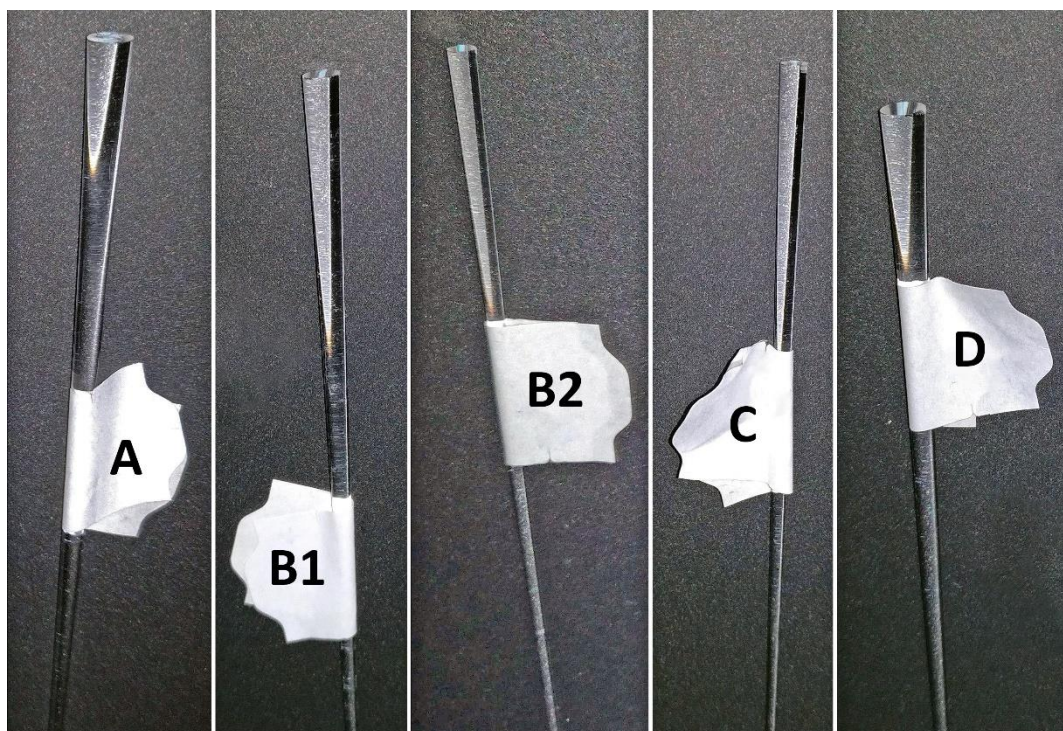


Fig. 36: Tapered OFEs available for experiments at UTK

3.5.1. Measurement of surface contact angles and zeta potentials

With the aim of proposing a surface modification of the quartz glass (Suprasil®) to ameliorate cell adsorption, the zeta potentials and contact angles of both the cells and the quartz glass were measured. The surface properties of the *P. putida* TVA8 cells, in the form of algal layers on membranes filters, and the APTES-modified quartz were characterized by contact angles (CA). Bacterial cells were deposited on a filter (nitrate cellulose membrane, 0.45 μm pore size, 47 mm diameter, Whatman Sigma–Aldrich, USA) under negative pressure. The microbial lawns thus obtained were then deposited on agar plates to stabilize the moisture content, then were fixed on a microscopic glass slide and allowed to dry for 30 min. The CA measurements of both the algal lawns and silica glass slides were performed by the sessile drop technique (volume of $\approx 3 \mu\text{L}$) using a CAM 200 goniometer (KSV Instruments, Finland). The measurements were performed at 25 °C with three test liquids (water, formamide, 1-bromnaphthalene), readings were taken after 0.5 s of deposition, and each sample was tested ten times. The total surface tension and its components, and the values of the free energy of interaction between cells and carrier in water were calculated in accordance with van Oss et al. (2006). (76)

The zeta potential (ZP) of the bacteria was measured using a Zetasizer Nano-ZS (Malvern, UK) in LB medium at pH 7. The surface charge of APTES-modified quartz was determined in an adjustable gap cell on SurPASS (Anton Paar, Austria) in contact with 170 mM KCl (ionic strength of LB medium) at pH 7. For the zeta potential determination, a streaming current approach and the Helmholtz–Smoluchowski equation were used. (46)

3.6. Surface modification of the OFE

(3-Aminopropyl)triethoxysilane (APTES) - Surface modification had the purpose of increasing surface charge of the OFE, so the cells would more likely adhere to its surface and create a biofilm-like layer. OFE was first washed with detergent and rinsed with deionized water. OFE was then immersed in a piranha solution at 70 °C for 30 min, washed in deionized water and dried at 110 °C for about 1 h. The OFE was then immersed in a mixed solution of (3-Aminopropyl)triethoxysilane (APTES) (5 mass %) in dry toluene at ambient temperature for about 24 h. Lastly the element was rinsed with toluene and acetone and dried at 110 °C for about 1 h.

Polyethylenimine (PEI) – This was an alternative modification technique which was tested when the APTES modification was not sufficient. OFE was first washed with detergent and rinsed with deionized water. OFE was then immersed in a piranha solution at 70 °C for 30 min, washed in deionized water and dried at 110 °C for about 1 h. After drying, the OFE was immersed in 0.2% solution of PEI in deionized water for 30 min, and then air-dried.

3.7. Cell adsorption on the modified OFE

***P. putida* TVA8** - The modified end of the OFE was fixed vertically in a flask filled with 150 mL of LB containing kanamycin (10 gL⁻¹) and overnight culture of *P. putida* TVA8 (1 mL). The cells were left to grow and adsorb on the element end in the shaker for 4 days, at 25 rpm and at 28 °C. Previous experiments proved this is the minimal time needed for *P. putida* TVA8 cells to be adsorbed.

***E. coli* 625T7** - Growth of *E. coli* 652T7 on the APTES modified OFE surface was inadequate. Addition of FeCl₃ to the growth medium with OFE in the final concentration of 150 μM, which was reported to ameliorate adhesion of cells by decreasing the separation distance, was unsuccessfully tested. The PEI modified surface was attempted as an alternative. A 20 mL aliquot of an overnight culture of *E. coli* 652T7 in 150 ml LB_{kan} medium was centrifuged at 3000 g for 5 min. The pellet was resuspended in 20 mL MSM and centrifuged again at 3000 g for 5 min. The pellet was then resuspended in 20 mL of 0.2% PEI in MSM and left in a shaker for 30 min at 100 rpm and 28 °C. Finally, the culture was centrifuged at 3000 g for 5 min and the pellet resuspended in 20 mL of MSM. The wider end of the PEI modified OFE was then immersed in the 20 mL suspension of *E. coli* 652T7 and shaken at 50 rpm for 30 min and 28 °C. (77) (78)

***S. cerevisiae* BLYR** - Growth of *S. cerevisiae* BLYR on the APTES modified OFE surface was inadequate. Addition of FeCl₃ to the growth medium with OFE in the final concentration of 150 μM was unsuccessfully tested. The PEI modified surface was attempted as an alternative. A 20 mL aliquot of an overnight culture of *S. cerevisiae* BLYR in 50 ml YMM medium was centrifuged at 3000 g for 5 min. The pellet was resuspended in 20 mL MSM and centrifuged again at 3000 g for 5 min. The pellet was then resuspended in 20 mL of 0.2% PEI in MSM and left in a shaker for 30 min at 100 rpm and 28 °C. Finally, the culture was centrifuged at 3000 g for 5 min and the pellet resuspended in 20 mL of MSM. The wider end of the PEI modified OFE or cone was then immersed in the 20 mL suspension of *S. cerevisiae* BLYR and shaken at 50 rpm for 30 min and 28 °C.

3.8. Measurement of induced bioluminescence

The thinner end of the OFE was connected to a light guiding tube or directly to a photon counter placed in a light-tight box, which minimized noise background in the measured signal (Fig. 37). The wider end with adsorbed cells was fixed 4 ± 1 mm from the bottom of a 50 mL glass beaker, filled with 10 mL of induction solution (Figs. 37-38). Reflective aluminum foil was placed underneath the beaker. The wide face of the OFE was pointing down to prevent a sediment formation (Fig. 38). Every day, the end of the OFE was gently washed with MSM using a pipette and re-immersed in a fresh induction solution. The exceptions were the

1–4 day pauses for weekends and holidays when the element was immersed in the induction solution for more than 24 h.

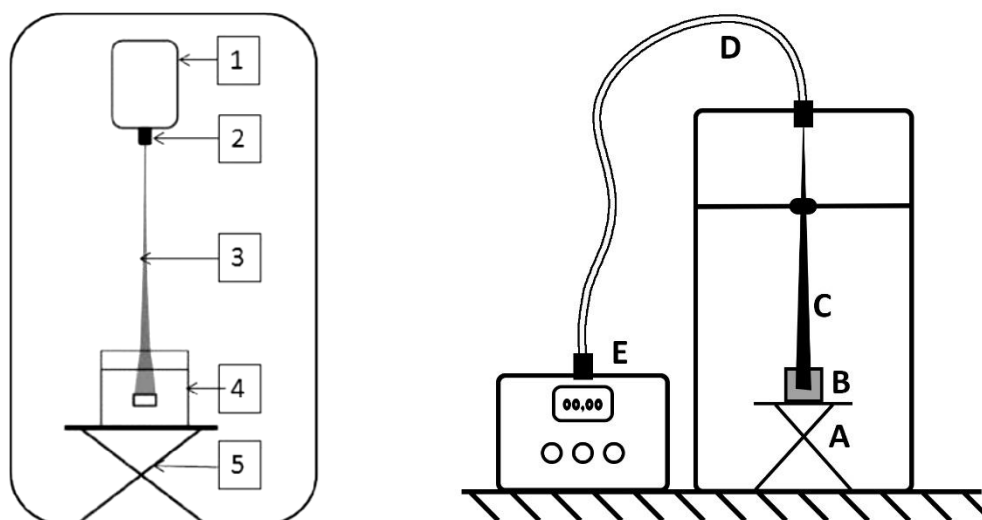


Fig. 37: Experimental set-ups for monitoring bioluminescence, used at ICP (left) (2) and at UTK (right), 1,E-photon counter; 2,SMA connector; D-light guiding cable; 3,C-OFE; 4,B-induction solution; A,5-stand

Intensity of the bioluminescence measured with Perkin-Elmer photon counter at ICP was recorded continuously for about 18 h (10 s integration times). Temperature in the measurement box varied between 25 °C and 29 °C. Due to high noise, the raw data were smoothed in OriginPro software.

Bioluminescence measured with Oriel 7070 measurement system at UTK was recorded with a web camera and values were registered manually every 20-60 min. Accelerating voltage of the photon multiplier tube was set to 850 V and the generated current was then read from the Oriel 7070 detection system in nano-Amperes (nA). Standard laboratory temperature was measured to be 21 °C.

The cells adsorbed on the element “0” were induced by “Aqua43” (polluted water sample, containing BTEX) on days 69, 70 and on day 71 by immersion in “Aqua43” diluted with PB (vol. ratio 9:1). On day 78 the biorecognition layer of the element was induced with LB medium and on day 135 by LB medium with kanamycin and 26.5 mg/l toluene.



Fig. 38: OFE immersed in the induction solution. Setup was placed in a light-tight box

3.9. Scanning electron microscope visualization

SEM was used to verify the attachment of *P. putida* TVA8 to its APTES modified OFE. Since the OFEs themselves could not be processed for SEM imaging, quartz cones were used as an alternative (Fig. 39). Quartz cones were surface modified with APTES and *P. putida* TVA8 cells were immobilized as explained above. Surface modified quartz cones with adhered cells were placed in a 50 mL beaker containing 30 mL of toluene induction solution. Bioluminescent signaling by the cells was verified by taking light measurements in a Perkin-Elmer IVIS Lumina K imaging system. After two days of immersion, SEM imaging was performed. The quartz cones with immobilized cells were fixed in McDowell–Trump Fixative (Fischer Scientific), gold coated (SPI Module Sputter Coater), and then viewed in a Zeiss Auriga SEM. Samples of biofilm grown for 2 days and 130 days were compared.



Fig. 39: Quartz cones

4. Results and discussion

4.1. Tapered optical fiber element

The OFE was designed to amplify a weak bioluminescent signal by increasing the number of light sources (bioreporter cells) on its face. The shape of OFE contributes to the amount of bioluminescence transmitted from the bioreporters to a detector. Mathematical model was developed by Kalabova et al. (2018) with the aim to optimize OFE parameters and maximize its light transmittance (T), which represents the fraction of light transmitted through an OFE to a detector. The amount of transmitted light is represented by the OFE efficiency, which can be calculated as a product of transmittance and number of $1\mu\text{m}$ cells which could be fit on wider end of an OFE. Because this concept of OFE efficiency is dependent on the size of a certain microorganism strain, author of this thesis proposed a more generalized model. Author used OFE face area, instead of the cell count, to calculate planar OFE efficiency (equation C). This concept allows to compare OFE efficiencies without considering different immobilized microorganisms or even other biological sensing elements in general (i.e. bacteria and yeast; or bacteria and enzymes). Note that this concept doesn't account bioluminescence intensity produced by a microorganism strain. (75)

$$E = T * A \quad (C)$$

Where E is OFE efficiency, T is OFE transmittance and A is area of wider end of an OFE.

The model suggested that the best place to immobilize light sources is on the very surface of the OFE face. Bioreporters immobilized in a matrix are separated by a small distance from the OFE (Kalabova et al. (2018) immobilized bioreporters in 2-3 mm thick silica gel), thus it is advantageous to immobilize the bioreporters in a form of biofilm-like layer on the glass surface. Bioreporters immobilized on the OFE side wall does not significantly contribute to the detected signal (<1 %) due to the laws of geometrical optics as described by Pospíšilová et al. (2015). (18)

Using the previously developed software (75), T was calculated for several theoretical OFE geometries with the same length, D_{min} , and D_{max} (Fig. 40, left). Increasing T (Fig. 40, right) of OFE shapes from the most curved to nearly linear confirmed the assumption that the best shape of an OFE is a frustum cone. The limits to this construction

are the numerical aperture of an OFE (refractive index of OFE material and refractive index of cladding material or air), aperture of a sensor or diameter of an optical fiber to which is the OFE connected (maximal output diameter), and maximum possible length that would maximize the size of the OFE face and thus the number of light sources. Kalabova et al. (2018) compared two different OFE geometries and conditions under which they were produced. Nevertheless, the provided information doesn't suggest the ideal drawing parameters, thus further experiments are needed (75).

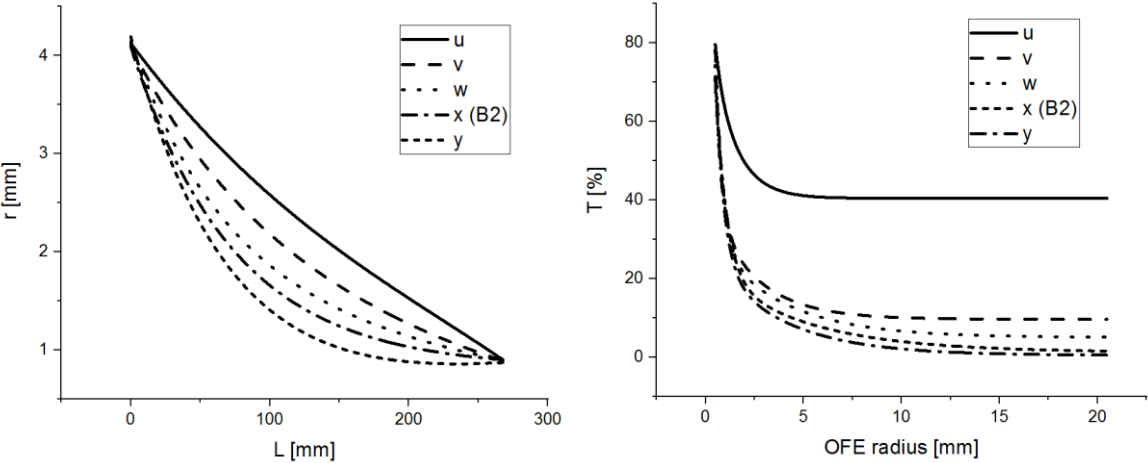


Fig. 40: Geometrical shape of theoretical OFEs (u, v, w, x, y) with identical D_{min} and D_{max} , but different bends (left), OFE “ x ” is identical to OFE “B2” used in the experiments (left); calculated Transmittance vs. OFE radius for each theoretical OFE (right).

Table 5 compares calculated transmittance, cell number and OFE efficiency of five available OFEs. The theoretical number of cells on the face of each OFE was determined based on the assumption that the cells are spheres with 1 μm diameter, organized in one layer on the surface of an OFE face (75). OFE efficiency was calculated as a product of the cell number and the OFE transmittance (18).

Table 5: Calculated transmittance, cell number and OFE efficiency

OFE	Transmittance [%]	OFE face area [mm ²]	Number of cells	OFE efficiency *10 ⁵	OFE efficiency planar [mm ²]
A	1.41	19.4	2.47×10^7	3.48	0.27354
B1	1.62	13.2	1.68×10^7	2.72	0.21384
B2	2.21	13.2	1.68×10^7	3.71	0.29172
C	1.51	7.26	0.92×10^7	1.39	0.10963
D	5.00	18.47	2.35×10^7	11.75	0.92350

4.2. OFE surface characterization - contact angles and zeta potential

Table 6: Zeta potential of tested samples

Material	Zeta Potential [mV]
Quartz	-21±2
APTES quartz	-3±0.4
<i>P. putida</i> TVA8	-15.6±0.6

Table 7: Contact angles of tested samples for 3 different liquids

Material	Water [°]	Formamide [°]	1-Bromonaphthalene [°]
Quartz	24.6±1.1	19.1±0.8	33.8±2.2
APTES quartz	71.8±2.5	63.2±1.7	30.3±1.6
<i>P. putida</i> TVA8	28.9±0.6	41.2±0.8	45.5±1.4

In the thermodynamic approach to microbial adhesion, the adhesion between solid surfaces in water are energetically favorable when $\Delta G_{TOT} < 0$ and unfavorable when $\Delta G_{TOT} > 0$. The thermodynamic approach does not include the role of long-range electrostatic interactions, hence it is only valid at close contact (Bos et al., 1999). An unfavorable (positive) total adhesion energy balance (Table 6-7) was obtained for both bacteria–water–quartz (33.3 mJ m⁻²) and bacteria–water–APTES quartz (13.5 mJ m⁻²) systems. This conflicts with the *P. putida* TVA8 cell adsorption observed onto APTES quartz. (45)

Since the thermodynamic model was not able to predict the adhesion of the bioreporter cells onto the APTES quartz, the extended DLVO (XDLVO) theory was used subsequently. This combines the conventional non-covalent Lifshitz–van der Waals (LW) and electrostatic (EL) interactions with the Lewis acid–base (AB) interactions (van Oss, 2008). Given the rod-shaped cells, the simulations in accordance with the XDLVO theory were made for the cylinder-flat plate interactions (Adamczyk, 2006), the Hamaker constant (van Oss, 2006) was estimated from the ΔG_{LW} value (Table 6-7) and the characteristic decay length of 0.6 nm for AB interactions in water was used (Bos et al., 1999). The profile of total interaction free energy (G_{TOT}) vs. the separation distance predicted favorable energy balances

for adhesion of the *P. putida* TVA8 bioreporter cells to the APTES quartz with a total absence of potential energy barriers (Fig. 41). This XDLVO model prediction supports the experimental observations of rapid bioreporter cell adsorption onto APTES quartz. At the same time, the XDLVO model prediction for *P. putida* TVA8 adhesion to unmodified quartz is characterized by the presence of a high energy barrier (6911 kT at 0.5 nm; Fig. 41). In the frame of the colloidal interaction model (XDLVO), this energetically unfavorable barrier prevents close contact between the bacteria and the quartz surface. This model prediction was confirmed by the absence of *P. putida* TVA8 adhesion to unmodified quartz. (46) (79) (76) (45)

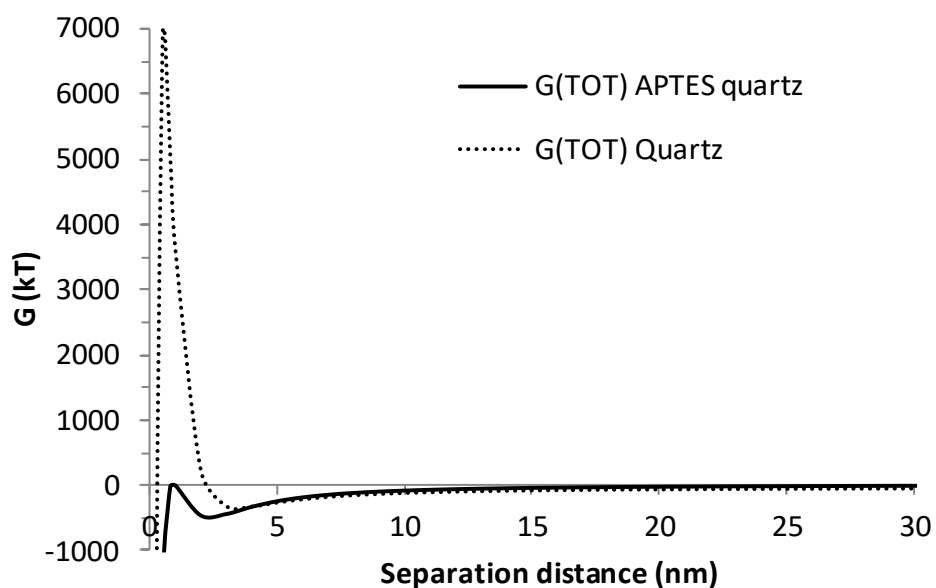


Fig. 41: Total free energy of interaction (G_{TOT}) as function of separation distance between bacteria *P. putida* TVA8 and surface of either quartz or APTES modified quartz as calculated according to XDLVO theory.

It was experimentally proven, that the *P. putida* TVA8 does not spontaneously adhere onto unmodified quartz surface. The measured Zeta potential of the unmodified glass and reporter cells has a negative surface charge. To support the cell adhesion to the bare OFE, the quartz surface was modified by APTES, which added aminopropyl functional groups to its surface. This increased the original charge from -21 mV to -3 mV. *P. putida* TVA8 cells were than more-likely to get closer to the quartz surface and colonize it. The modification also led to increased surface hydrophobicity, as can be seen from the contact angle values before and after the modification.

4.3. Repeated immobilization of bioreporters and their visualization in SEM

By measuring surface charges and zeta potentials of used microorganism, authors previously showed that the surface modification with APTES will lead to increase of quartz surface hydrophobicity and enhanced adsorption of *P. putida* TVA8. The same approach was used to immobilize strain 652T7.

OFE modification with APTES leads to successful formation of TVA8 biofilm layer on its surface. Nevertheless, this approach was unsuccessful with the 652T7 strain. Visible TVA8 biofilm developed on all five available OFEs. Two days after beginning of the bioluminescence inductions, lumps of cell colonies (100-1000 μm apart) between much smaller scattered clusters or single cells were observed on the glass surface under SEM, which corresponds to standard biofilm establishment characteristics (Kokare et al., 2009). The cell layer kept developing until it covered the entire OFE face surface, as it could be seen from the SEM sample that was visualized after 130 days of repeated inductions (Fig 42). (47)

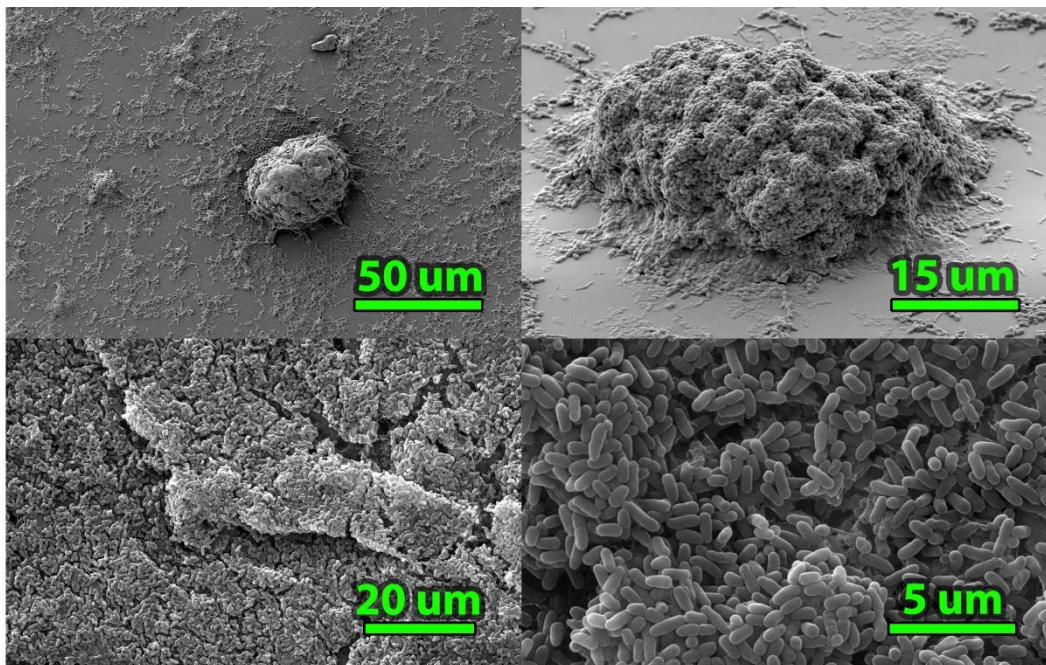


Fig. 42: *P. Putida* TVA8 biofilm-like layer, island colonies and scattered cells across OFE surface, 2 days after initial immobilization (top). *P. Putida* TVA8 biofilm layer, covered surface, 130 days after initial immobilization (bottom). (4)

4.4. Time records of induced bioluminescence - ICP

Time-records of daily inductions of bioluminescence of *P. putida* TVA8 immobilized on OFE "0" are shown in Figs. 43-46. Y-axis denotes detected bioluminescence intensity in cps integrated over 10 s (denoted as A.U.). X-axis denotes time from the induction of bioluminescence in hours. The experiment lasted 135 days. Chart legends denote the measurement day number.

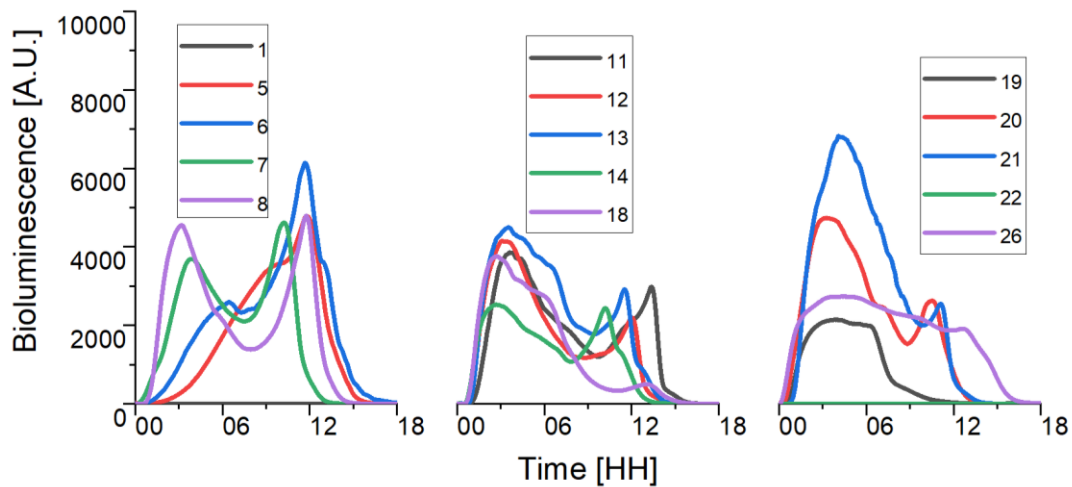


Fig. 43: OFE – 0 - X axis: time (HH); Y axis: bioluminescence (A.U.), legend shows day number

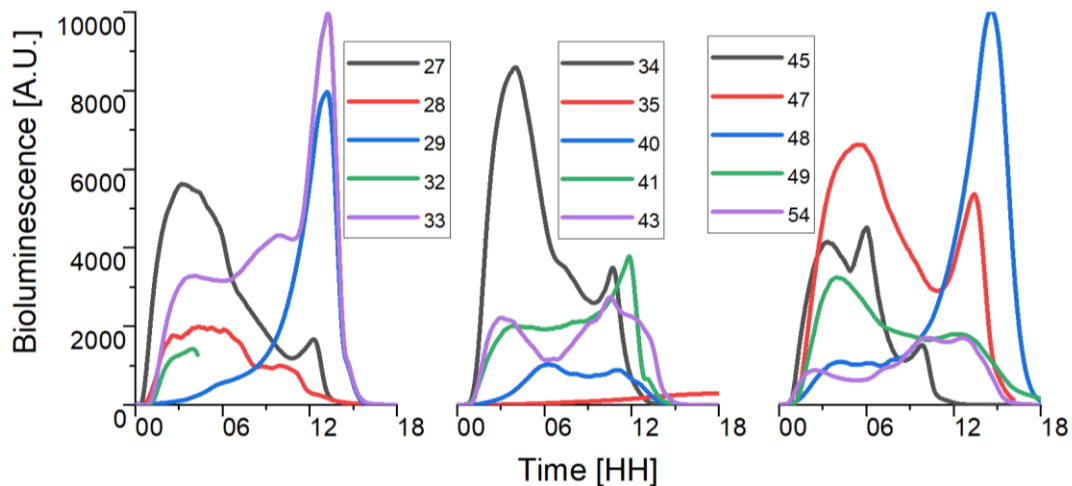


Fig. 44: OFE – 0 - X axis: time (HH); Y axis: bioluminescence (A.U.), legend shows day number

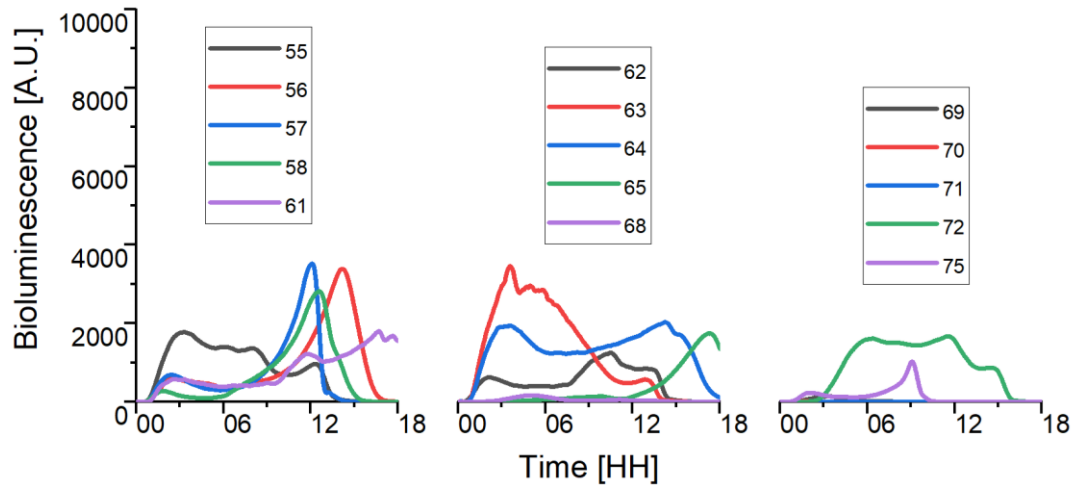


Fig. 45: OFE – 0 - X axis: time (HH); Y axis: bioluminescence (A.U.), legend shows day number

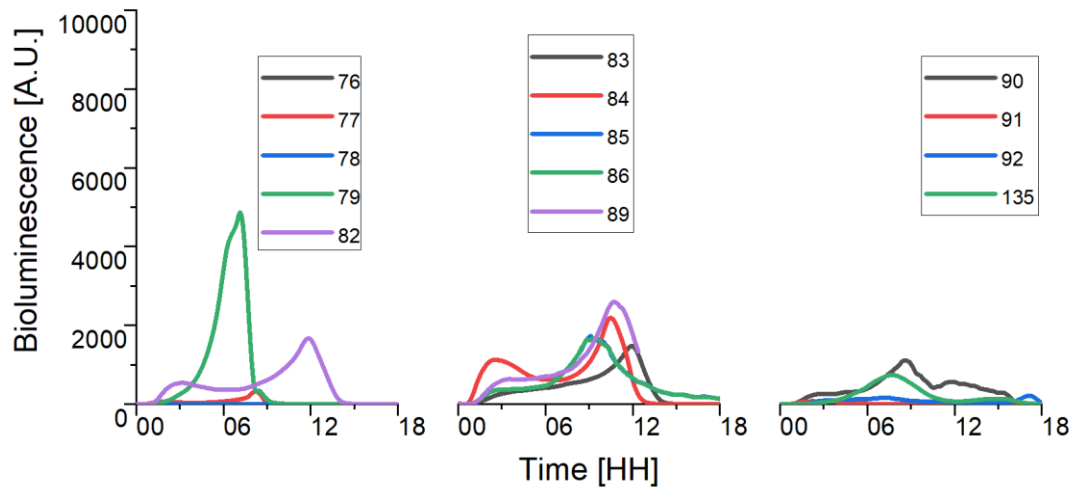


Fig. 46: OFE – 0 - X axis: time (HH); Y axis: bioluminescence (A.U.), legend shows day number

4.5. Time records of induced bioluminescence - UTK

Time-records of daily inductions of bioluminescence of *P. putida* TVA8 immobilized on each of the five available OFEs (A, B1, B2, C, D) are shown in Figs. 47-51. Background noise of 0.26 nA was subtracted from the measured data. Y-axis denotes detected bioluminescence intensity in nA at 850 V. X-axis denotes time from the induction of bioluminescence in hours. Each experiment lasted 15–19 days (A 10x, B1 14x, B2 16x, C 15x, D 14x). Chart legends denote the measurement day number.

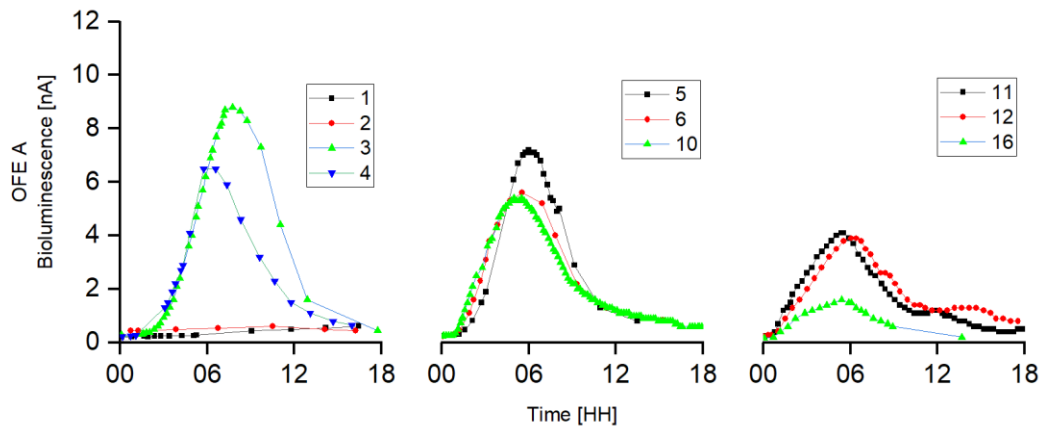


Fig. 47: OFE-A – Time-records of daily inductions of bioluminescence

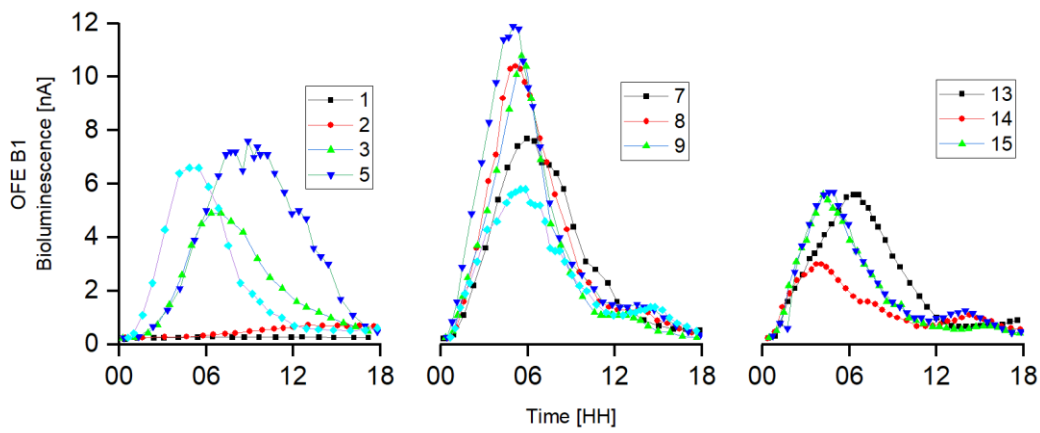


Fig. 48: OFE-B1 – Time-records of daily inductions of bioluminescence

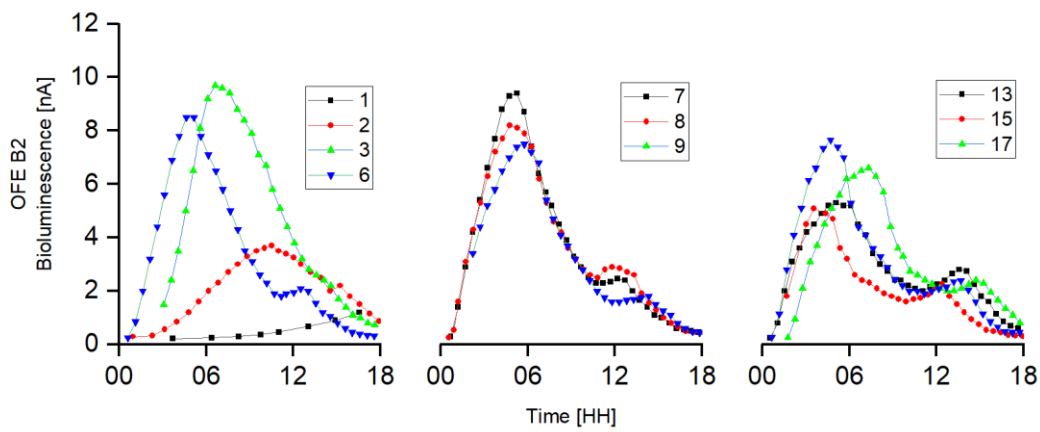


Fig. 49: OFE-B2 – Time-records of daily inductions of bioluminescence

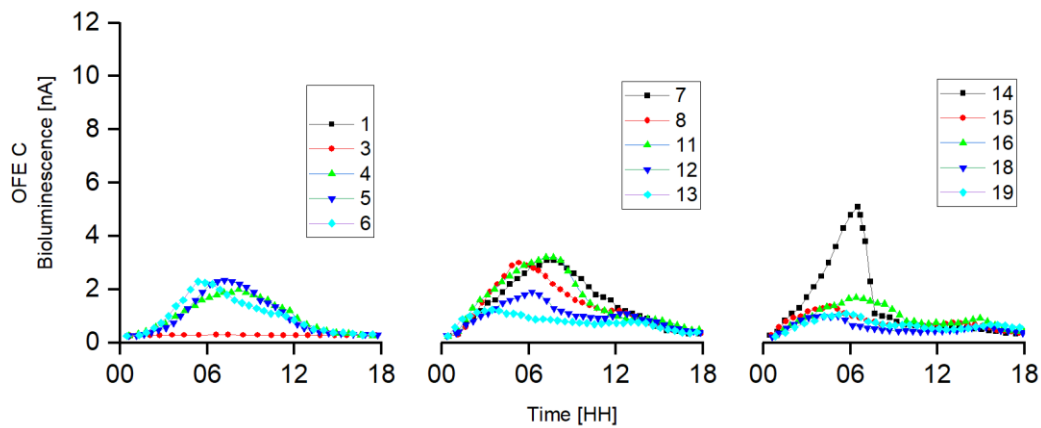


Fig. 50: OFE-C – Time-records of daily inductions of bioluminescence

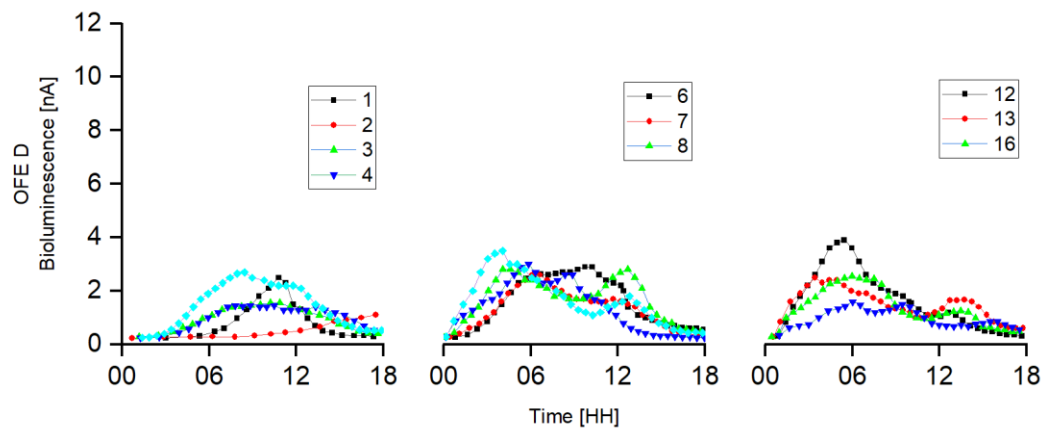


Fig. 51: OFE-D – Time-records of daily inductions of bioluminescence

Successful colonization of the OFEs surface was proved by induced bioluminescence. Results among the repeats of the trial varied significantly, nevertheless, these common features were observed:

1) Two bioluminescence maxima were observed on the daily records of induced bioluminescence (Fig. 52). The first peaks B1 were caused by adsorbed biofilm cells. The second peaks B2, which appeared 8–12 h after B1, were the results of cells growth that were often released from the adsorbed layer into the solution. The proof of delayed bioluminescence from the induction solution can be also found in the supplement 5.3.

Small second peaks confirmed experimental calculations, which suggested the best place to immobilize bioreporters is on the very surface of OFEs wider end. The size or presence of the second peak depended on the distance of the OFE from the bottom of beaker with induction solution, and thus on the varying amount of induction solution with different number of bioreporter cells underneath the OFE face (see beaker on adjustable stand in Fig. 37). This distance changed every time the induction solution was changed, and the stand with the baker was set again. The size and nature of the B2 make it an insignificant element for the purpose of toluene detection. (4)

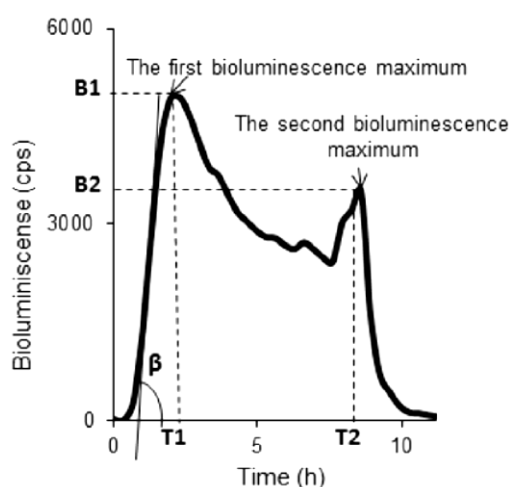


Fig. 52: Typical time-record (smoothed) of daily induction of *P. putida* TVA8 adsorbed on the wider end of tapered quartz optical fiber modified with APTES. The inductor (toluene 26.5 mg L^{-1}) was added at time = 0. (4)

2) During the first several days of the experiment, the bioluminescence maxima of the principal peak were gradually developing (Fig. 53) and were achieved in shorter times (Fig. 54). Times of appearance of the B1 maxima decreased within first 5 days and was between 2 – 4 h after the induction, and stabilized at about 4 h 46 min (Fig. 54). Nevertheless, any signal above twice the amount of background noise of the detector (Oriol module - $2 \times 0.26 \text{ nA}$; Perkin Elmer module $2 \times 20 \text{ cps}$ integrated over 10s) could reliably confirm the presence of toluene in the sample. Such an increase in bioluminescence appeared within 0.5 h after immersion in the induction solution. This growth was observed in all inductions (for all OFEs) with exceptions over the first two days. During this initial period, the cell layers were likely not matured and performed slowly, with low bioluminescent responses.

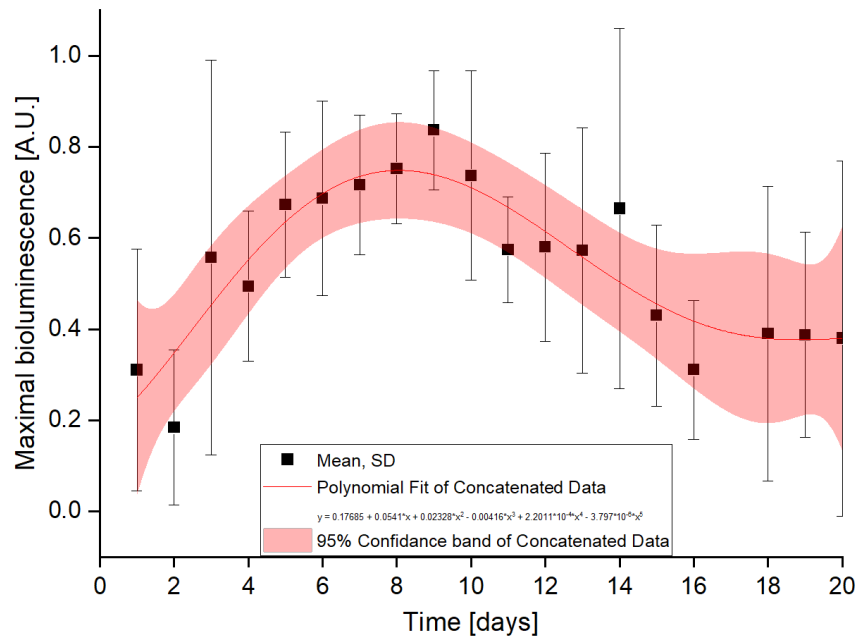


Fig. 53: Daily bioluminescence maxima (B1) normalized to 1. Aggregated data from six OFEs.

3) During the second week of the experiments all the lines showed two peaks. The intensities of the detected light (B1) were low during the first few days after induction and then gradually increased (Fig. 53). This might be ascribed to an advanced covering of the base of the OFE with cells. Light intensities (B1) decreased after 8-14 days and were fluctuating across a wide range (Fig. 53). Number of leaked cells increased over time, resulting in higher bioluminescence intensities from the solution (B2).

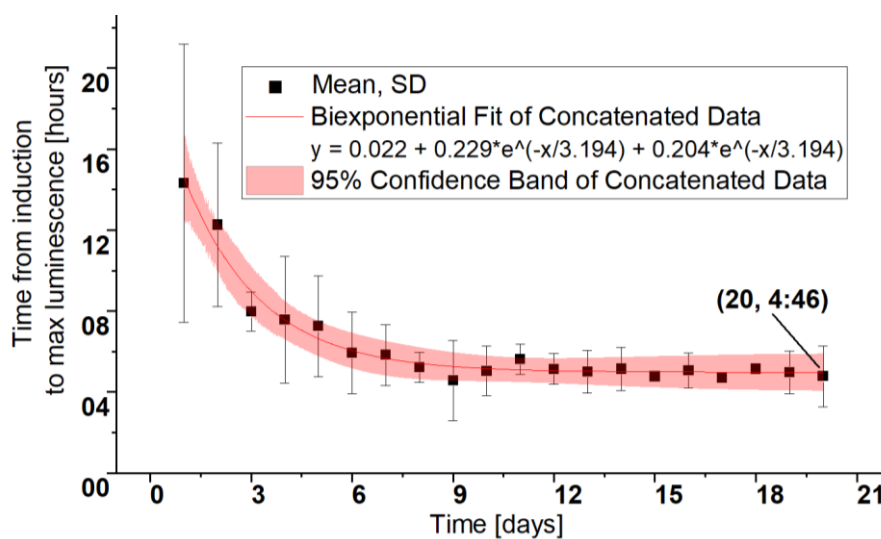


Fig. 54: Time of the first bioluminescence maxima; aggregated data of six OFEs.

4.6. ICP experiment

The experiment carried out at ICP was aimed to test the longevity of inductions. The cells adsorbed on the element were induced 68 times with toluene and 4 times with contaminated ground water over the course of 135 days.

The sum of emitted light (S), was tested, comprising the contributions of light emitted from both the adsorbed and leaked cells and the rate by which the bioluminescence increased (β). The bioluminescence maxima ($B1$, $B2$) and the times at which they were achieved ($T1$, $T2$) from the longest trial with the element are shown in Fig. 55.

While the bioluminescence maxima ($B1$, $B2$) fluctuated across a large range, the times of appearance of the first bioluminescence maxima ($T1$) were between 2 h and 4 h and for $T2$ were between 10 h and 14 h. The courses and fluctuations of S and β were similar to the fluctuations of $B1$ or $B2$. The reproducibility of all the analytical responses tested ($B1$, $B2$, $T1$, $T2$, S , β) remains so low that the element with adsorbed cells is plausible only for identification of the presence of bioavailable BTEX. In contrast to studies such as from Rassinger et al. (2005) or Zhong et al. (2011), the fiber biosensor with adsorbed bioluminescent bioreporters was repetitively induced with toluene for more than 2 months, which is the longest time-interval reported for the service of such a biosensor. The technique of cell adsorption and the conditions of bioluminescence inductions require optimization to achieve better reproducibility. (80) (81)

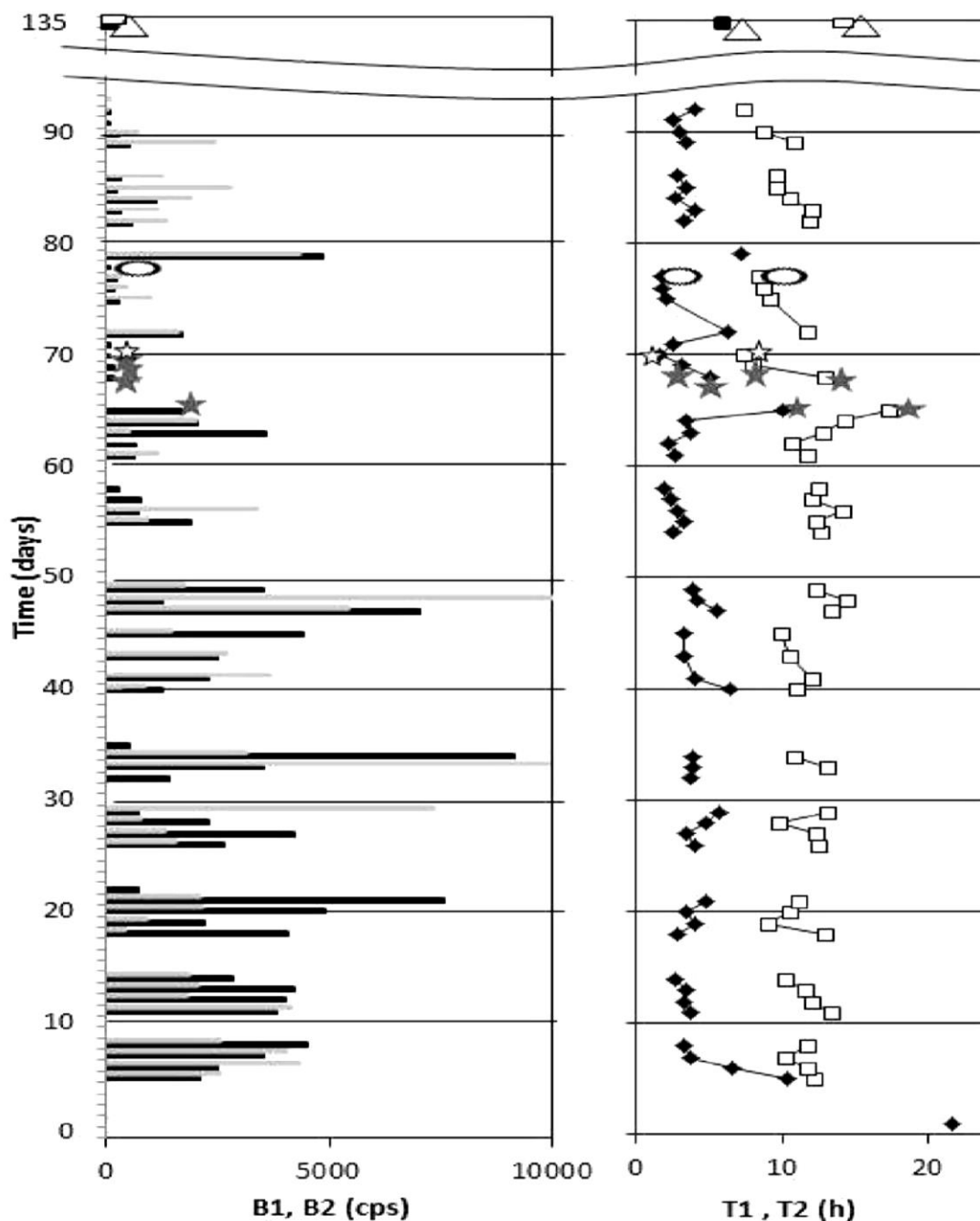


Fig. 55: Tapered sensor with adsorbed cells of *P. putida* TVA8 induced daily with toluene solution (26.5 mg L^{-1}). Intensities of bioluminescence of first principal peak, B1 -- and the second maxima, B2 --. Times of bioluminescence maxima, of first principal peak, T1 \diamond and second principal peak, T2 \square .

On days 65–70 cells were induced with real contaminated water Aqua43 \star . On day 71 the cells were induced with Aqua43 diluted with PBS \star . On day 78 the cells were immersed in LB \circ and on day 135 in LB_{kan} with toluene (26.5 mg L^{-1}) Δ .

4.6.1. Contaminated water induced bioluminescence

The biofilm-like layer on OFE was induced with “Aqua43” 60 days after immobilization. At that time, the bioluminescence responses to the induction solution were lower than during the first 30 days. Nevertheless, the intensities of bioluminescence induced with this contaminated water were much lower than expected based on the content of toluene (172 mg L^{-1}) and were also lower than the intensities induced with the induction solution (26.5 mg L^{-1}) (Fig. 55). This decrease in induced bioluminescence probably results from a toxic effect of high concentrations of toluene and xylenes and increased temperature above $30 \text{ }^{\circ}\text{C}$ on the days of measurement. On day 71, the ten-times diluted “Aqua43” did not increase the bioluminescence of adsorbed cells. Nevertheless, the following day-72, the maximum of the bioluminescence response was higher. This one-day delay in the increase in bioluminescence maxima might be a lag-time needed for cells adaptation.

On day 78 the element was immersed in a growth medium with the aim to support the viability of adsorbed cells. The following day the intensity of bioluminescence induced with the induction solution reached 4900 counts. Despite this restoration of light production, the bioluminescence responses decreased over the following days. After 135 days the presence of the bioluminescent bioreporter *P. putida* TVA8 on the element was confirmed by induction with a toluene solution containing kanamycin, which inhibits the growth of bacteria other than TVA8, and detection of bioluminescence.

The study demonstrated the repetitive inductions of bioluminescence of the adsorbed cells of a bioluminescent bioreporter. The cells were adsorbed on an APTES-modified tapered optical fiber element. The adsorbed cells performed a two-fold higher number of repetitive inductions than cells entrapped in silica gel. The element is conceivable as a detection probe for multiple use in a laboratory and the online monitoring of bioavailable contamination in remote localities.

4.7. UTK experiment

The experiment at UTK was aimed to test the repeatability of inductions and to compare different OFE geometries. The cells adsorbed on 5 different elements over the course of 2-3 weeks. The cells adsorbed on the element were induced 10-16 times with toluene over the period of 20 days. Besides the B1 bioluminescence maxima, the sum of emitted light (integral of bioluminescence peak) was also tested. B1 maxima and the sum of its bioluminescence correlated, as it could be seen from the Fig 56.

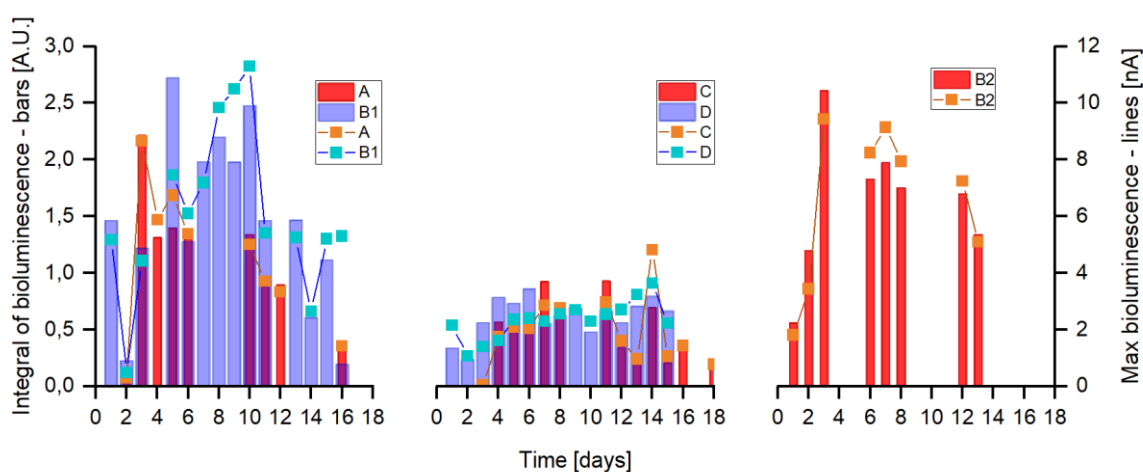


Fig. 56: Main peak bioluminescence integrals and main peak max bioluminescence of each OFE within 20 days.

Table 8 compares time-records, bioluminescence maxima, integrals of bioluminescence, and OFE efficiencies. Unbiased OFE efficiency parameter suggested the highest bioluminescence signal should be detected with the OFE "D". Our calculations did not fully match the real measurements. Transmittance differences of tenths of a percent did not result in a significant difference of detected bioluminescence.

Table 8: Sums of bioluminescence intensities and maxima of bioluminescence for five OFEs

OFE	BL sum of light, average value [A.U.]	BL sum of light, max value [A.U.]	BL average value [nA]	BL max value [nA]	OFE efficiency x 10 ⁵
A	1.1056044	2.2179	4.4899	8.65	3.48
B1	1.4585701	2.7255	6.1605	11.30	2.72
B2	1.6217301	2.6090	6.5433	9.44	3.71
C	0.4597357	0.9305	1.8573	4.82	1.38
D	0.6002724	0.8607	2.2790	3.63	11.75

Ranks from the highest to the lowest

B2>B1>A>D>C B1>B2>A>C>D B2>B1>A>D>C B1>B2>A>C>D D>B2>A>B1>C

These results confirmed previous observations that OFEs adhering with *P. putida* TVA8 can be repeatedly used as a detector for toluene after a few days of the stabilization of immobilized cells. A stabilization period of two to four days was observed, even if the cells were immobilized in silica gel. (41) (82)

Kalabova et al. (2018) was able to predict a different outcome of experiments comparing an OFE and a PCS fiber, but in authors experimental results the effect of used bioreporter cells surpassed the differences in OFE transmittances. Used mathematical model is useful for the design and better understanding OFEs in terms of coupling and transmitting bioluminescence to a detector, the best shape, size, and ideal place for bioreporter immobilization. (69)

Possible ways to improve the stability of bioluminescence signal responses include engineering a cell strain with two reporter genes (one under control of an analyte of interest and one constitutively present to monitor cell viability) (Roda et al., 2011). An alternative to this is the use of two independent bioreporters (constitutive and inducible) derived from the same strain (Angelaalincy et al., 2018). Nevertheless, in the optical fiber arrangement, this resolution requires two fibers, which complicates the sensor construction. The analyte-specific signal must be than corrected according to cell viability; or genetical manipulation of a bacterial strains ability to create and dissolve biofilm structure (Wei and Ma, 2013). (83) (84) (85)

4.7.1. Immobilization and induction of *E. coli* 652T7

In the LB_{Kan} growth medium, *E. coli* 652T7 did not adhere on the APTES modified base of the OFEs regardless of the addition of ferric chloride which was added to theoretically enhance the adhesion of microorganisms by lowering the repulsion forces (52). Cell attachment was observed only at the interface of growth medium and air (Figure 57). At this interface, photon-OFE binding efficiency is < 1%, thus bioluminescence of these attached cells would not significantly contribute to detected light.

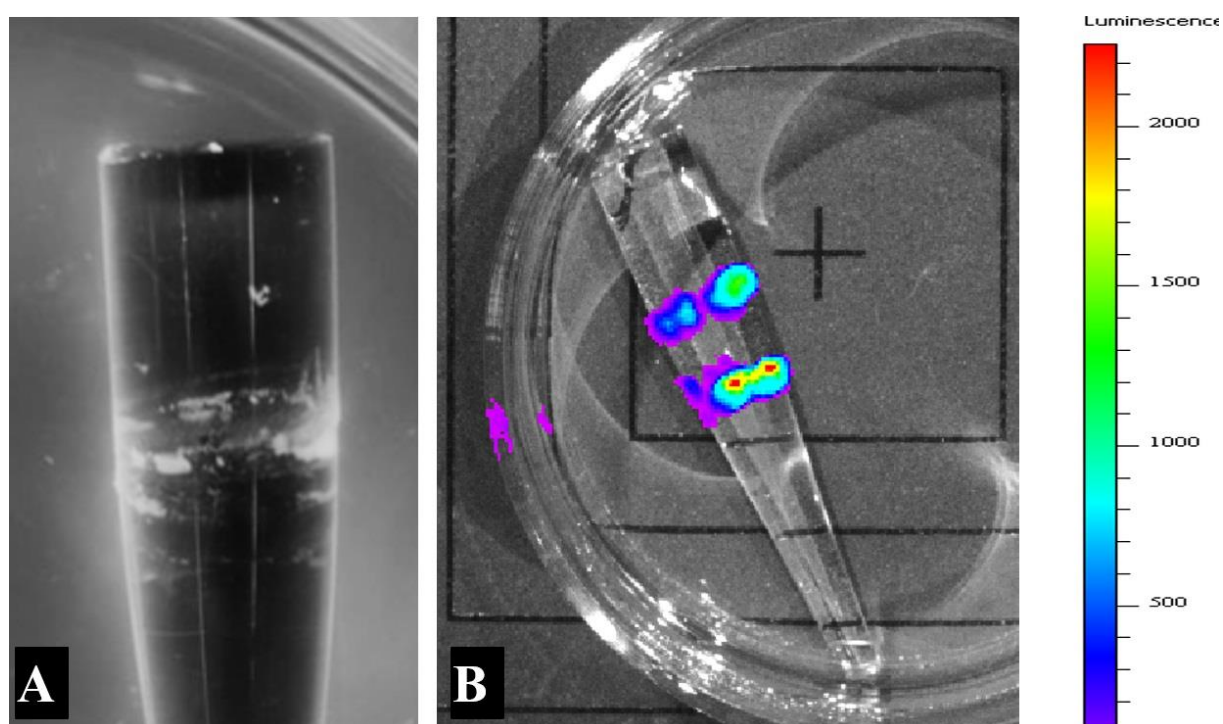


Fig. 57: *E. coli* 652T7 on the surface of an APTES modified quartz cone after 4 days in LB_{Kan} cultivation medium (A). Bioluminescence of *E. coli* 652T7 induced after immersion in LB medium as measured in an IVIS Lumina K imager (photons/sec/cm²/steradian) (B).

E. coli 652T7 was immobilized on the base of OFE-D with PEI. The time records of daily inductions with LB medium is presented in Fig. 58. Except for the first induction intensities, bioluminescence increased within 15 min after immersing the OFE into the LB solution. The intensities remained stable for 18 h on the first day, 6-9 h on all other days, and then sharply decreased due to a depletion of nutrients. To test the OFE with immobilized *E. coli* 652T7 as a biosensor for biotoxicity, HCl was added to the induction solution on the 8th day. This caused pH lowering to pH = 6 and decreased the bioluminescence, which did not

recover after the following two inductions. These results imply that an OFE immobilized with *E. coli* 652T7 is sensitive to influences that affect cell viability but cannot be repetitively used as a biosensor since cells are dying and not recovering.

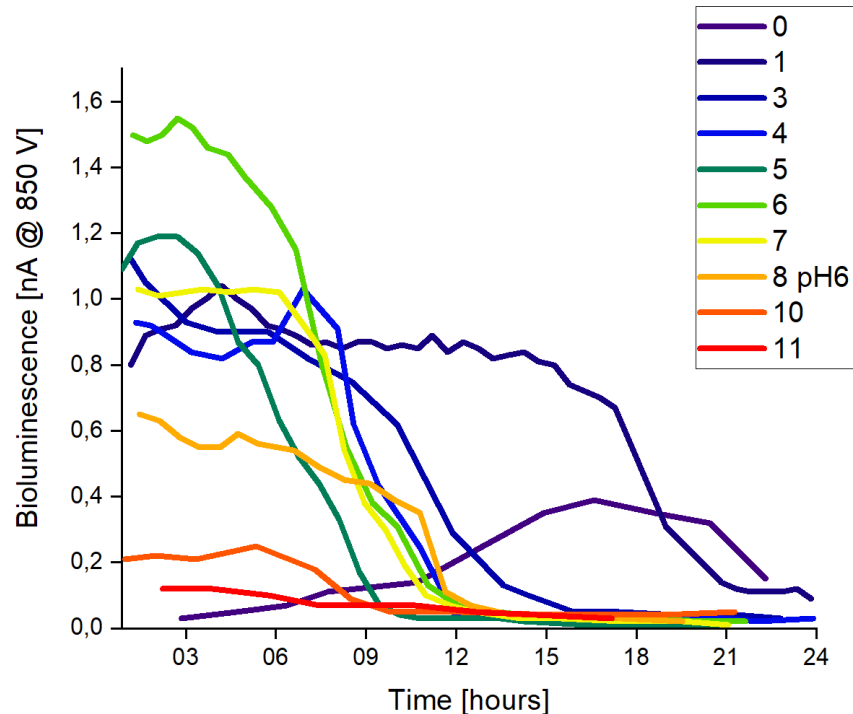


Fig. 58: Time records of bioluminescence of *E. coli* 652T7 immobilized on OFE D in PEI. Legend denotes the days after the immobilization.

In the UTK study we immobilized the bioluminescent bioreporter *P. putida* TVA8 on a tapered OFE in order to prepare a biosensor for the detection of liquid toluene. This study broadened our previous research where we used physico-chemical models, using contact angles and zeta potential, to facilitate the attachment of *P. putida* TVA8 to quartz surfaces after treatment with APTES. Biofilm development of *P. putida* TVA8 with time was quantified and the repeatability of the biofilm preparation and the repeatability of bioluminescence detection was determined. Except for a short maturation period (~2-4 days), the OFEs exhibited a stable bioluminescent response for at least 20 days.

We additionally immobilized the constitutively bioluminescent toxicity bioreporter *E. coli* 652T7 on a PEI modified OFE and demonstrated its potential use as a biosensor for cytotoxicity. Also, the immobilization process that we used, without any bulky matrix requirements, could be applied towards many other microbial bioreporters for the biosensing of a variety of different analytes. However, since the reproducibility of bioreporter responses remains low, the developed biosensor can be used for online, rapid and multiplexed monitoring of the presence of a pollutant, but not its concentration.

5. Outcomes and future course of research

Author made a literature research on pollution, effect of pollutants on human health, current detection methods of toluene, and the areas where the principle of bio-sensing is used. Author also become familiarized with the work and procedures used in a microbiological laboratory.

The use of tapered fiber element in a sensor design, which is a novel approach that increases the detected bioluminescence signal intensity, was described. The geometry of a fiber element allows to immobilize larger amounts of bioreporter organisms on its wider end in comparison with a regular optical fiber, making such a whole-cell optical fiber biosensor significantly more sensitive to a compound of interest. Ideal parameters of an optical fiber element were described, immobilization techniques were discussed, laboratory setup for toluene detection was proposed.

Pseudomonas putida TVA8 cells were successfully immobilized without an inorganic carrier in a biofilm-like layer on a bare tapered optical fiber element. A biosensor capable of long-term detection of liquid toluene in a laboratory sample was prepared. Repeatability of sensor preparation and stability of measured signals were described. Sensitivity of the developed sensor was also successfully tested on a real polluted water sample. Additionally, several different microorganisms were tested in the biosensor design. It was demonstrated that constitutively bioluminescent toxicity bioreporter *Escherichia coli* 652T7, immobilized on a PEI modified fiber element, could potentially serve as a biosensor for cytotoxicity. The immobilization process, modified or unmodified, could be applied towards many other microbial bioreporters for the biosensing of a variety of different analytes.

Cooperation between the teams from the Faculty of Biomedical Engineering of the Czech Technical University, the Institute of Chemical Processes of the Czech Academy of Sciences, and the Center for Environmental Biotechnology of the University of Tennessee resulted in publication of two articles in impacted journals, and three international conference contributions (attachments 6.1-6.2).

Author made a literature research on pollution, effect of pollutants on human health, current detection methods of toluene, and the areas where the principle of bio-sensing is used. Author also become familiarized with the work and procedures used in a microbiological laboratory.

The use of tapered fiber element in a sensor design, which is a novel approach that increases the detected bioluminescence signal intensity, was described. The geometry of a fiber element allows to immobilize larger amounts of bioreporter organisms on its wider end in comparison with a regular optical fiber, making such a whole-cell optical fiber biosensor significantly more sensitive to a compound of interest. Ideal parameters of an optical fiber element were described, immobilization techniques were discussed, laboratory setup for toluene detection was proposed.

Pseudomonas putida TVA8 cells were successfully immobilized without an inorganic carrier in a biofilm-like layer on a bare tapered optical fiber element. A biosensor capable of long-term detection of liquid toluene in a laboratory sample was prepared. Repeatability of sensor preparation and stability of measured signals were described. Sensitivity of the developed sensor was also successfully tested on a real polluted water sample. Additionally, several different microorganisms were tested in the biosensor design. It was demonstrated that constitutively bioluminescent toxicity bioreporter *Escherichia coli* 652T7, immobilized on a PEI modified fiber element, could potentially serve as a biosensor for cytotoxicity. The immobilization process, modified or unmodified, could be applied towards many other microbial bioreporters for the biosensing of a variety of different analytes.

Cooperation between the teams from the Faculty of Biomedical Engineering of the Czech Technical University, the Institute of Chemical Processes of the Czech Academy of Sciences, and the Center for Environmental Biotechnology of the University of Tennessee resulted in publication of two articles in impacted journals, and three international conference contributions (attachments 6.1-6.2).

5.1 Future goals

- To further test polluted water samples and evaluate cytotoxicity of commonly present compounds.
- To characterize surface properties of microorganisms, other than *P. Putida* TVA8, suitable for the detection of BTEX, EDCs, and other compounds of interest.
- To characterize surface properties of quartz glass functionalized with different agents, other than APTES, to ameliorate biofilm growth.
- To test chosen EDCs with the developed sensor.
- To develop in-situ setup for BTEX and EDCs detection.
- To test the in-situ setup in real conditions.

6. Attachments

6.1. List of author's publications

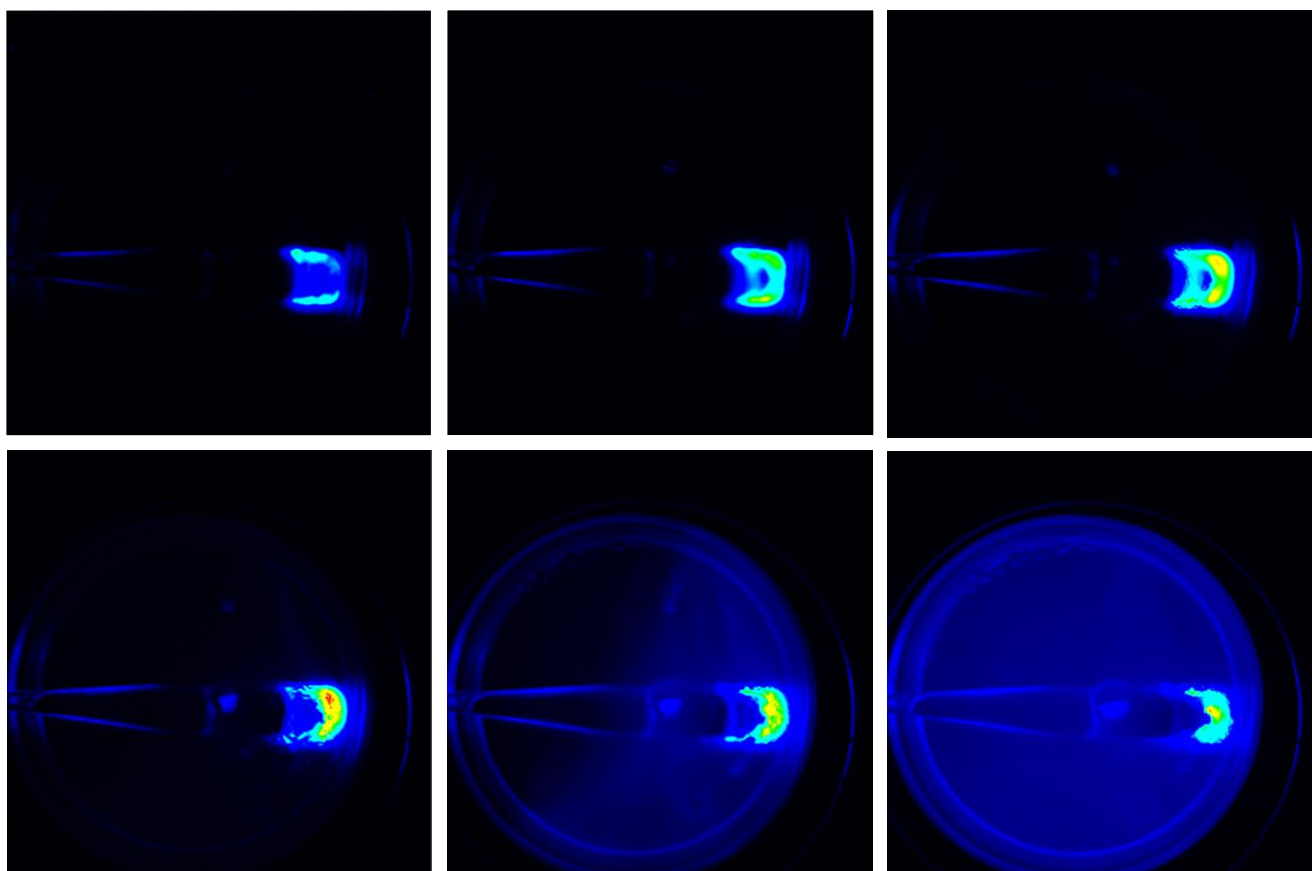
- Zajíc J., Traplová L., Matějec V., Pospíšilová M., Barton I. **Optical pH Detection with U-Shaped Fiber-Optic Probes and Absorption Transducers.** *Hindawi - Conference Papers in Science* **2015**, 1-8; doi: 10.1155/2015/513621
- Zajíc J., Bittner M., Brányik T., Solovyev A., Šabata S., Kuncová G., Pospíšilová M. **Repetitive inductions of bioluminescence of *Pseudomonas putida* TVA8 immobilized by adsorption on optical fibre.** *Chemical Papers* **2016**, 70, 877–887; doi: 10.1515/chempap-2016-003
- Zajíc J., Kuncová G., Ripp S., Pospíšilová M., Trögl J. **Whole-cell detectors of contaminants constructed by immobilization of bioreporters in form of biofilm on special optical fiber elements.** *IEEE International Conference on Sensors and Nanotechnology*, conference proceedings **2019**; doi: 10.1109/SENSORSNANO44414.2019.8940080
- Zajíc J., Ripp S., Trögl J., Kuncová G., Pospíšilová M. **Repetitive Detection of Aromatic Hydrocarbon Contaminants with Bioluminescent Bioreporters Attached on Tapered Optical Fiber Elements.** *Sensors* **2020**, 20, 3237; doi: 10.3390/s20113237
- Zajíc J., Ripp S., Kuncová G., Trögl J., Pospíšilová M., Morava J. **Whole-Cell Detectors of Aromatic Hydrocarbon Contaminants Constructed by Immobilization of Bioreporters on Special Optical Fiber Elements.** *Instruments and Methods for Biology and Medicine*, conference proceedings **2020**; ISBN: 9788001067963

6.2. List of author's conference contributions

- **Absorption optical fiber sensors; *BIO-OPT-XUV workshop*; Kladno, Czech Republic, 2014**
- **Optical pH Detection with U-Shaped Fiber-Optic Probes and Absorption Transducers; *Materiaux et Applications aux Dispositifs et Capteurs*; Mahdia, Tunisia, 2015**
- **Whole-cell detectors of contaminants constructed by immobilization of bioreporters in form of biofilm on special optical fiber elements; *IEEE Sensors and Nano 2019*, Penang, Malaysia, 2019**
- **Whole-Cell Detectors of Aromatic Hydrocarbon Contaminants Constructed by Immobilization of Bioreporters on Special Optical Fiber Elements; *Instruments and Methods for Biology and Medicine*, Kladno, Czech Republic., 2020**

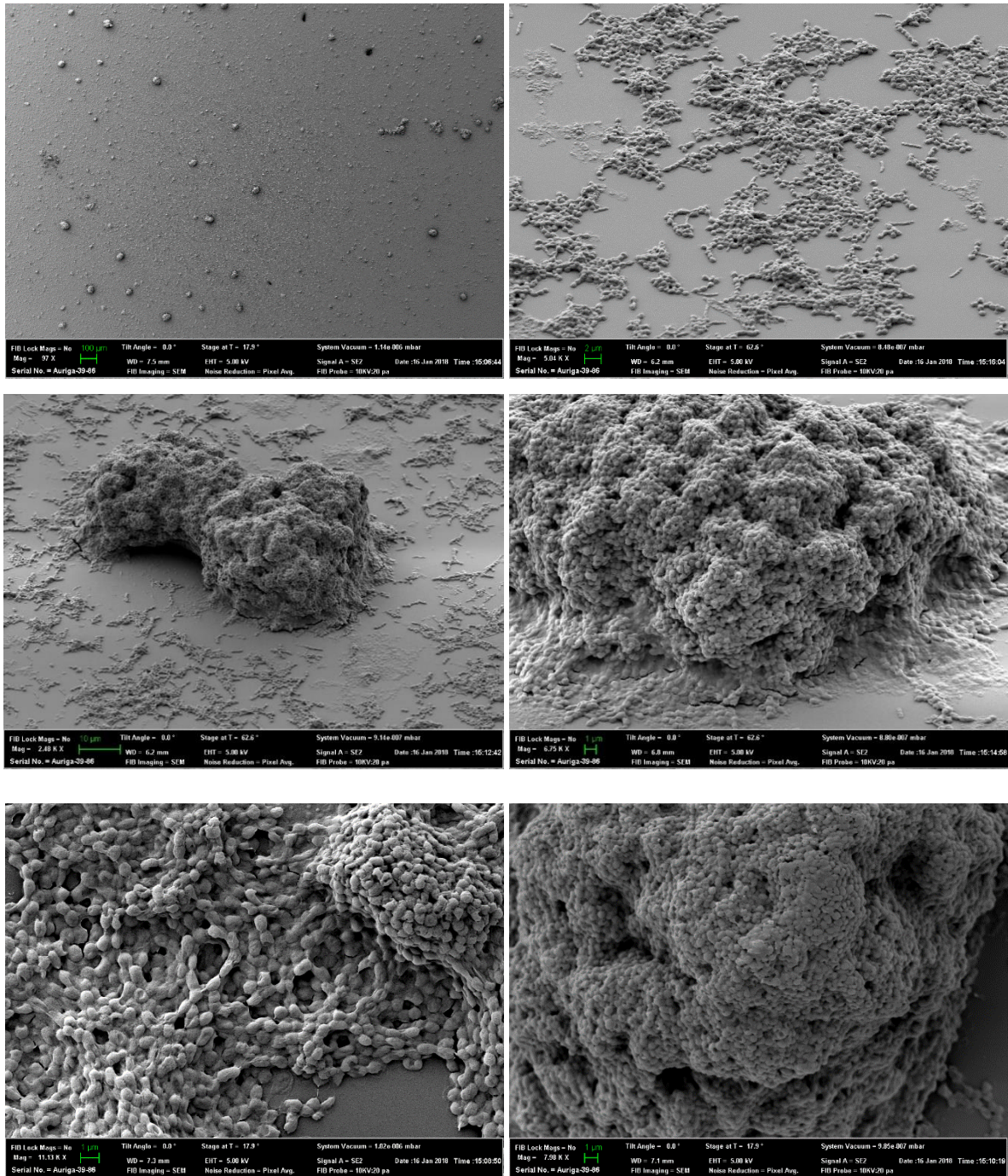
6.3. Proof of first and second bioluminescent peak

Induction of *P. putida* TVA8 adhered on an OFE cone. A gradual increase in bioluminescence of cells adhering on the APTES modified surface, the base, and the part of the cone, was followed by a high bioluminescence intensity located only on the base (this corresponds to the first bioluminescent peak). The bioluminescence of these attached cells fell below the detection limits and at the end (12–15 h) a low light signal emerged in the induction solution (this corresponds to the second bioluminescent peak).

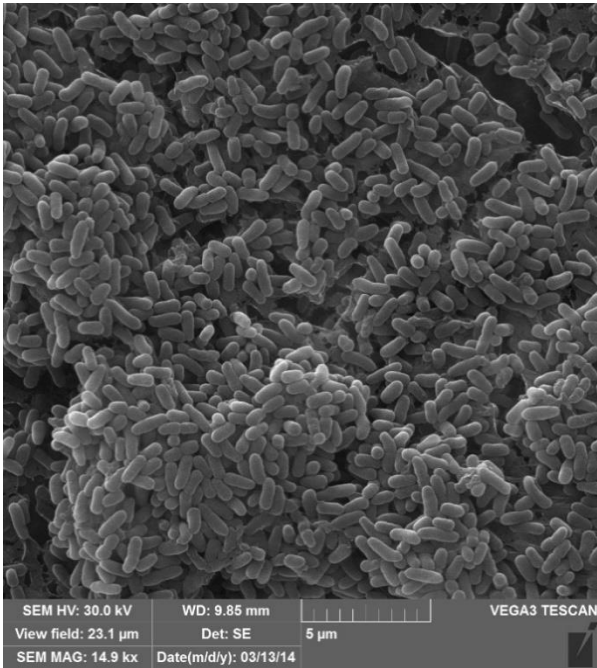
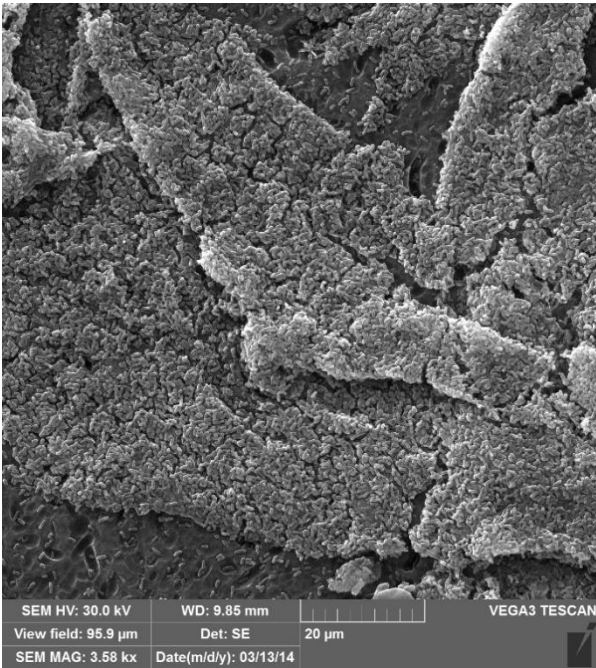


6.4. SEM images of immobilized *P. putida* TVA8

After 2 weeks from immobilization on APTES modified quartz surface:



After 135 days from immobilization on APTES modified quartz surface:



6.5. Real polluted water sample composition test



AQUATEST a.s.
 AQUATEST- testing laboratories
 Workplace Geologická 4, 15200 Prague 5
 Head of laboratories Tel. 234607180, Fax.
 234607710
 Reception of samples –Tel. 234607422
 Results Tel - 23467321, Fax. 234607781

Testing laboratory accredited by Czech Accreditation Institute, No 1243 according ČSN EN ISO/IEC 17025:2005

Test Protocol No. 1097/14

Order party: AQUATEST a.s. Liberec

Page 1/3

Responsible person: Lederer

Name of the action: Nanorem

Action No.: 668138003018

Locality: Site 2

Sampling: Patka Mgr. (employ of Aquatest a.s.)

Sample: RWA-43

Laboratory No.: 3528/14

Depth (m): not mentioned

Material: groundwater

AQUATEST a.s. Liberec
Husitská 133/49
Liberec
460 09

Data of sampling: 26.02.14

Date of receipt: 27.02.14

Date of analysis: 27.02.14 - 06.03.14

Results are only related to tested items. The test protocol must be reproduced complete. The parts of the protocol might be reproduced only with written permission of the laboratory.

The laboratory is liable only for results of tests of the sample in the state in which was delivered by a customer.

Name of indicator	SOP	Method	Result	Unit	Uncert.	A/N
Amonium ions	SOP 1.8.1.	Spectroquant MERCK	0,66	mg/l	±12%	A
Chlorides	SOP 1.1.3.	ČSN EN ISO 10304-1	297	mg/l	±8%	A
Nitrates	SOP 1.1.2.	ČSN EN ISO 10304-1	<1.50	mg/l		A
Nitrites	SOP 1.1.2.	ČSN EN ISO 10304-1	<1.00	mg/l		A
Fluorides	SOP 1.1.3.	ČSN EN ISO 10304-1	<5.00	mg/l		A
ANC 4.5	SOP 1.13.1	ČSN EN ISO 10304-1	18.3		±5%	A
BNC 8.3	SOP 1.14.1	ČSN 75 7372	1.64		±15%	A
pH	SOP 1.3.1	ČSN ISO 10523	7.53		±0.1%	A
Sulphates	SOP 1.1.3	ČSN ISO 10523	34.8	mg/l	±8%	A
Conductivity	SOP 1.13.1	ČSN EN 27888	239		±3%	A
Phosphates	SOP 1.7.1	ČSN EN ISO 6878	7.9	mg/l	±10%	A
CO2 agrasive	SOP 1.19.1	ČSN 83 0520-35 (complete a sum)	0.00	mg/l		A
CO2 free	SOP 1.14.1	ČSN 75 7372 ČSN 75 7373 (complete a sum)	72.2	mg/l	±15%	A
Bicarbonates	SOP 1.13.1	ČSN EN ISO 9963-1 ČSN 75 7373	1120	mg/l	±5%	A
Carbonates	SOP 1.13.1	ČSN EN ISO 9963-1 ČSN 75 7373	0			A

Name of indicator	SOP	Method	Result	Unit	Uncert./	A/N
Colour		visually	Yellow			N
Sediment		visually	without			N
Smell		sensoric	organic			N
COD-Cr		ČSN ISO 15705, manual Hach	390	mg/l	±10%	A
Potassium dissolved		ČSN EN ISO 11885	6.89	mg/l	±15%	A
Magnesium dissolved		ČSN EN ISO 11885	2.8	mg/l	±15%	A
Manganese dissolved		ČSN EN ISO 11885	0.500	mg/l	±15%	A
Silicium oxide dissolved		ČSN EN ISO 11885	27.1	mg/l	±15%	A
Sodium dissolved		ČSN EN ISO 11885	532	mg/l	±15%	A
Calcium dissolved		ČSN EN ISO 11885	15.2	mg/l	±15%	A
Calcium and magnesium		complete a sum	0.49	mmol/l	±20%	A
Iron dissolved		ČSN EN ISO 11885	7.34	mg/l	±15%	A
Benzene		ČSN EN ISO 10301, EPA 8015 D	264	µg/l	±30%	A
Toluene		ČSN EN ISO 10301, EPA 8015 D	172000	µg/l	±30%	A
Ethylbenzene		ČSN EN ISO 10301, EPA 8015 D	7820	µg/l	±30%	A
Xylenes		ČSN EN ISO 10301, EPA 8015 D	20000	µg/l	±30%	A

Uncertainty is expressed as a double of standard uncertainty . Uncertainty characterized interval of values in which one can expect true value with probability 95%. This uncertainty does not include uncertainty of sampling and is not mentioned in cases of results below limits of determination.

A - Accredited method

N - Nonaccredited method

Information related to certain test or facts related to deviations from test specifications:

Elemental analysis (SOP5.13.1, 5.20.1, 5.9.1) – pretreatment: In the laboratory before the determination of dissolved metals the sample was filtrated (0,45 µm) and subsequently was conserved by addition of acid (HNO₃).

Responsibility of technical aspects of the protocol:

J.Hůková
Staffer of exit of results

Authorization on behalf of the laboratories:

Ing. Radana Mračková Dvořáková
Director of the laboratory section

In Prague: 06.03.2014

END OF THE PROTOCOL

TEST PROTOCOL No. 1097/14

Page 3/3

Information written below are out of the framework of the accreditation. The values of concern were calculated and evaluated on the base on a comparison with related regulations.

CATIONS	mg/l	mmol/l	ANIONS	mg/l	mmol/l
NH ₄ ⁺	0.66	0.0367	Cl ⁻	297	8.3773
Ca ²⁺	15.2	0.3792	NO ₃ ⁻	<1.50	<0.0242
Mg ²⁺	2.8	0.11582	NO ₂ ⁻	<1.00	<0.0217
K ⁺	6.89	0.1762	F ⁻	<5.0	<0.2632
Mn	0.500	0.0091	HPO ₄ ²⁻	7.9	0.0823
Na ⁺	532	23.1407	SO ₄ ²⁻	34.8	0.3623
Fe celk.	7.34	0.1314			
SUMA (mval)		24.62	SUMA (mval)		27.56

CALCULATED VALUES:	mmo/l		mg/l
Water hardness complete	0.49	Complete mineralization	2048
Calcium hardness	0.3792	CO ₃ ²⁻	0
Magnesium hardness	0.1152	HCO ₃ ⁻	1116
H ⁺	0.0000	CO ₂ agres	0
OH ⁻	0.0000	CO ₂ free	72.16
		Langel. index	-0.389

ASSESMENT OF WATER :

Chemical type of water: Na, Cl⁻, HCO₃

Reaction: alcalic

Hardness: very soft

ČSN-EN 206-1 Concrete - part 1: Specification, properties, production nonagresive

Remarks to English stranslation:

Translated: G. Kuncova

SOP = Standard operating procedure

<http://aquatest.cz.kappa.nen.cz/en/>

ANC, BNC, see - Stumm W., Morgan J. J.: *Aquatic Chemistry.*, Wiley, New York 1970 a 1996.

ČSN = Czech technical standards

7. Bibliography

1. Co je biomedicínské inženýrství. *Fakulta biomedicínského inženýrství*. [Online] <https://www.fbmi.cvut.cz/uchazeci/co-je-bmi>.
2. Harrison, Roy M. *Pollution: Causes, Effects and Control*. 4th. Cambridge : The Royal Society of Chemistry, 2001. ISBN 0-85404-621-6.
3. Hill, Marquita K. *Understanding Environmental Pollution*. 3rd. Cambridge : Cambridge University Press, 2010. ISBN-13: 978-0-521-51866-6.
4. *Repetitive inductions of bioluminescence of Pseudomonas putida TVA8 immobilized by adsorption on optical fiber*. Jakub Zajíc, Gabriela Kuncová, Milan Bittner, Tomáš Brányik, Andrey Solovyev, Stanislav Šabata, Marie Pospíšilová. 7, s.l. : Chemical Papers, 2016, Vol. 70, pp. 877-887.
5. Diamanti-Kandarakis E, Bourguignon JP, Giudice LC, Hauser R, Prins GS, Soto AM, Zoeller RT, Gore AC. Endocrine-disrupting chemicals: an Endocrine Society scientific statement. *Endocrine reviews*. 30, 6 2009, Vol. 4, pp. 293-342.
6. Benzene, Toluene, Ethylbenzene, and Xylene. *EUGRIS: portal for soil and water management in Europe*. [Online] <http://www.eugris.info/FurtherDescription.asp?Ca=2&Cy=0&T=Benzene,%20toluene,%20ethylbenzene,%20and%20xylene&e=6>.
7. *Chemically-induced alterations in sexual and functional development - the wildlife/human connection*. Bern HA, Blair P, Brasseur S, Colborn T, Cunha GR, Davis W, et al. Wingspread Racine WI : Statement from the Work Session on Chemically-Induced Alterations in Sexual Development: The Wildlife/Human Connection, 1991, pp. 1-8. 978-0-911131-35-2.
8. Dioxins and their effects on human health. <https://www.who.int/>. [Online] 10 4, 2016. [Cited: 19, 2020.] <https://www.who.int/news-room/fact-sheets/detail/dioxins-and-their-effects-on-human-health>.
9. *Research needs for the risk assessment of health and environmental effects of endocrine disruptors: a report of the U.S. EPA-sponsored workshop*. Kavlock RJ, Daston GP, DeRosa C, Fenner-Crisp P, Gray LE, Kaattari S, Lucier G, Luster M, Mac MJ, Maczka C, Miller R, Moore J, Rolland R, Scott G, Sheehan DM, Sinks T, Tilson HA. (Suppl 4), s.l. : Environ Health Perspect, 1996, Vol. 104. PMCID: PMC1469675.

10. Nicolopoulou-Stamati P, Maipas S, Kotampasi C, Stamatis P, Hens L. Chemical Pesticides and Human Health: The Urgent Need for a New Concept in Agriculture. *Front Public Health*. 4, 2016, Vol. 148.
11. Patisaul, Heather B. Endocrine disruption by dietary phyto-oestrogens: impact on dimorphic sexual systems and behaviours. *Proceedings of the Nutrition Society*. 176, 5 2017, Vol. 2, pp. 130-144.
12. Thomas H. Miller, Keng Tiong Ng, Samuel T. Bury, Sophie E. Bury, Nicolas R. Bury, Leon P. Barron. Biomonitoring of pesticides, pharmaceuticals and illicit drugs in a freshwater invertebrate to estimate toxic or effect pressure. *Environment International*. 129, 2019, pp. 595-606.
13. *Fiber optic monooxygenase biosensor for toluene concentration measurement in aqueous samples*. Z. Zhong, M. Fritzche, S. B. Pieper, T. K. Wood, K. L. Lear, D. S. Dandy, K. F. Reardon. s.l. : Biosensors and Bioelectronics, 2010, Vol. 26/2011. doi:10.1016/j.bios.2010.10.021.
14. *Repetitive Detection of Aromatic Hydrocarbon Contaminants with Bioluminescent Bioreporters Attached on Tapered Optical Fiber Elements*. Zajíc, Jakub and Ripp, Steven and Trögl, Josef and Kuncová, Gabriela and Pospíšilová, Marie. 11, s.l. : Sensors, 2020, Vol. 20. 1424-8220.
15. Deric P. Jones, Joe Watson. *Biomedical Sensors*. London : Momentum Press, 2010. 1606500562.
16. John Vetelino, Aravind Reghu. *Introduction to Sensors*. s.l. : CRC Press, 2010. 1439808538, 9781439808535.
17. Patranabis, D. *Sensors and Transducers*. s.l. : Prentice-Hall of India, 2004. 8120321987.
18. *Fiber-optic chemical sensors and fiber-optic bio-sensors*. Marie Pospíšilová, Gabriela Kuncová, Josef Trögl. 10, s.l. : Sensors, 2015, Vol. 15, pp. 25208-25259. ISSN 1424-8220.
19. Zajíc, Jakub. *Detection of pH with Fiber-Optic Detection Elements*. České vysoké učení technické v Praze, Fakulta biomedicínského inženýrství v Kladně, 2013. Diploma thesis.
20. *Miniaturized fiber-optic hybrid sensor for continuous glucose monitoring in subcutaneous tissue*. Alen Pasic, Hans Koehler, Ingo Klimant, Lukas Schaupp. 8, s.l. : Sensors and Actuators B: Chemical, 2007, Vol. 1, pp. 60-68.
21. *Chemiluminometric enzyme sensors for flow-injection analysis*. U. Spohn, F. Preuschoff, G. Blankenstein, D. Janasek, M. R. Kula, A. Hacker. 1, s.l. : Analytica Chimica Acta, 1995, Vol. 300, pp. 109-120.

22. *A disposable biosensor based on immobilization of laccase with silica spheres on the MWCNTs-doped screen-printed electrode.* Yuanting Li, Li Zhang, Meng Li, Zhigang Pan & Dawei Li. 103, s.l. : Chemistry Central Journal, 2012, Vol. 6.
23. *Whole-cell biosensor for detection of environmental pollution — enhancement of detected bioluminescence.* Hana Kalabova, Marie Pospisilova, Marcel Jirina, Gabriela Kuncova. 1, s.l. : Current Opinion in Biotechnology, 2013, Vol. 24. doi:10.1016/j.copbio.2013.05.056.
24. *A disposable fiber optic SPR probe for immunoassay.* Mai Z, Zhang J, Chen Y, Wang J, Hong X, Su Q, Li X. s.l. : Biosens Bioelectron, 2019, Vol. 144.
25. *Nucleic acid functionalized fiber optic probes for sensing in evanescent wave: optimization and application.* Xiyu Zhu, Ruoyu Wang, Kaidong Xia, Xiaohong Zhou, Hanchang Shi. 4, s.l. : RSC Advances, 2019.
26. *Fiber-Optic Chemical Sensors and Biosensors (205-2019).* Xu-dong Wang, Otto S Wolfbeis. 1, s.l. : Analytical Chemistry, 2020, Vol. 92, pp. 397-430.
27. *Application of genetically engineered microbial whole-cell biosensors for combined chemosensing.* Wei He, Sheng Yuan, Wen-Hui Zhong, Ashaduzzaman Siddiquee, Chuan-Chao Dai. s.l. : Applied Microbiology and Biotechnology, 2015, Vol. 100.
28. *Dual-color bioluminescent bioreporter for forensic analysis: evidence of androgenic and anti-androgenic activity of illicit drugs.* Luca Cevenini, Elisa Michelini, Marcello D'Elia, Massimo Guardigli & Aldo Roda. s.l. : Analytical and Bioanalytical Chemistry, 2013, Vol. 45, pp. 1035–1045.
29. *Controlled Field Release of a Bioluminescent Genetically Engineered Microorganism for Bioremediation Process Monitoring and Control.* Ripp Steven, Nivens David, Ahn Yeonghee, Werner Claudia, Jarrell, Easter James, Cox Chris, Burlage Robert, Sayler Gary. s.l. : Environmental Science & Technology, 2000, Vol. 34, p. 2068.
30. Union, European. Chemicals and GMO Legislation. *Handbook on the Implementation of EC Environmental Legislation.* Szentendre : s.n., 2014, Vol. Section 8, pp. 93–126.
31. Gutiérrez, Juan & Amaro, Francisco & Martín-González, Ana. Heavy metal whole-cell biosensors using eukaryotic microorganisms: An updated critical review. *Frontiers in Microbiology.* 6, 2015, pp. 1-8.
32. Xu T., Perry N., Chuaham A., Sayler G. S., & Ripp S. Microbial Indicators for Monitoring Pollution and Bioremediation. [book auth.] Surajit Das. *Microbial Biodegradation and Bioremediation.* s.l. : Elsevier, 2014, pp. 115-132.

33. Depagne, C., Roux, C. & Coradin, T. How to design cell-based biosensors using the sol–gel process. *Analytical and Bioanalytical Chemistry*. 400, 2011, pp. 965–976.
34. Roda, Elisa Michelini & Aldo. Staying alive: new perspectives on cell immobilization for biosensing purposes. *Analytical and Bioanalytical Chemistry*. 402, 2012, pp. 1785–1797.
35. Nivens DE, McKnight TE, Moser SA, Osbourn SJ, Simpson ML, Sayler GS. Bioluminescent bioreporter integrated circuits: potentially small, rugged and inexpensive whole-cell biosensors for remote environmental monitoring. *Journal of Applied Microbiology*. 96, 2004, Vol. 1, pp. 33-46.
36. Elisa Michelini, Luca Cevenini, Maria Maddalena Calabretta, Silvia Spinozzi, Cecilia Camborata & Aldo Roda. Field-deployable whole-cell bioluminescent biosensors: so near and yet so far. *Analytical and Bioanalytical Chemistry*. 405, 2013, pp. 6155–6163.
37. Thomas Charrier, Marie José Durand, Mahmoud Affi, Sullivan Jouanneau, H el ene Gezekel, G erald Thouand. Bacterial bioluminescent biosensor characterisation for on-line monitoring of heavy pollution in waste water treatment plant effluents. [book auth.] Pier Andrea Serra. *Biosensors*. s.l. : Intechopen, 2010, 11.
38. Michal Bittner, Sergio Jarque, Kl ara Hilscherov a. Polymer-immobilized ready-to-use recombinant yeast assays for the detection of endocrine disruptive compounds. *Chemosphere*. 132, 2015, pp. 56-62.
39. Charles., Johnson Patrick & Muttill Pavan & Mackenzie Debra & Carnes Eric & Pelowitz Jennifer & Mara Nathan & Mook William & Jett Stephen & Dunphy Darren & Timmins Graham & Brinker. Spray Dried Multiscale nano-biocomposites containing living cells. *ACS nano*. 9, 2015.
40. J. Tr ogla, S. Ripp, G. Kuncov a, G. S. Sayler, A. Churav a, P. Pař ik, K. Demnerov a, J. H alov a, L. Kubicov a. Selectivity of whole cell optical biosensor with immobilized bioreporter *Pseudomonas fluorescens* HK44. *Sensors and Actuators B: Chemical*. 107, 2005, Vol. 1, pp. 98-103.
41. Gabriela Kuncov a, Takayuki Ishizaki, Andrey Solovyev, Josef Tr ogl, Steven Ripp. The Repetitive Detection of Toluene with Bioluminescence Bioreporter *Pseudomonas putida* TVA8 Encapsulated in Silica Hydrogel on an Optical Fiber. *Materials*. 9, 2016, Vol. 467.
42. Nagar E, Schwarz R. To be or not to be planktonic? Self-inhibition of biofilm development. *Environmental Microbiology*. 17, 2015, Vol. 5, pp. 1477-86.
43. Donlan, Rodney M. Biofilms: Microbial Life on Surfaces. *Emerging Infectious Diseases*. 8, Sep 2002, Vol. 9, pp. 881–890.

44. Mengxue Diao, Tuan A.H. Nguyen, Elena Taran, Stephen Mahler, Anh V. Nguyen. Differences in adhesion of *A. thiooxidans* and *A. ferrooxidans* on chalcopyrite as revealed by atomic force microscopy with bacterial probes. *Minerals Engineering*. 61, 2014, pp. 9-15.
45. Rolf Bos, Henk J. Busscher. Role of acid–base interactions on the adhesion of oral streptococci and actinomyces to hexadecane and chloroform—influence of divalent cations and comparison between free energies of partitioning and free energies obtained by extended DLVO analysis. *Colloids and Surfaces B: Biointerfaces*. 14, 1999, Vols. 1-4, pp. 169-177.
46. Oss, Carel Jan van. Chapter Three - The Extended DLVO Theory. *Interface Science and Technology*. s.l. : Elsevier, 2008, 3, pp. 31-48.
47. Kokare, C.R., et al. Biofilm: Importance and applications. *Indian Journal of Biotechnology*. 8, 2009, pp. 159-168.
48. *Experimental bacterial endocarditis. IV. Structure and evolution of very early lesions*. Durack, D T. [ed.] 115. s.l. : PubMed, 1975, The Journal of Pathology.
49. *Biofilm and biofilm-related encrustation of urinary tract devices*. M M Tunney, D S Jones, S P Gorman. s.l. : PubMed, 1999, Methods in Enzymology, Vols. 310:558-66.
50. Yi Lu, Dominique Macias, Zachary S. Dean, Nicole R. Kreger, Pak Kim Wong. A UAV- Mounted Whole Cell Biosensor System for Environmental Monitoring Applications. *IEEE Transaction on Nanobioscience*. 14, 2015, Vol. 8, 15, pp. 811-816.
51. *Strategies of Immobilizing Cells in Whole-cell Microbial Biosensor Devices Targeted for Analytical Field Applications*. Nadine Lobsinger, Wendelin J. Stark. 8, s.l. : Analytical Sciences, 2019, Vol. 35, pp. 839-847.
52. *Bioluminescent whole cell optical fiber sensor to genotoxicants: system optimization*. Boris Polyak, Efim Bassis, Alex Novodvoretz, Shimshon Belkin, Robert S. Mark. 1-3, s.l. : Sensors and Actuators B: Chemical, 2001, Vol. 74.
53. Bartkow, Frederic Leusch and Michael. A short primer on benzene, toluene, ethylbenzene and xylenes (BTEX) in the environment and in hydraulic fracturing fluids. <https://environment.des.qld.gov.au>. [Online] 2010. [Cited: 5 2, 2020.] https://environment.des.qld.gov.au/__data/assets/pdf_file/0020/87140/btex-report.pdf.
54. *Leukemia and Benzene*. Snyder, Robert. 8, s.l. : NCBI, 2012, International Journal of Environmental Research and Public Health, Vol. 9.

55. Severochema. Bezpečnostní list - Toluén. Liberec : s.n., 2017. Vol. 4.
56. Services, U.S. Department of Health and Human. 14th Report on Carcinogens. <https://app.knovel.com/hotlink/pdf/id:kt0116Z3I1/14th-report-carcinogens/polychlorinated-biphenyls>. [Online] 2016. [Cited: 1 19, 2020.] <https://app.knovel.com/hotlink/pdf/id:kt0116Z3I1/14th-report-carcinogens/polychlorinated-biphenyls>.
57. *Pseudo-outbreak of Pseudomonas putida in a hospital outpatient clinic originating from a contaminated commercial anti-fog solution.* Romney M, Sherlock C, Stephens G, Clarke A. Ottawa : Canadian Medical Association, Nov 2000, Canada communicable disease report, Vol. 26, pp. 183-184. 1188-4169.
58. Cornelis, Pierre. *Pseudomonas: Genomics and Molecular Biology.* Norfolk : Caister Academic Press, 2008. 978-1-904455-19-6.
59. Parales, Rebecca. *Pseudomonas putida F1. JGI Genome Portal.* [Online] [Cited: 2 19, 2018.] <https://genome.jgi.doe.gov/portal/psepu/psepu.home.html>.
60. *A Chromosomally Based tod-luxCDABE Whole-Cell Reporter for Benzene, Toluene, Ethylbenzene, and Xylene (BTEX) Sensing.* Applegate BM, Kehrmeyer SR, Sayler GS. 7, Knoxville : APPLIED AND ENVIRONMENTAL MICROBIOLOGY, 1998, Vol. 64. 0099-2240/98/\$04.0010.
61. Rahn, Jennifer Joy. Independent Expression of the Gene todX in the Bioluminescent Reporter Strain Pseudomonas putida TVA8. *trace.tennessee.edu.* [Online] 2000. [Cited: 2 20, 2018.] http://trace.tennessee.edu/utk_chanhonoproj/423/.
62. *Bioluminescent bioreporter Pseudomonas putida TVA8 as a detector of water pollution. Operational conditions and selectivity of free cells sensor.* Gabriela Kuncova, Jarmila Pazlarova, Alena Hlavata, Steven Ripp, Gary S. Sayler. 3, s.l. : Elsevier, May 2011, Ecological Indicators, Vol. 11, pp. 882-887.
63. Donnenberg, Michael. *E. coli: Genomics, Evolution and Pathogenesis.* s.l. : Elsevier, 2002. 0080494811, 9780080494814.
64. Liyu Du, Kelly Arnholt, Steven Ripp, Gary Sayler, Siqun Wang, Chenghua Liang, Jingkuan Wang, Jie Zhuang. Biological toxicity of cellulose nanocrystals (CNCs) against. *Ecotoxicology.* 2015, Vol. 24, pp. 2049–2053.

65. Shi Wen-Juan, Menn Fu-Min, Xu Tingting, , Zhuang Zibo T., Beasley Clara, Ripp Steven, Zhuang Jie, Layton Alice C., Sayler Gary S. C60 reduces the bioavailability of mercury in aqueous solutions. *Chemosphere*. 2014, Vol. 95, pp. 324-328.
66. Gershman MD, Kennedy DJ, Noble-Wang J, Kim C, Gullion J, Kacica M, Jensen B, Pascoe N, Saiman L, McHale J, Wilkins M, Schoonmaker-Bopp D, Clayton J, Arduino M, Srinivasan A. Multistate outbreak of *Pseudomonas fluorescens* bloodstream infection after exposure to contaminated heparinized saline flush prepared by a compounding pharmacy. *Clinical Infectious Diseases*. 47, 12 2008, Vol. 11, 1372-9.
67. Brittan S. Scales, Robert P. Dickson, John J. LiPuma, Gary B. Huffnagle. Microbiology, Genomics, and Clinical Significance of the *Pseudomonas fluorescens* Species Complex, an Unappreciated Colonizer of Humans. *Clinical Microbiology Reviews*. 2014, Vol. 27, 4, pp. 927–948.
68. Archana Chauhan, Alice C. Layton, Daniel E. Williams, Abby E. Smartt, Steven Ripp, Tatiana V. Karpinets, Steven D. Brown, Gary S. Sayler. Draft Genome Sequence of the Polycyclic Aromatic Hydrocarbon-Degrading, Genetically Engineered Bioluminescent Bioreporter *Pseudomonas fluorescens* HK44. *JOURNAL OF BACTERIOLOGY*. 9 2011, Vol. 193, 18, pp. 5009–5010.
69. Hana Kalabová, Marie Pospíšilová, Romana Šíroková, Gabriela Kuncová. A biosensor with encapsuled bioreporters—optical fiber element for enhanced detection of bioluminescence. *Measurement Science and Technology*. 29, 2018, Vol. 7.
70. *Saccharomyces* species. *drfungus.org*. [Online] <https://drfungus.org/knowledge-base/saccharomyces-species/>.
71. Eldridge ML, Sanseverino J, Layton AC, Easter JP, Schultz TW, Sayler GS. *Saccharomyces cerevisiae* BLYAS, a new bioluminescent bioreporter for detection of androgenic compounds. *Applied Environmental Microbiology*. 73, 2007, Vol. 19, pp. 6012–6018.
72. *Detection of Benzene, Toluene, Ethyl Benzene, and Xylenes (BTEX) Using Toluene Dioxygenase-Peroxidase Coupling Reactions*. Zhaohui Xu, Ashok Mulchandani, Wilfred Chen. 6, s.l. : Biotechnology Progress, 2003, Vol. 19. 10.1021/bp0341794.
73. Ishizaki, Takayuki. *Fiber-optic whole cell bioluminescent sensor*. Kladno : Czech Technical University, Bachelor thesis, 2013.
74. Kalábová, Hana. *Influence of geometry and active layer of optical elements on sensitivity of biosensor*. Kladno : Czech Technical University, Diploma thesis, 2010.

75. Kalabova H, Pospisilova M, Jirina M, Kuncova G. Mathematical Model for Laboratory System of Bioluminescent Whole-Cell Biosensor with Optical Element. *Journal of Biosensors & Bioelectronics*. 9, 2018, Vol. 1, 250.
76. Oss, Carel J. van. *Interfacial Forces in Aqueous Media*. 2nd. s.l. : CRC Press, 2006. 1420015761, 9781420015768.
77. Fletcher, M. Attachment of *Pseudomonas fluorescens* to glass and influence of electrolytes on bacterium-substratum separation distance. *Journal of Bacteriology*. 170, 1988, Vol. 5, pp. 2027-2030.
78. S. F. D'Souza, J. S. Melo, A. Deshpande, G. B. Nadkarni. Immobilization of yeast cells by adhesion to glass surface using polyethylenimine. *Biotechnology Letters*. 8, 1986, pp. 643-648.
79. Adamczyk, Zbigniew. *Particles at Interfaces: Interactions, Deposition, Structure*. s.l. : Academic Press, 2006. Zbigniew Adamczyk.
80. *Evaluation of an FIA Operated Amperometric Bacterial Biosensor, Based on Pseudomonas Putida F1 for the Detection of Benzene, Toluene, Ethylbenzene, and Xylenes (BTEX)*. Rasinger, Josef, et al. 10, s.l. : aylor & Francis, 2005, nalytical Letters, Vol. 38, pp. 1531-1547. 0003-2719.
81. *Fiber optic monooxygenase biosensor for toluene concentration measurement in aqueous samples*. Zhong Zhong, Michael Fritzsche, Sean B Pieper, Thomas K Wood, Kevin L Lear, David S Dandy, Kenneth F Reardon. 5, 2011, Biosensors & Bioelectronics, Vol. 26, pp. 2407-2412.
82. *Optical Fiber Whole Cell Bioluminescent Sensor*. Kuncova, Gabriela, Pospisilova, Marie and Solovyev, Andrey. Orillia, ON, Canada : Proceedings of the XX International Conference on Bioencapsulation, 2012. pp. 96-97. proceedings reference P_01.
83. *Analytical strategies for improving the robustness and reproducibility of bioluminescent microbial bioreporters*. Aldo Roda, Barbara Roda, Luca Cevenini, Elisa Michelini, Laura Mezzanotte, Pierluigi Reschiglian, Kaisa Hakkila & Marko Virta. s.l. : Analytical and Bioanalytical Chemistry, 2011, Vol. 401, pp. 201–211.
84. *Biofilm Engineering Approaches for Improving the Performance of Microbial Fuel Cells and Bioelectrochemical Systems*. Maria Joseph Angelaalincy, Rathinam Navanietha Krishnaraj, Ganeshan Shakambari, Balasubramaniam Ashokkumar, Shanmugam Kathiresan and Perumal Varalakshmi. 63, s.l. : Frontiers in Energy Research, 2018, Frontiers in Energy Research, Vol. 6.
85. *Biofilm Matrix and Its Regulation in Pseudomonas aeruginosa*. Qing Wei, Luyan Z. Ma. s.l. : International Journal of Molecular Sciences, 2013, Vol. 14. 20983-21005.

86. Long-range and short-range mechanisms of hydrophobic attraction and hydrophilic repulsion in specific and aspecific interactions. Oss, Carel Jan van. 4, 2003, Journal of molecular recognition, Vol. 16, pp. 177-190.

